# The application of Dendrimers for catalysis and purification and analysis for protein binding.


**Abdullah Neda Alotaibi**

**Department of Chemistry**
**The University of Sheffield**

**Submitted to the University of Sheffield**
**In fulfilment of the requirements for the degree of**
**Doctor of Philosophy**

**September 2022**

**ACKNOWLEDGEMENTS**

I wish to offer up my success to my dearly loved parents, whose presence in my life gives me untold joy, as well as to my wife, brothers and sisters, who have all supported me throughout every stage of my career.

I would like to extend my thanks to my supervisor, Dr Lance Twyman, who gave me the opportunity to participate in this project, and offered generous support, advice and encouragement during the entire research process. And I would like to thank Dr. Azrah Abdulaziz for her suggestion and help. I also owe a debt of gratitude to Dr Ibrahim Altobaiti, who worked with me on the project, and not only shared his extensive knowledge, but also made many sound and useful suggestions, as well as he guided me in choosing the right university and supervisor for this project, and his input was invaluable and I greatly appreciate whose warm welcome to the department and encouragement put me at ease on arrival.

Ms Heather Grievson, Mr Simon Thorp and Mr Nick Smith provided me with valuable technical assistance, and I wish to thank them, as well as everyone in the department of Chemistry, particularly the staff in the teaching lab, NMR, mass spectrum and the IT services, for their unflagging help.

I would like to offer my sincere thanks to Ms Amal for her recent help in the lab. and thanks to Mr Mohamad Alassaf and Mr Sultan Almutairi who played in making me feel settled and happy in Sheffield . Many thanks are also due to the Twyman group: Mr Abdelfatah Blau, Mr Abdullatif, Mrs Enas , and Mr Reyad.

Finally, I wish to acknowledge Imam Mohammad Ibn Saud Islamic University, whose financial assistance made it possible to undertake and complete these PhD studies.

**ABSTRACT**

The aim of this thesis was two-fold. Firstly, to demonstrate how dendrimers, and internally functionalized dendrimers could be used to speed up the rate of a reaction. Secondly, to develop a new non-covalent methodology towards selective or specific protein binding. The results for each are summarised below:

For the catalysis systems we synthesised a series of neutral water soluble dendrimers as model enzyme systems. These PAMAM dendrimers significantly increased the rate of the ester cleavage reaction (trans-esterification) in water, using the hydrophobic PNPA substrate. These rate accelerations did not require the use of acid or base, and could take place at neutral pH. In this respect, they resemble the action and properties of an enzyme. Dendrimers with 4, 8 and 16 end groups were studied (G 0.5, 1.5 and 2.5 respectively), and it was clear that the larger dendrimers were able to speed up the reaction to a greater extent. This was due to the fact the larger dendrimers had a more hydrophobic interior that was more ordered and could bind the PNPA substrate more tightly, and in closer proximity to the larger number of internal and external functionality (required for reaction and stabilisation), The catalytic process was also studied at pH 7.5, 8.0 and 8.5. In all cases, the rates were significantly faster, with the fastest occurring at pH 8.5. Over this pH range, we also observed that the change in relative rate was significantly lower for the dendrimers when compared to the simple control reaction (without dendrimers). In an attempt to develop a synthetic metallo-enzyme, copper was inserted into each of the dendrimers by reacting them with excess copper sulphate. The copper stoichiometry per dendrimer was determined by Job plots, which identified a stoichiometry of 1, 2 and 4 coppers for the G0.5, G1.5 and G 2.5 dendrimers respectively. These copper dendrimers were subjected to the same rate studies carried out for the non-functionalised dendrimers, and similar results and trends were obtained across all pHs studied (with the copper dendrimers being slightly faster). This included the ability to significantly increase rates at neutral pH, and the very small increase in relative rate with respect to pH (compared to the control). Overall, we concluded that the dendrimers were able to speed up PNPA cleavage through an initial hydrophobic binding, which placed the substrate in close proximity to the dendrimer's reactive and stabilising groups. The pH rate experiments confirmed that the dendrimer reactions proceeded by a completely different mechanism, and gave a different product, to those occurring in the simple hydrolysis reaction (the control).

The second area of study was aimed at generating new macromolecules as inhibitors to protein-protein binding and for use in protein purification. To achieve this, neutral OH ended PAMAM dendrimers were used as host molecules to support a number of different functional groups on its surface. The functional groups would be attached to linear chains, which would bind via a series of non-covalent interactions (hydrophobic and H-bonding) to the interior of the dendrimer. The dynamic nature of these interactions would allow the functionalised chains to move and maximise their interactions with a protein surface. In effect, the protein would template its optimum dendrimer based ligand, with the relative position of the linear chains and their functional groups controlled by the protein surface.

A tyrosine and valine linear chain was synthesis, as these groups are known to respectively strengthen and weaken binding to a number of target proteins. The chains were synthesised using a standard Boc peptide methodology to generate beta-alanine based chains with three hydrogen bonding amides in the backbone (designed to interact with the internal amides of the PAMAM dendrimers). The initial stages of the synthesis progressed well, but due to solubility problems in the later stages, and despite many purification attempts, we were not able to obtain the desired chains in good purity. Nevertheless, we used the crude material to generate dendrimer-linear chain complexes (with the tyrosine and valine chains). Inhibition experiments were used to assess binding to chymotrypsin, with strong inhibition be directly related to strong binding. In our experiments we observed that the tyrosine based complex had a $K_i$ value of 1.23 M, which was 25% higher than the valine derived complex. Control studies confirmed that the dendrimer and the linear chains were required for binding and that no inhibition/binding occurred when either were used on their own.

**ABBREVIATIONS**

**PAMAM** Poly(amido amine)
**PAMAM-OH** Neutral Hydroxyl Terminated PAMAM
**PAMAM-COOH** Acid Terminated PAMAM
**DCC** Dynamic combinatorial chemistry
**DCLs** Dynamic combinatorial libraries
**DCM** Dichloromethane
**DCCI** Dicyclohexyl carbodiimide
**DCU** Dicyclohexyl urea
**DMSO** Dimethylsulphoxide
**EDA** Ethylenediamine
**EDC** 1-Ethyl-3-(3-dimethylaminopropyl)carbodiimide
**DMAP** 4-Dimethylaminopyridine
**MA** Methyl Acrylate
**BTNA** N-benzoyltyrosine-p-nitroanilide
**$^{1}$H NMR** Proton Nuclear Magnetic Resonance Spectrometry
**$^{13}$C NMR** Carbon-13 Nuclear Magnetic Resonance Spectrometry
**IR/FTIR** Infra Red/Fourier Transfer Infra Red Spectrometry
**ES-TOF MS** Electron Spray Time-Of-Flight Mass Spectrometry
**MALDI-TOF MS** Matrix Assisted Laser Desorption Ionisation Time of Flight
**Chy** $\alpha$-chymotrypsin
**NaOH** Sodium Hydroxide
**$K_2CO_3$** Potassium Carbonate
**TRIS** Tris(hydroxymethyl)aminomethane
**UV/Vis Spectrometry** Ultra Violet/Visible Spectrometry
**Ɛ** Extinction coefficient
**nm** Nanometre.
**DLS** Dynamic light scattering
**TRIS** Tris(hydroxymethyl)aminomethane.
**3HB-LC-Boc-Tyr** Three hydrogen bonding of linear chain with Boc Tyrosine
**3HB-LC-Tyr** Three hydrogen bonding of linear chain with Tyrosine
**3HB-LC-Boc-Val** Three hydrogen bonding of linear chain with Boc Valine
**3HB-LC-Val** Three hydrogen bonding of linear chain with Valine

# Table of Contents

# CHAPTER 1
## Dendrimers: an introduction

## 1.0 Introduction polymers

The Greek words "poly" (many), "mono" (one), and "meros" were incorporated to create the names "polymer" and "monomer", with polymers being the large-scale materials (macromolecules) made up of multiple microscopic units known as monomers. Polymers can be created artificially or organically, with the synthetic polymers created industrially including plastics, textiles, and rubbers. Examples of natural polymers include proteins (polypeptides), starches, latex, and cellulose. Despite this wide range of polymer products, however, polymers exist in only three types of molecular architecture: cross-linked, branching, and linear (Figure 1.1).[1]

A long chain of monomers becomes a linear polymer, while any side branching attached to this chain creates a branched polymer. In cross-linked polymers, neighbouring linear chains are covalently connected, with links either between distinct chains or between different locations of the same chain, rather than just at the ends. Branched polymers may, however, also have side branches that join along the chain, and the term "dendritic polymer" refers to a novel type of branching polymer that has recently been produced.[2]


Figure 1.1: Polymer Architectures

## 1.1 Introduction to Dendritic Polymers

The most common way in which dendritic polymers are defined is as particular branching, tree-like structures that consist of multifunctional monomers. When compared to linear polymers, their physical characteristics are strikingly different due to their branching structure, with several system features arising from the numerous functionalised groups that emerge from a high degree of branching.

Dendrons, dendrimers, star polymers, and hyperbranched polymers are examples of the varying branched topologies that may contain dendritic polymers: the type of branching observed is thus used to make distinctions between these formations.[3]

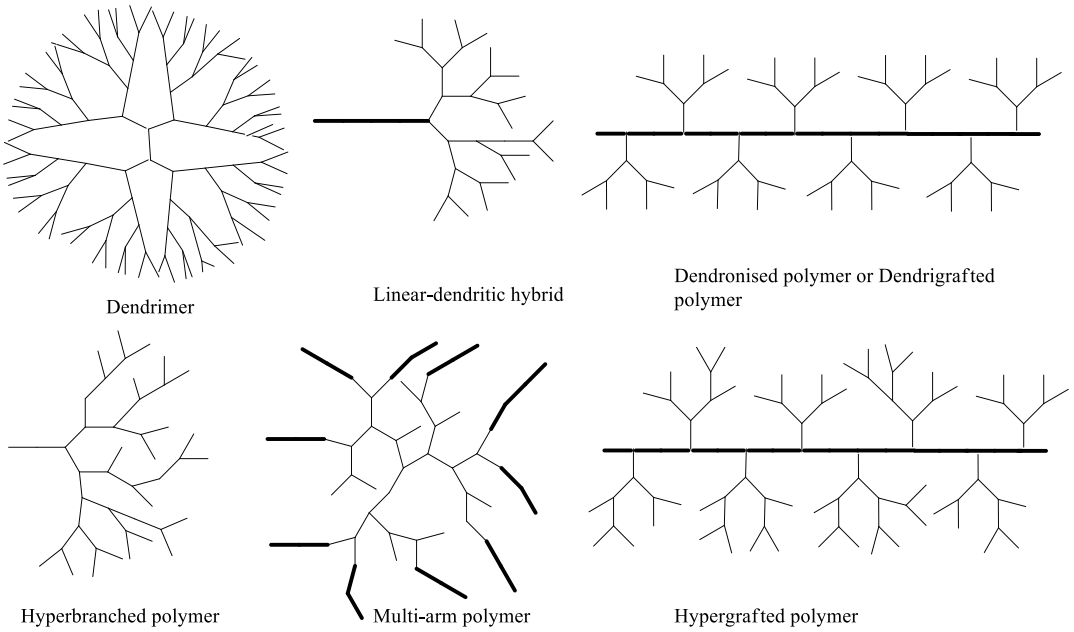


Figure 1.2: Examples of dendritic polymers

### 1.1.1 Dendritic Polymer Synthesis

In terms of dendritic polymer chemistry, the work done by Flory in 1952 marked the beginning of a new era.[4] The essential idea of the researcher's hypothesis was the condensation of ABx (where $x \geq 2$) monomer molecules. The earliest iterative synthetic technique for dendrimer synthesis, which was based on aliphatic amine $AB_2$ type monomer molecules, was thus proposed by Vögtle et al.[3] based on this idea, while the creation of so-called "cascade" polymers was facilitated by condensation. As monodispersed symmetrical macromolecules, dendrimers require tight synthetic control, which is made possible by using a layered construction method in which every step involves a variety of deprotection, protection, and purification steps; this thus leads to a highly complicated synthesis procedure. There are now two major categories of synthesis processes, both of which were initially developed in 1978: the divergent approach and the convergent method.[4]

## 1.2 Divergent Approach

Divergent dendrimer synthesis was developed based on the branched model created by Tomalia et al.[5]. This begins with an initiator core, with layers then added through a series of coupling and activation phases as a way to build outward in the direction of the molecule's periphery. Figure 1.3 shows the growth of a dendrimer using the divergent method, which highlights that every generation's terminal groups react with the monomer unit's corresponding reactive group,[6] such that branch points are established at each location, increasing the number of terminal functionalised groups. This is thus known as the coupling step. The activation stage, in which latent functional groups are energised, begins once the initial connection stage has been finished, which point the monomer is

allowed to react, boosting generation.[7] The number of branches in the macromolecular intermediate thus depends on the amount of active hydrogen available, and these are connected to the other inner generations in a distinct and regular order.[8]

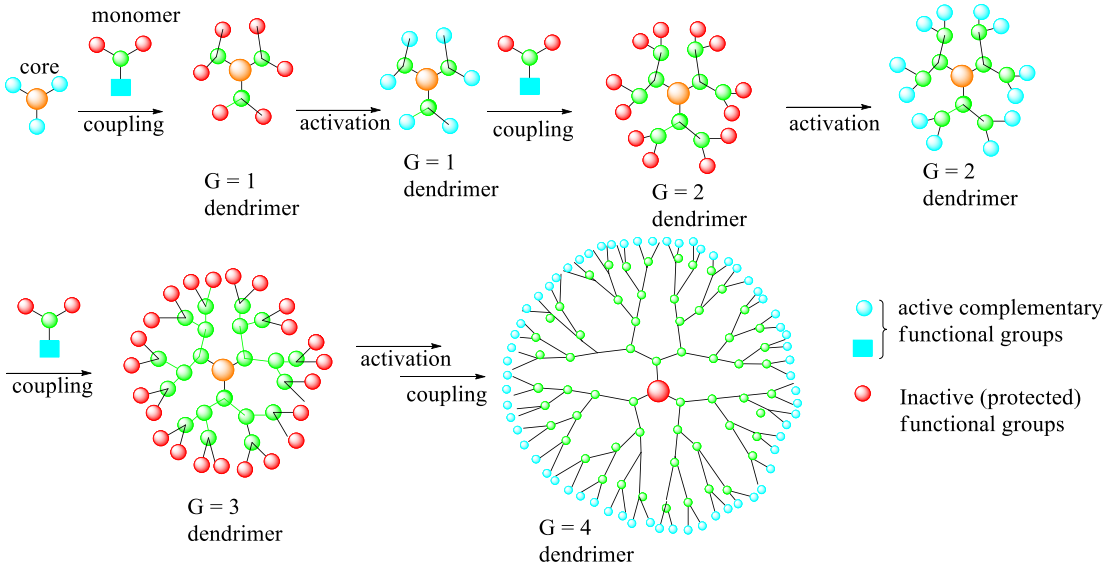


Figure 1.3: Divergent dendrimer synthesis

Divergent dendrimer synthesis is advantageous due to both its simplicity and the fact that, if suitable reagents are used and viable reaction conditions maintained, it makes industrial scale synthesis feasible. The number of reactions needed at the perimeter, however, increases exponentially based on the order of activation and coupling reaction phases required. A significant surplus of reagents is therefore needed to ensure that each reaction step proceeds as planned. Another drawback is the way in which the number of coupling reactions required scales with each generation, increasing the risk of unfavourable side effects and the ensuing potential for incomplete by-products. To prevent the development of superfluous dendritic structures, the activating reagent must also be entirely removed after the process is complete.[7]

The first family of dendrimers to be synthesised and subsequently made commercially available was the polyamido amines (also known as "starburst" dendrimers), which were first described by Tomalia et al. in 1985.[9] Many additional details are available in the literature for this family of dendrimers, as it has since been thoroughly investigated.[10]

### 1.3 Convergent Approach

The convergent method for dendritic polymer synthesis was first documented by Fréchet and Hawker.[11-15] This method produces a reactive dendron by beginning with the edge of the final dendritic structure and working inward. The collection of dendrons then reacts with a multifunctional core molecule to create a globular dendritic architecture.[16] This differs from divergent synthesis due to the fact that the core is incorporated into the macromolecule during the final reaction phase.[17] Figure 1.4 provides an illustration of the convergent method.

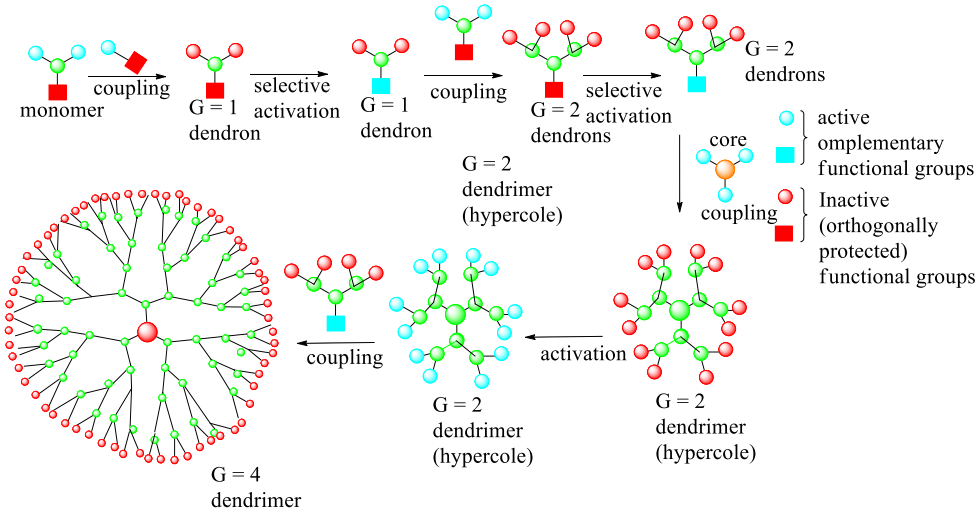


Figure 1.4: Convergent dendrimer synthesis

After coupling, the focus point of the dendron can be triggered via an activation procedure. This method thus offers a high degree of architectural control by working from the periphery to the core, which means that fewer coupling reactions are needed at each phase.

Thus, in contrast to the divergent strategy, only a small surplus of **reagents is required,** which aids in the purifying process. The convergent technique's ability to disperse functional groups across the architecture selectively is another way in which it outperforms the divergent approach.[17]

The methods utilised in this technique to produce both symmetrical and unsymmetrical dendrimers are accurate and offer high degrees of definition. Steric crowding may develop as a result of the approach's passage from the interior to the periphery, however, making large generation dendrimers more difficult to synthesis and prone to structural flaws. This method was used by Grayson and Fréchet to make poly(benzyl ethers).[18]

### 1.4 Applications of Dendrimers

Catalysis, drug delivery, anion binding, biomimetic, and many other potentially significant applications have been either imposed or proposed for dendrimers.[19] The majority of these rely on additional functionalisation added either to the outside or inside of the dendrimer. However, current methods for internal functionalisation either focus on adding functionality after the dendrimer has been synthesised or on inserting this within the monomer or repeat unit.[20] The first method, however, occasionally results in an excessively functionalised molecule, while the second method always entails the synthesis of unsymmetrical dendrons that demand numerous protection/deprotection processes and challenging purifying techniques. The internal post-synthetic functionalisation of a water-soluble dendrimer can be achieved via a straightforward quaternisation approach, however, and this broad strategy can enable the incorporation of a number of functional groups inside the interiors of various dendrimers, allowing the generated molecules to be of use in a number of different fields.[19,20]

## 1.5 Catalyst Introduction

In the chemical industry, polymers have been utilised in catalysis for many years. Such modifications have prompted scientists to look for ways to reduce the amount of waste produced by such chemical reactions, with one goal being to create a catalyst that could be readily recovered from the chemical process without any loss of effectiveness to permit repeated use. As well as reducing costs, the environment would be significantly protected if this goal were to be accomplished, making it crucial to create a catalyst with these particular qualities.[17-19]

## 1.6 Enzymes in the catalyst role

The three-dimensional structure of enzymes drives their functions, and these may thus significantly speed up the rate of reactions as extremely selective catalysts. Numerous enzymatic actions are thus possible.[16] They can reduce activation energy by decreasing the transition state, offering different pathways and establishing an environment that allows the transition state to be stabilised, leading to faster reactions. Additionally, they may offer an ideal environment for substrate and transition state binding.[18] Such transition state binding mechanisms result in stabilisation, which again reduces activation energy and speeds up various processes, as shown in Scheme 1.


Whereas, E= Enzyme, S= Substrate, ES= Enzyemsubstrate complex and P= Product

Scheme 1.1: Enzyme-Substrate in catalysis process

## 1.7 Catalysis Types, Advantages, and Disadvantages

In the chemical industry, catalysis is already a significant process, yet this branch of chemistry is still being developed to meet both environmental and economic needs. The traditional definition of catalysis is the use of a catalyst to speed up chemical reactions, yet a more expansive definition may now be required due to the discovery that catalysts may also support other crucial functions including selectivity and recoverability.[14] Catalysts typically offer a different route to the reaction product, lowering the activation energy and thus speeding up the reaction rate, as seen in Figure 1.5.

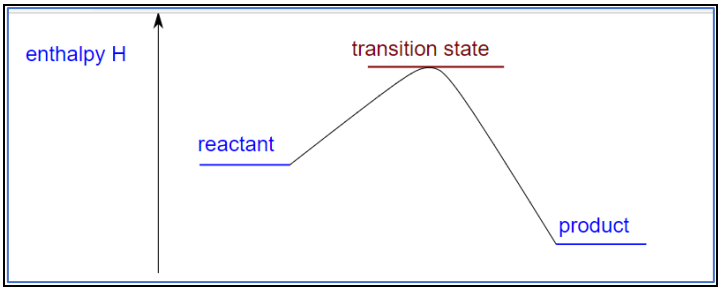


Figure 1.5: Transition state of a catalyst

Although the primary function of a catalyst is to speed up the chemical reaction process, catalysts are occasionally used to alter the reaction's selectivity towards other products. Enantioselectivity, for example, may be controlled by a catalyst, allowing a reaction to proceed at a more cost-effective and convenient temperature and pressure.[13,15]

Catalysts can be categorised as positive, negative, homogeneous, or heterogeneous. A negative catalyst (inhibitor), in contrast to a positive catalyst, slows down chemical reactions, which plays a crucial role in some forms of production. For instance, oxygen

inhibits free radical processes, which are crucial for the production of polymers, and as a result, such reactions must be carried out without oxygen.[12, 16]

Heterogeneous catalysts are insoluble in the reaction phase, while homogeneous catalysts are soluble in the same phase as the reactant. Heterogeneous catalysts are often more stable than homogeneous catalysts and may have considerably stronger catalytic activity; they also have the advantage of allowing for easy product separation from the catalyst.[19] However, as reaction processes are frequently opaque, heterogeneous catalysis can be challenging to analyse fully. Nevertheless, as a solid catalyst can be quickly separated from any liquid products using simple, affordable means such as filtration or decantation, heterogeneous catalysts are generally straightforward to separate from the reaction mixture, and they are thus employed more frequently in the chemical industry due to both this simplicity of separation and their greater heat stability.[20,21] Homogeneous catalysts have much more significant issues with respect to the recovery process; thus, in order to make use of these catalytic processes' unique reactivity, catalyst recovery must be carefully considered.[22]

The recovery of homogeneous catalysts has received increased attention recently due to their superior catalytic activity coupled with their problematic separation from the reaction product.[21] The recovery of a homogeneous catalyst is only readily feasible if the generated product is volatile; otherwise, more difficult processes are required. The simplest effective separating method is commonly distillation, yet since the majority of homogeneous catalysts operate in organic solvents, waste issues commonly arise in such cases. As a result, good, efficient separation procedures have been sought recently as a potential remedy for homogenous catalyst separation utilising polymer-supported ligands.[14]

The underlying concept entails attaching the catalyst to the polymer, which can then be filtered out due to the polymer's comparatively large molecular weight. Numerous examples have been explored with respect to the separation and recovery of homogeneous catalysts, and several have proven to be effective and beneficial, including the use of polyethylene, alkene oxide, N-isopropyl acrylamide, fluorous polymers, and amphoteric polymers.[23] In terms of their key characteristics, these examples vary significantly, however. For instance, polyethylene can be used for catalytic separation for two key reasons: it is chemically inert, ensuring that catalysis is not hampered, and its solubility is significantly influenced by temperature, making its utilisation is more appealing due to the manipulability of the relationship between solubility and temperature.[24] In particular, at standard industrial room temperatures, the solvent and catalyst combine to form a biphasic solution which, as illustrated in Figure 1.6, blends together on heating to create a homogeneous solution.

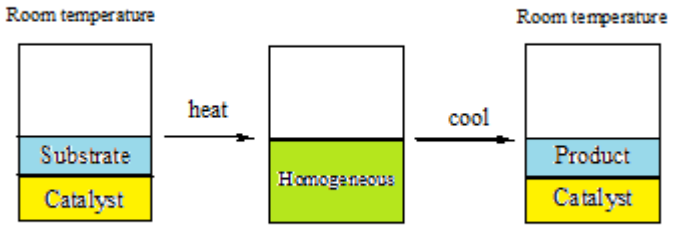


Figure 1.6: Temperature Effects in the Homogeneous Catalyst Separation Step

The biphasic system (product/catalyst) reappears once the reaction is complete and the reaction mixture is cooled to room temperature, allowing the catalyst to be rapidly separated from the product.

## 1.8 Naturally occurring biosynthetic enzymes

The use of biomolecules, particularly enzymes or entire cells, as catalysts for the creation of new materials is referred to as biocatalysis. The number of biocatalytic applications available has increased significantly over the last few decades as a result of major advancements in enzyme technology and the development of understanding of structure-function correlations.[20-24] However, the tremendous potential of biocatalysis has not yet been fully exploited, despite many successful improvements in the use of specific compounds and the increased number of applications available. Importantly, biocatalysts can increase a reaction's speed without changing its thermodynamic characteristics.[21]

Biocatalysts' primary advantages also include high stereoselectivity, regioselectivity, and chemoselectivity.[17,18] For industrial synthesis, such high levels of selectivity are very desirable, offering a number of benefits that include a decreased or eliminated requirement for protecting groups, fewer side reactions, speedier separation, and reduced environmental effect. High catalytic efficiency and comfortable working conditions are two additional advantages for commercial applications. The drawbacks of biocatalysis do, however, include the inhibition of substrate and product, the need to perform reactions in aqueous solutions, and a requirement for very precise environmental conditions.[16]

Methyltransferases;[20] Diels-Alderases, which catalyse cycloadditions;[21]halogenases;[22] uridine diphosphate-dependent glycosyltransferases;[23] laccases;[24] and pyridoxal phosphate-dependent enzymes[25] are all natural product biosynthetic enzymes that have been used in

chemical synthesis. However, these biosynthetic enzymes are generally slow catalysts, with Michaelis constant $k_{cat}$ values typically 30 times lower than those of primary metabolism,[26] potentially due to limitations arising from their evolutionary histories.[26,27] Nevertheless, biosynthetic enzymes have become the basis for multiple attempts to enhance catalysis rates and substrate tolerance, as well as to enhance stability and solubility in preferred solvents such as ionic liquids and water-soluble organic solvents. [28]

### 1.9 Dendrimers as biosynthetic enzymes

Despite its traditional focus on organic chemistry, the biocatalysis community has recently started to actively investigate the development of molecular complexity and scaffold synthesis.[17] Catalytic processes carried out in an environmentally friendly solvent, such as water, are in particular demand, as catalysis is pertinent to many areas of environmental science.[16] Dendritic macromolecules are a relatively recent class of polymers that are potentially suitable for such applications, and since this type of polymer first appeared, the study of polymeric chemistry has received increased attention. Dendrimers and hyperbranched polymers are the two basic forms of dendritic polymers (HBPs).[19]

The initial steps of several different types of chemical catalysis are similar to those of enzyme catalysis. Enzymes function similarly to other catalysts by creating a distinct path for the reaction product, which decreases activation energy and considerably enhances the rate of reaction.[16] Numerous studies have thus focused on replicating the behaviour of such enzymes in an effort to duplicate their exceptional properties[16,17,18]; however, this is complex, due to the three-dimensional layout of these natural systems (enzymes), which is

in turn responsible for their great catalytic efficiency.[28] An electronic effect resulting from the polarity difference between an enzyme's inner and outer surfaces also impacts results, and this also pertains to the steric effect and the catalytic site concealed within each enzyme molecule. In order to dissolve organic molecules, these effects must thus be exploited to enclose and isolate the molecules inside an enzyme, and, as a result, enzymes can be used to carry out highly selective and precise reactions.

Zeolites[28] and micellar[29] molecules were widely employed before the emergence of dendritic polymers to replicate the site isolation of natural molecules (enzymes). Zeolite catalysts are particularly significant in the chemical industry, as zeolites' distinctive microporous structures perfectly regulate access for both reactants and products (a steric effect). Zeolites also have a reputation for functioning as shape-selective catalysts. Following the discovery of dendritic macromolecules with three-dimensional structures that resemble enzymes structurally, researchers have recreated such systems and shown how well they can imitate the controlled environment that enzymes provide, however. Such dendritic polymers were able to separate molecules from their surrounding environment by means of a process known as "dense packing", achieved by limiting access to the core, especially among higher generation dendrimers.[30]

Small molecules can be contained in the internal chambers of dendrimers in a manner related to their three-dimensional branching nature[31]. Meijer et al.[25] utilised this feature to employ dendrimers as container molecules, encapsulating small organic molecules inside the dendritic “box” of the dendrimers and then controlling the release of these guest

molecules by modifying the terminal end-groups. This property allows dendrimers to be used to separate core and internal components, shielding the interior environment from the exterior.

Dendrimers thus possess both the steric and electrical capabilities required to manipulate their environment. The fact that the nature of the end-groups may be adjusted is the most crucial factor in terms of adjusting solubility and thermal stability, which provides crucial control over various properties, particularly in catalytic applications. One of the most crucial characteristics of any catalytic processes is control over the surroundings. Dendrimers thus have an advantage because they can be used to perform reactions in a controlled microenvironment, allowing them to operate in a water-based bulk solvent that is ecologically benign. Such dendritic macromolecules can thus be uniquely applied across various applications, such as catalysis and drug delivery, a process enhanced by the improvement of new methods to incorporate molecules into the dendritic polymers' periphery or to encapsulate them in the cavities within such polymers[32-36]

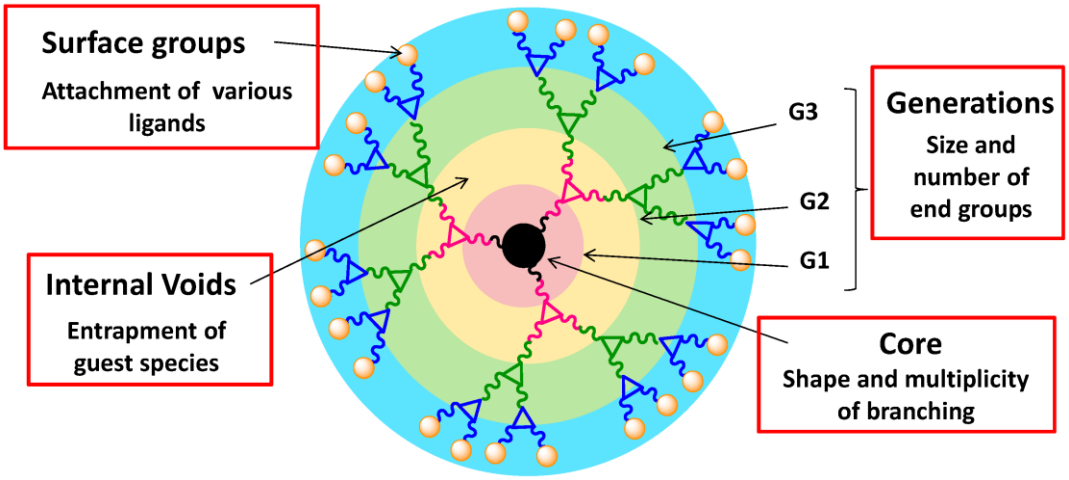


Figure 1.7: Dendrimer structure suitable for functionalisation.

Dendrimer structures can be further exploited for functionalisation, as demonstrated in Figure 1.7. All such enzyme-created functions can be carried out by PAMAM dendrimers, which can bind substrates and create particular conditions for the substrates, intermediates, and lower transition states. PAMAM dendrimers can be used as catalysts based on binding a metal within their cavities, thus allowing them to imitate the remarkable properties of enzymes.

## 1.10 Conclusions

The majority of the examples presented in this paper demonstrate how catalytic groups buried inside precisely defined and regulated dendrimer environments can have significant influence on both regio- and stereoselectivity. Other instances demonstrate the impact of a dendrimer's internal physical characteristics on the catalysis process. Reactions may thus be catalysed by the type of integrated group, the microenvironment (whether polar or non-polar), or both. However, currently, the challenging nature of dendrimer-based catalysis prevents the full scope of industrial and commercial use.

# CHAPTER 2
# Aims and Objectives

## 2.0 Aims and Objectives

In natural processes, water-soluble macromolecules (enzymes) serve as catalysts for a variety of reactions: in fact, enzymes are required in almost every chemical reaction that takes place in biological cells. There are a variety of factors involved in the catalysis process, including hydrophobic binding, transition state stabilisation, and substrate concentration. As Figure2.1 shows, enzymes use electric charges to create a stable reactant state. Within each enzyme, there is an active site at which the reactant molecules (substrate) join together. The combination of such molecules within the binding site is known as the transition state, and during the creation and breaking of bonds, the substrate binds to the enzyme, which nevertheless remains unchanged, after which the product is created. This product can thus be separated into the desired product and the enzyme. Enzymes enable all such reactions to occur in water; thus, mimicking this action of enzymes permits unusual chemical reactions to be undertaken to obtain different isomers or to catalyse important reactions that do not have specific natural catalysts within water. The enzyme catalysis process is ostensibly very similar to other chemical catalysis processes that create alternative pathways to facilitate a reaction, thus reducing the activation energy and causing a significant increase in reaction rate.

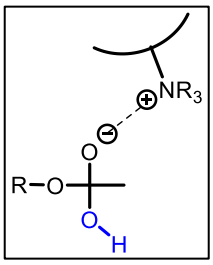


Figure 2.1: Stabilisation of TS/intermediate - charge

The three-dimensional architecture of enzymes is responsible for their efficiency, while an electronic effect within the enzyme is due to as the difference in polarity between the inside (active site) and outside of its protein structure. In addition to the electronic effects at the enzyme's active/catalytic site, steric effects related to the size of the organic substrates and whether or not they (or the TS) can fit inside the enzyme also occur. As a result of these electronic and steric effects, enzymes can carry out reactions with high levels of specificity, based on chemo-, regio- and or stereoselectivity.

Human bodies, being essentially "sacks of water", rely on a range on organic reactions that are only possible without the specific microenvironment provided within enzymes. Due to their size, polymers have commonly been used to try to mimic an enzyme structure and its ability to control a steric and electronic microenvironment. Although there have been some successes using linear polymers, these are generally not suitable for use as enzyme mimics due to their dynamic structure and flexibility that means permanent structures or active sites cannot effectively form. This means that any interactions and reactions that take place between linear polymers and organic molecules are "non-specific" in nature, which in turn means that these types of systems have had some success when applied to the catalysis of non-specific reactions.

For example, the simple hydrolysis of esters. In order to achieve selectivity or specificity, a water soluble polymeric system with a fixed structure and a controlled microenvironment (interior) is required, however. In this respect, dendrimers may be better able to offer the structural, electronic, and solubilising properties required, as seen in the PAMAM dendrimers similar to the one shown in Figure 2.

One possible design maybe a dendrimer with neutral polar terminal groups, which provide water solubility, as well as possessing a hydrophobic internal environment that can bind to or dissolve organic material. This ability to encapsulate organic molecules has been widely used to increase the aqueous solubility of drug molecules, improving their therapeutic effectiveness and ability to transport and deliver hydrophobic drugs. It has also been shown that several important secondary interactions provided by the internal functionality within these dendrimers can increase drug interactions, supporting greater loading and retention within the body.

PAMAM dendrimers have a number of amides that can form hydrogen bonds with suitable groups on a drug, and the encapsulation and delivery of acidic drugs that can form ion pair interactions with internal amines has been previously investigated. These properties can also be exploited to bind substrates, intermediates, and transitions states and therefore to catalyse reactions in a similar manner to enzymes with respect to structural properties. The key objective of this study is thus to functionalise the interiors of dendrimers and to investigate the impact of this on the internal microenvironment in order to determine whether or not dendrimers can be applied as effective enzyme mimics.

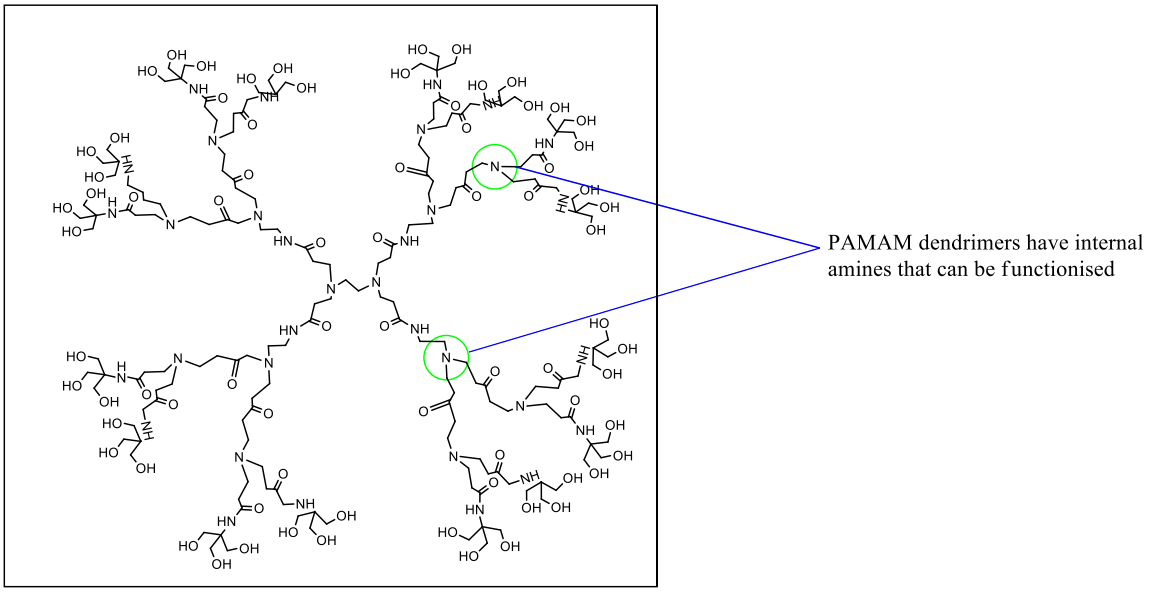


Figure 2.2: Structure of a water soluble dendrimer. The dendrimer possesses internal functionality that can be exploited to bind and interact with a variety of species, including drug moles, substrates, and transition states.

Dendrimers all have unique architectures, based on their three-dimensional, spherical shapes and their extremely regular branching nature. Although accurate control is required to construct them initially, they can be adapted for multiple different uses due to their unique features. Dendrimers' globular forms, especially at higher generation levels, also mean that they are ideal for filtration and precipitation at the end of reactions, which makes recovery easier. Furthermore, dendrimers have large numbers of terminal groups at their periphery that can be easily modified, making them soluble in both organic and aqueous environments, as sown in Figure 2.

Nevertheless, they are basic enough to deprotonate acidic substrates, depending on the relative pKa of the acid, while PAMAM dendrimers can isolate substrate molecules within their internal cavities and maintain relatively controlled geometry with regard to any

internal groups that may be able to interact with subsequent transition states. In this respect, they can mimic the structure of enzymes closely, thereby enhancing the rates of some reactions.

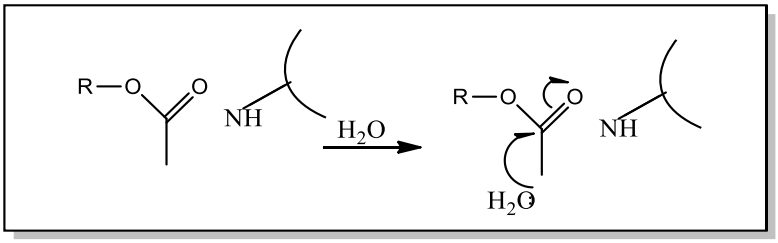


Figure 2.3: Intermediate interaction with internal amides

This work will initially looks at simple dendrimers and investigates their ability to catalyse reactions based on their pre-existing internal functionality. For example, during a hydrolysis reaction, a charged intermediate will form; thus, if this intermediate can be stabilised, then the activation energy will be lowered, and the rate of reaction will increase. The process is shown schematically in Figure3, though the substrate must be carefully considered, as its properties or products are required to monitor the rate of reaction. While non-catalysed hydrolysis reactions are strongly dependant on pH, enzymes operate at neutral pH. A secondary, but no less important target of this work is to investigate the role and dependence of pH on the rate of dendrimer-catalysed hydrolysis reactions.

As well as considering the substrate with care, it is important that the specific dendrimer selected for use as an enzyme mimic is also considered. Previously, amine ended dendrimers that could react with an ester to be converted to terminal amides, were used as shown in Figure4. Although this was successful, some of the terminal amines tended to become protonated, making it hard to control or even determine the number of reactive

groups in the solution. Furthermore, the level of protonation differed with pH level, again making it harder to control or determine the number of reactive groups). Consequently, this work proposes the use of neutral OH terminated dendrimers, as these should be less sensitive to protonation and thus allow a simple hydrolysis reaction to be the dominant process.

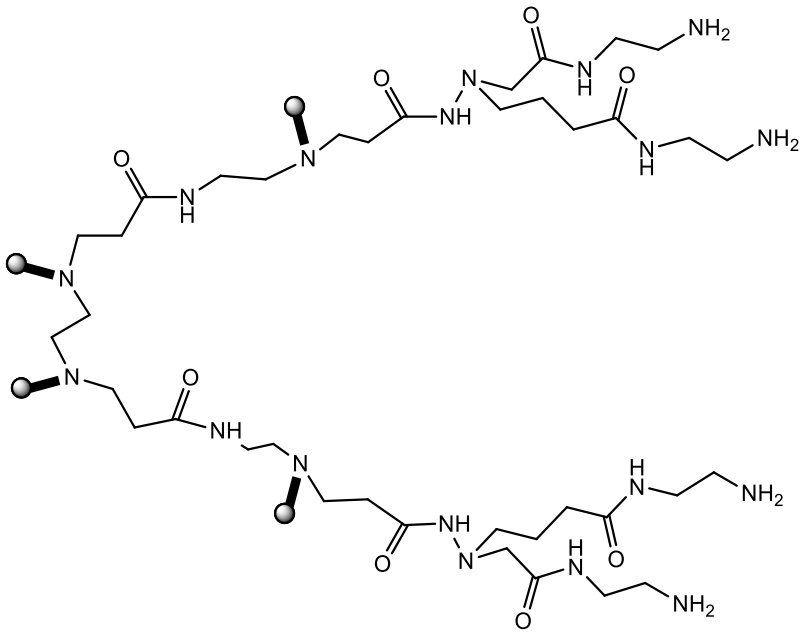

Figure 2.4: Amine dendrimer reacting with an ester to give amide dendrimers and OH ended dendrimers encapsulating the substrate, thus catalysing hydrolysis.

In addition, and in a similar manner to previous studies on dendrimer catalysis, this work also seeks to explore the effect of dendrimer size of catalytic rates. After investigating simple dendrimers and the ability of their pre-existing functional groups to catalyse a hydrolysis reaction, it thus investigates post- synthetically modified PAMAM dendrimers to determine any effect on catalytic ability. To achieve this, modification of the interior of the dendrimer with groups that allow better interaction with the tetrahedral

intermediate/transition state of the hydrolysis reaction will initially be achieved through the post-synthetic metalation of the dendrimer's interior via coordination of the internal amines. The metal should thus bind the carbonyl oxygen of the ester and polarise the bond, increasing the positive character of the carbon and thus enhancing its reactivity towards nucleophiles (including water). This process is a feature of some metallo-enzymes and is similar in mechanism to the use of Lewis acid catalysis. Alternatively, the interior may be modified to include charged regions by means of simple quarterisation reactions. In such cases, the charge generated will interact with the negatively charge oxygen that forms when the carbonyl π bond of an ester is broken during hydrolysis. As with the amide stabilisation discussed above, binding the tetrahedral intermediate will thus result in lower activation energy and a faster reaction. The synthesis of both systems and their interactions with substrates and charged intermediates is shown in

Figure 3.2: Dendrimers' structural features were utilised as a catalyst.

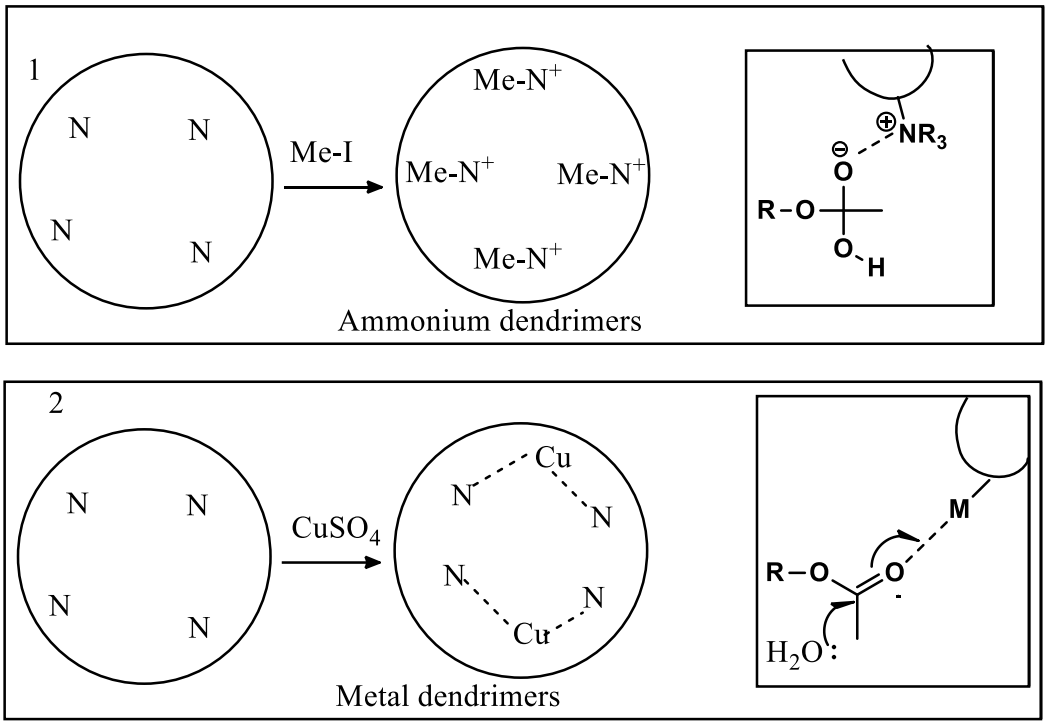


Figure 2.5: Incorporation of specific functionality designed to interact with the charged intermediate from ester hydrolysis. Metals in the dendrimers facilitate the binding of the amine group dendrimer to the substrate.

# CHAPTER 3
# Dendrimers as enzyme catalysts

## 3.0 Introduction

Dendritic polymers have been used extensively as catalysts, based on two main advantages. One of these is that large polymers with a large number of active sites can be constructed, as these catalysts are a hybrid of heterogeneous and homogeneous catalysts and can thus be easily separated through filtration.[37] The second important reason is their ability to encapsulate a single catalytic site whose activities can be enhanced by the dendritic superstructure.

Dendrimers have distinct architectures, with three-dimensional or globular shapes and highly branched structures. These properties allow them to be assembled under precise control and tailored for specific applications. The globular shapes, particularly at higher generations, make them suitable for filtration or precipitation at the end of a reaction, further easing recovery, while the large number of terminal groups at the periphery can be easily tailored to allow dendrimers to be soluble in both organic and aqueous solvents. Dendrimers also have multifunctional surfaces that incorporate a catalytically active site.[38] Metals, for example, can thus be encapsulated and transported into a solvent within the interior of a dendrimer.

The catalytic groups can be characterised by location: at the core of the dendrimer, on the surface of the dendrimer, or encapsulated within the dendrimer.[39]

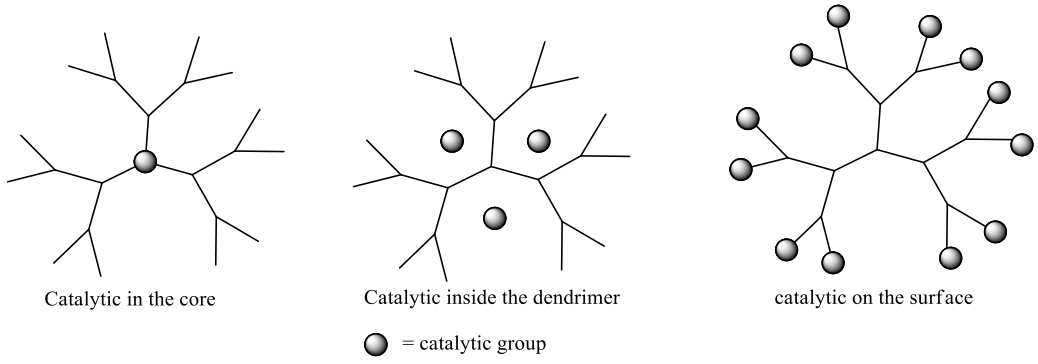


Figure 3.1: Different Positions of Catalytic Groups

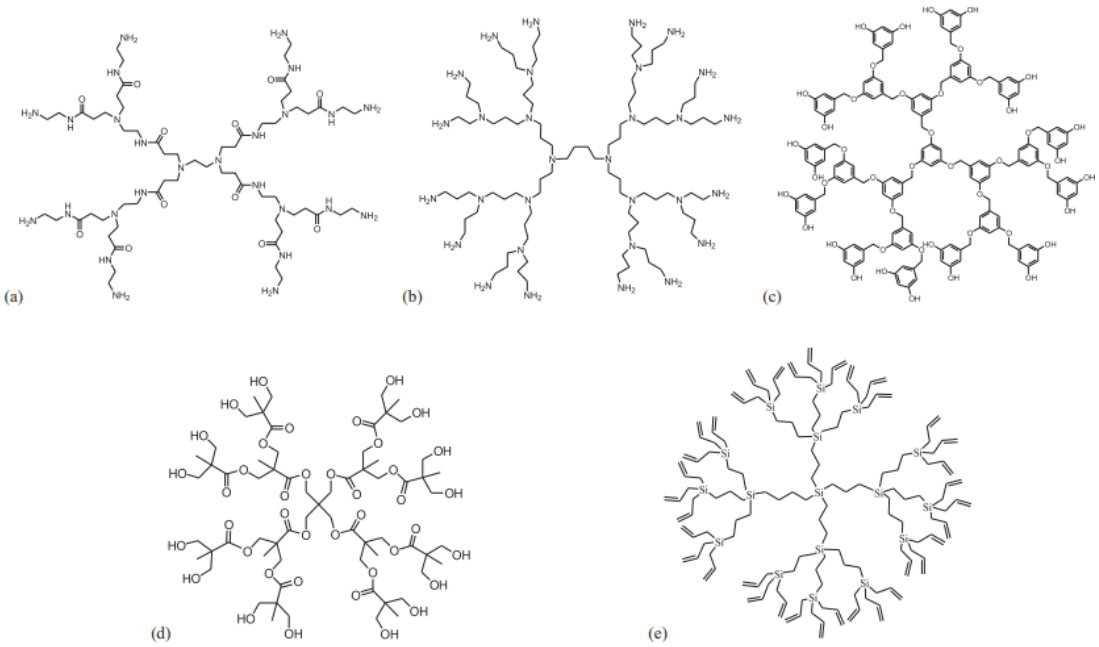


Figure 3.2: Dendrimers' structural features were utilised as a catalyst.

The position of the catalytic groups directly affects the catalyst's ability to function. For instance, the microenvironment will differ more significantly from that of the bulk solution when the catalytic group is positioned at the core as the catalyst loading will be low. This can create an isolated environment, with an exterior and interior distinct from one another, that can be utilised to catalyse an organic reaction using an aqueous solvent at the water-soluble dendrimer's core. Due to the globular structure of the dendrimer, catalytic groups

are easily accessible for reaction in those situations where they are connected on the periphery, especially at higher generations.[40]

These systems all have significant loading capacities, and in the third instance, the dendrimer's internal structure acts as a potent porous stabiliser due to the encapsulation of the catalytic groups inside the dendrimers.[41] These types of catalytic group combine the benefits of precise microenvironmental control and high catalytic group loading around a catalyst-like core case.

### 3.1 Catalytic core group

The steric, photophysical, and electrochemical properties of a dendrimer can be regulated by positioning the catalytic group at its centre, which offers spatial control of functions. The ability to employ a dendrimer's bulk and surroundings to catalyse and regulate a chemical process was initially demonstrated by Fréchet et al.[15], who used the alkoxide-containing poly(aryl ether) dendrimer to initiate anionic ring opening polymerizations (Fig. 1.3). The outcomes of these dendrimer-assisted reactions were notably better than those obtained from reactions using a standard alkali metal alkoxide initiator. Large molecular weight polymers with incredibly narrow polydispersities were generated when dendrimer was used as the initiator, with the low molecular weight polymers with unusually broad molecules offering an effective contrast. Chow et al. similarly investigated the impact of dendrimer size on intermolecular selectivity. Their research compared two equivalent 1 + 1 combinations of dienophiles of various sizes with one equivalent of cyclopentadiene in order to compare the effects of steric demand on product distribution. The smaller dienophile responded faster than the bigger dienophile across all four dendrimers (from

generation 0 to generation 3) studied. This suggests that, during catalysis, the dendrimers can offer some steric selectivity.

Moore and Suslick[21-23] developed ester-linked dendrimers using metalloporphyrin cores as shape-selective catalysts, further exploring the hypothesis that sterics influence selectivity. The manganese-porphyrin dendrimers' potential as shape-specific oxidation catalysts was thus investigated after preparation up to the second generation. The dendrimers' UV-vis absorption spectra resembled those of basic porphyrins, but they were blue shifted, which was believed to be the result of the dendrimer generating a localised region of low polarity surrounding the porphyrin: similar outcomes for zinc dendrimer porphyrins have been reported. An increase in the rate of reaction was thus anticipated when utilising dendrophane, as dendrimers offer a favourable environment with regard to polarity without having any negative impact on binding affinity. The authors hypothesised that this decrease in activity might be caused by the rate-determining nature of a distinct reaction pathway step, however. A dendrimer might shorten the reaction's electron transfer step, which acts as the step that determines the reaction rate. The steric environment and the branches within the dendrimer may then also have a negative impact on other transition states.[24]

### 3.2 Catalysis within the dendrimer’s interior

The inside of a dendrimer can provide a concentrated setting that is ideal for binding and catalysis. It has been demonstrated that water-soluble dendrimers have the ability to dissolve microscopic hydrophobic molecules within them in a manner resembling the activity of a micelle.[25] This strategy contributes to generating a system that concentrates reactive species in a constrained, small-scale microenvironment; thus, as the concentration

rises, so will the reaction rate. Many organic reactions using traditional bases could thus be catalysed in bulk aqueous solutions.

Recently, research has demonstrated that a dendrimer's interior gaps can be exploited to bind and catalyse processes among hydrophobic guests, mimicking the function of the micelle's hydrophobic interior. In this study, the pace of an aminolysis reaction involving 64 terminal amine groups and the PAMAM dendrimer was assessed and compared to the rate attained when 64 equivalents of a less complex monomeric amine, acetyl ethylenediamine, were used

According to research by Crooks et al.[25], PAMAM dendrimers ending with 64 OH groups can be used to enclose anywhere between 12 and 60 positive platinum ions inside of their interiors. By absorbing a specified quantity of Pt (II) into the dendrimer and then reducing the ions with $BH_4$, noble metal nanoparticles can thus be created. These particles were precisely described using UV spectroscopy, as $PtCl_4$ exhibits a peak in its UV spectrum at 216 nm, and a new peak at 250 nm emerges when a dendrimer is added in known quantities.

This peak is proportional to the number of Pt (II) ions in the range of 0 to 60, and its strength increases with the quantity of dendrimer provided. This observation can be used to control loading. An isobestic point, which is a marker of a ligand exchange process, is also seen at 234 nm as more dendrimer is injected, as the dendrimer's tertiary nitrogens take the place of the chloride ligands. Control tests also show that the Pt (II) ions are complexed within the dendrimer rather than coordinated to the peripheral OH groups.

However, when dendrimer-modified silver electrodes (Pt 60) were utilised, a significantly larger catalytic effect was seen, and the peak potential moved to a positive value of 75 mV, indicating a sizable catalytic effect.[27] These findings are significant, as they indicate that the dendrimer's surface may exchange electrons with the surrounding electrode surface, making it accessible to reactants. Crooks et al. also created other dendrimer nanoparticles employing a range of metals, including as Cu, Pd, Ru, and Ni.

Such metal-dendrimer complexes have the same spectroscopic characteristics as the Pt-dendrimer complexes mentioned previously, and the fourth generation palladium-based dendrimers, which display outstanding potential as homogenous and size-selective hydrogenation catalysts, are among the most intriguing. N-isopropylacrylamide and allyl alcohol were both reduced using the G4-Pd and the bigger G8-Pd complexes (Figure3) as catalysts.

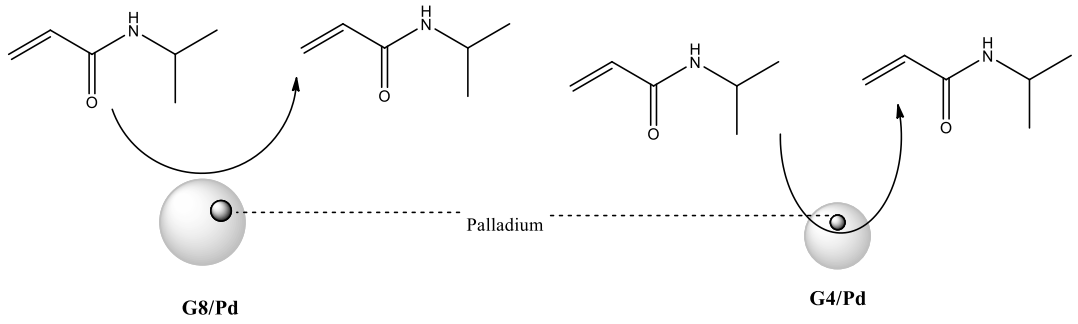


Figure 3.3: Size selective dendrimers. No reaction occurs because the huge acrylamide is too large to enter the dense surface of the G8 dendrimer, which is both enormous and contains palladium (left). The image was taken with permission from A. Carlmark, C. Hawker, A. Hult and M. Malkoch, Chem. Soc. Rev., 2009, 38, 352–362.

The bulky acrylamide group can reach the catalytic palladium units inside the smaller G4 dendrimer (right), where there is less congestion, so that reduction can occur. Both of these reactions are effectively catalysed by the G4-Pd complex, with turnover numbers of 372 and 218 for the reduction of acrylamide and allyl alcohol, respectively. These figures are comparable to those attained with Ru catalysts coupled to polymers, while a turnover number of 17 is obtained for the reduction of acrylamide when the bigger G8 dendrimer is utilised, and a turnover number of 134 is obtained for the reduction of alcohol in similar circumstances. The efficiency of the acrylamide process is drastically reduced, by up to 95 %, as compared to the values produced using the smaller G4 dendrimer; however, the efficiency of the allyl alcohol reduction is only reduced by 32 %.

The size of the substrate (N-isopropylacrylamide or allyl alcohol) and the steric crowding on the dendrimer's surface are the most likely causes of this discrepancy. Before any reactions may occur, the substrate must pierce the dendrimer's outer shell, due to the fact that the catalyst is buried inside the dendrimer.[36] This offers an excellent illustration of how the design of a dendrimer can be effectively employed to regulate size and shape selective reactions, while such selectivity is not feasible using catalysts attached to polymers.

### 3.3 Results and Discussion

As previously mentioned, in order to study and stabilise any intermediates and rate changes. PAMAM dendrimers were chosen. The purpose of the preliminary phase of this process was thus to determine whether neutral PAMAM dendrimers can be utilised for reactions with the substrate during hydrolysis reaction.

### 3.3.1 Synthesis of PAMAM Dendrimers

To allow the use of minimal generations, Tomalia et al.[6] introduced the divergent technique in 1985. The divergent method is still frequently chosen because it uses an easy-to-understand technique that is frequently easier than the convergent method. The Michael addition to attach ester groups (half generations) and the amidation step to add terminal amines are the two repeated synthetic stages that make up the general synthesis of PAMAM dendrimers (full generations). Large G4.5 dendrimers **9** with methyl end groups are produced through a series of processes that start with the fundamental compound ethylene diamine1. This makes it possible to accomplish the main goal since PAMAM dendrimers have polar terminals that make it possible for them to be water soluble. Additionally, the dendrimer's inside has a proper hydrophobic environment and other

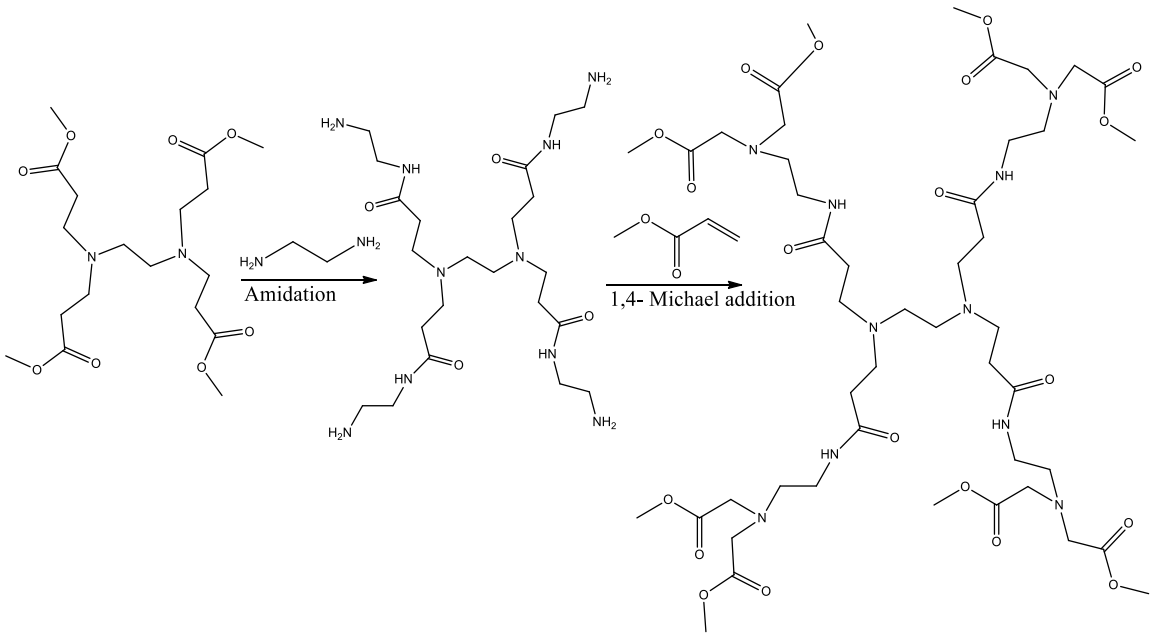


**Scheme 3.1:** Half and full generation of PAMAMs.

Alpha-beta unsaturated carbonyl compounds are used in a 1,4-Michael addition (conjugate addition) as the first step of the half generation in Scheme 3.2. These unsaturated carbonyl compounds include a double bond coupled to a carbonyl group, where α-carbon denotes the carbon atom after the carbonyl and β-carbon denotes the subsequent carbon atom. Typically, the unsaturated carbonyl's ability to pull electrons causes the α-carbon to have a positive delta charge, which resonance stabilises. The β-carbon then turns electropositive, making it vulnerable to a nucleophilic attack at this location. Methyl acrylate is the α-β unsaturated carbonyl system in this reaction, and ethylenediamine (EDA) is the nucleophile.

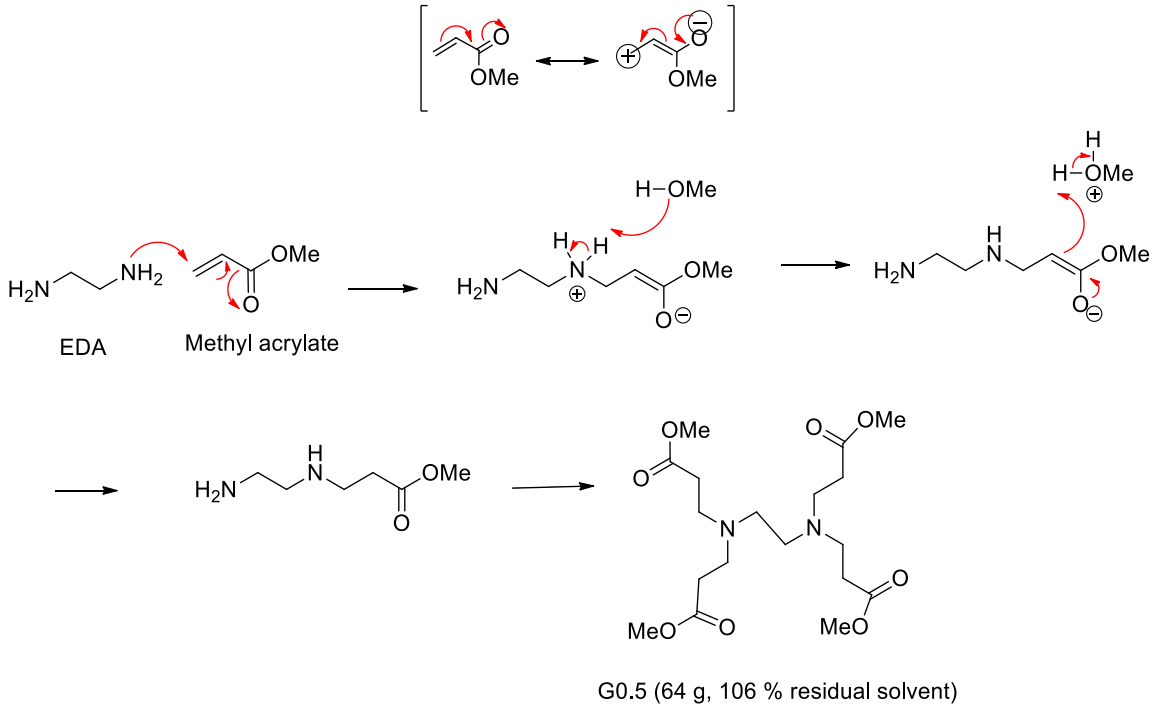


**Scheme 3.2:** The mechanism of 1, 4- Michael Addition

EDA and methyl acrylate were combined with methanol to create PAMAM G0.5 **1**. Methyl acrylate was used in slight excess, to prevent an imperfect Michael addition. A 1,4-conjugate addition process was used by the nucleophilic amine of EDA to attack the

electrophilic terminal -carbon in the methyl acrylate. Figure 3.4 illustrates how $^{1}H$ NMR analysis was later used to confirm that the reaction had been completed. The singlet at 2.57 ppm (a) was integrated as 4H and assigned to the core EDA, and the peak at 3.68 ppm was designated as the terminal methoxy group. While the $^{13}C$ NMR and FTIR spectra showed ester C=O at 177 ppm and 1,735 $cm^{-1}$ for the excess methyl acrylate, respectively, there was no peak 5-6 ppm for vinyl protons, indicating that it had been totally eliminated.

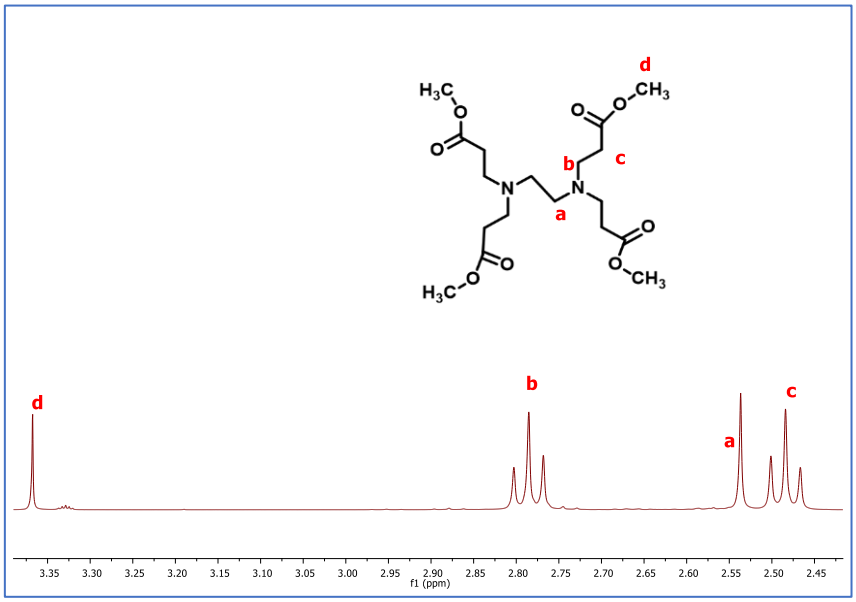


**Figure 3.4**: $^{1}$ H NMR spectrum of half generation (G0.5 **1)** dendrimer

The amidation reaction needed to create a full generation dendrimer is depicted in Scheme 2.4. A charged tetrahedral intermediate is created in this stage as a result of the EDA's nucleophilic lone pair on its nitrogen attacking the electrophilic carbonyl of the ester (C=O). Before the methoxy group departs, the amine from the same EDA group deprotonates the nitrogen using a helpful 5-membered cyclic TS. A whole generation dendrimer is produced by solvent-mediated deprotonation of the terminal ammonium ion. The G1.0 dendrimer (**2**)

is then created by mixing G0.5 (**1**) with too much EDA in methanol. A 9:1 azeotropic combination of toluene and methanol is then used to eliminate the extra EDA.

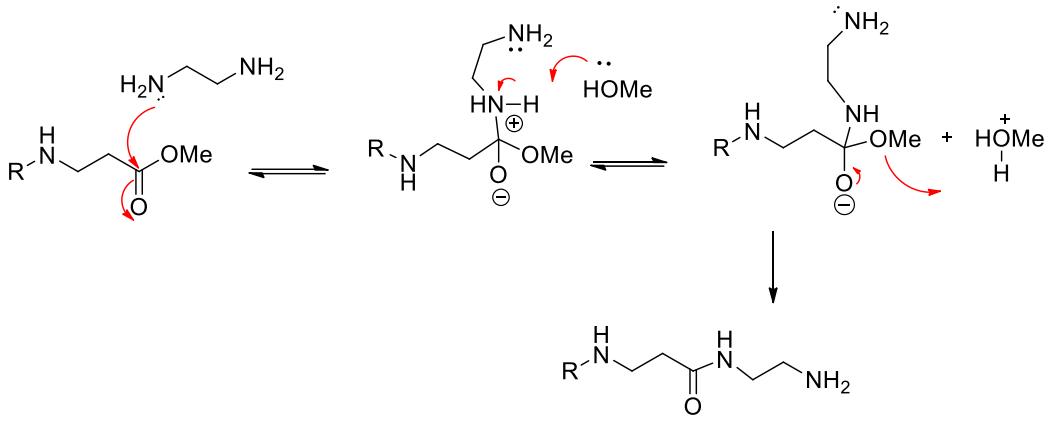


**Scheme 3.3**: Mechanism of Amidation Reaction

The $^{1}$H NMR spectroscopy, which revealed a disappearance of the carbonyl peak at 3.67 ppm, validated the purified G1.0 (**2**) dendrimer. In addition, the esters in the starting material's FTIR peak at 1,736 $cm^{-1}$ were no longer discernible. It was discovered that G1.0 (**2**) had a molecular ion at 517 ($MH^{+}$) when smaller generation dendrimers with molecular ions under 1,000 were examined using electrospray ionisation mass spectrometry (ES-MS). Following a second round of characterising dendrimers up to G4.5 (**9**), it was discovered that matrix-assisted laser desorption ionisation (MALDI) was the best ionisation technique for mass spectral analysis. Table 3.1 summarises the characteristics of half and full generation PAMAM dendrimers.

| Dendrimer Generation | Molecular Formula | Molecular weight (g/mol) | Terminal groups | Ester methyl NMR peak (∂ ppm, integration) | Mass ion ($MH^+$) obtained |
|---|---|---|---|---|---|
| G0.5 1 | $C_{18}H_{32}N_2O_8$ | 406 | $CO_2Me$ (4) | 3.68, 12H | 405 |
| G1.0 2 | $C_{22}H_{48}N_{10}O_4$ | 516 | $NH_2$ (4) | - | 517 |
| G1.5 3 | $C_{54}H_{96}N_{10}O_{20}$ | 1205 | $CO_2Me$ (8) | 3.69, 24H | 1206 |
| G2.0 4 | $C_{62}H_{128}N_{26}O_{12}$ | 1429 | $NH_2$ (8) | - | 1430 |
| G2.5 5 | $C_{126}H_{224}N_{26}O_{44}$ | 2807 | $CO_2Me$ (16) | 3.69, 48H | 2806 |
| G3.0 6 | $C_{142}H_{288}N_{58}O_{28}$ | 3256 | $NH_2$ (16) | - | 3257 |
| G3.5 7 | $C_{270}H_{480}N_{58}O_{92}$ | 6014 | $CO_2Me$ (32) | 3.69 ,96H | 6014 |
| G4.0 8 | $C_{302}H_{608}N_{122}O_{60}$ | 6913 | $NH_2$ (32) | | 6913 |
| G4.5 9 | $C_{558}H_{992}N_{122}O_{188}$ | 12411 | $CO_2Me$ (64) | 3.69,192 H | 12410 |

**Table 3.1**: Analysis of dendrimers (**1-9**).

## 3.4 Synthesis of neutral dendrimers for catalysts

To achieve the aim of this study, the next step was to synthesise a neutral PAMAM dendrimer. Newkome et al.[20] developed a method to convert a PAMAM dendrimer's ester or half generation end groups into hydroxyl end groups using ethanolamine via nucleophilic substitution. As ethanolamine is insufficiently reactive, the conditions used were different to those used in EDA substitution; nevertheless, the mechanism was similar, as shown in **Scheme 3..3**, utilising potassium carbonate as a base and DMSO as a solvent.

To synthesis neutral PAMAMs, ester-terminated PAMAM (G- 0.5, 1.5, and 2.5) was dissolved in a minimal amount of DMSO, and potassium carbonate and ethanolamine were then added. The reaction mixture was left to the stirrer at 50 °C for 3 days under nitrogen before the solution was filtered to remove any solid residues and the solvent was removed

at reduced pressure. To achieve purification, the crude products (dense oils) were dissolved in a minimum amount of water and acetone was added to facilitate the precipitation process. This process was repeated three times to ensure good purity of the final products, which were put in a vacuum oven overnight to dry and then collected as pale yellow viscous oils that offered the neutral PAMAMs G0.5, G1.5, and G2.5 at 55 %, 50 %, and 48 % yields respectively.

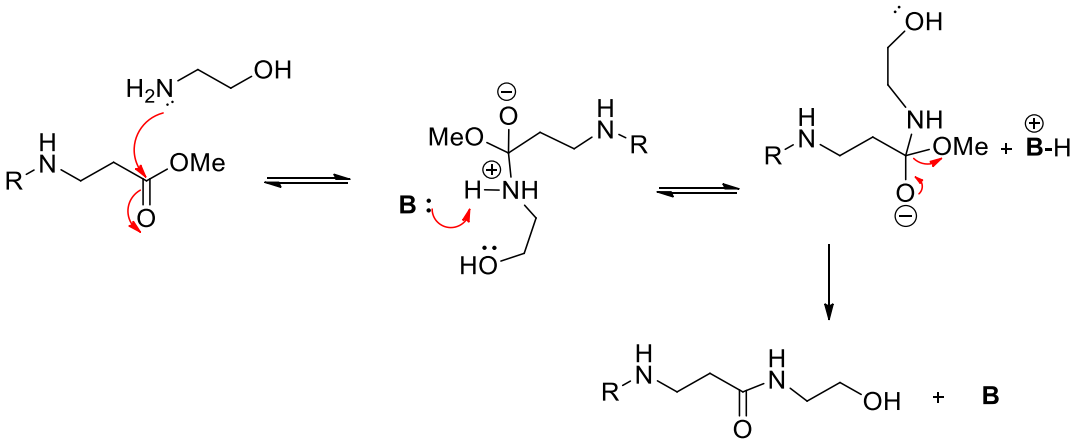


**Scheme 3.5**: Mechanism of ethanolamine groups reaction with potassium carbonate (**B**) to form neutral PAMAMs.

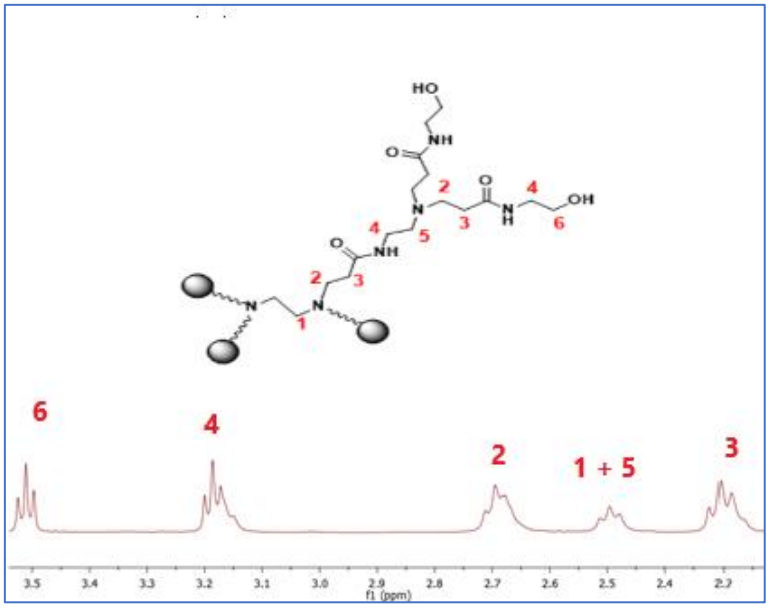


**Figure 3.5**: $^{1}$H NMR spectrum of purified G1.5-OH **13** (only one arm of the dendrimer is illustrated)

Figure depicts the $^{1}H$ NMR of the G1.5-OH **13**. New peaks for the methylene protons (near the terminal hydroxyl groups) are discernible as a triplet at 3.58 ppm, replacing the ester methyl peak at 3.69 ppm. Due to their proximity to the electronegative oxygen, these protons exhibit a little larger chemical shift than other methylene groups. The ester C=O did not exhibit any discernible peaks at 175 ppm or 1,735 $cm^{-1}$ for the $^{13}C$ NMR or FTIR, respectively, indicating that the reaction was successful. The spectra also showed peaks at 57.0, 48.7, 47.5, 38.4, and 32.9 ppm, which are associated with the C-NH, $CH_2$-N, and $CH_2$ core carbons.

A molecular ion at 1,438 on the MALDI spectrum was identified as an $MH^+$ ion. Neutral dendrimers up to G 2.5 with 16 OH **14** were synthesised using the same method and characterization approach. The compiled information for all synthesised neutral PAMAMs is displayed in Table 3.3.

| Dendrimer Generation | Chemical Formula | Expected Molecular weight (g/mol) | Number Of OH surface groups | Obtained Mass ion ($MH^+$) |
|---|---|---|---|---|
| G0.5-OH 12 | $C_{22}H_{44}N_6O_8$ | 520 | 4 | 521 |
| G1.5-OH 13 | $C_{62}H_{120}N_{18}O_{20}$ | 1438 | 8 | 1438 |
| G2.5-OH 14 | $C_{142}H_{272}N_{42}O_{44}$ | 3272 | 16 | 3272 |

Table 3.3. Analysis of synthesised neutral PAMAM-OHs (**12-14**)

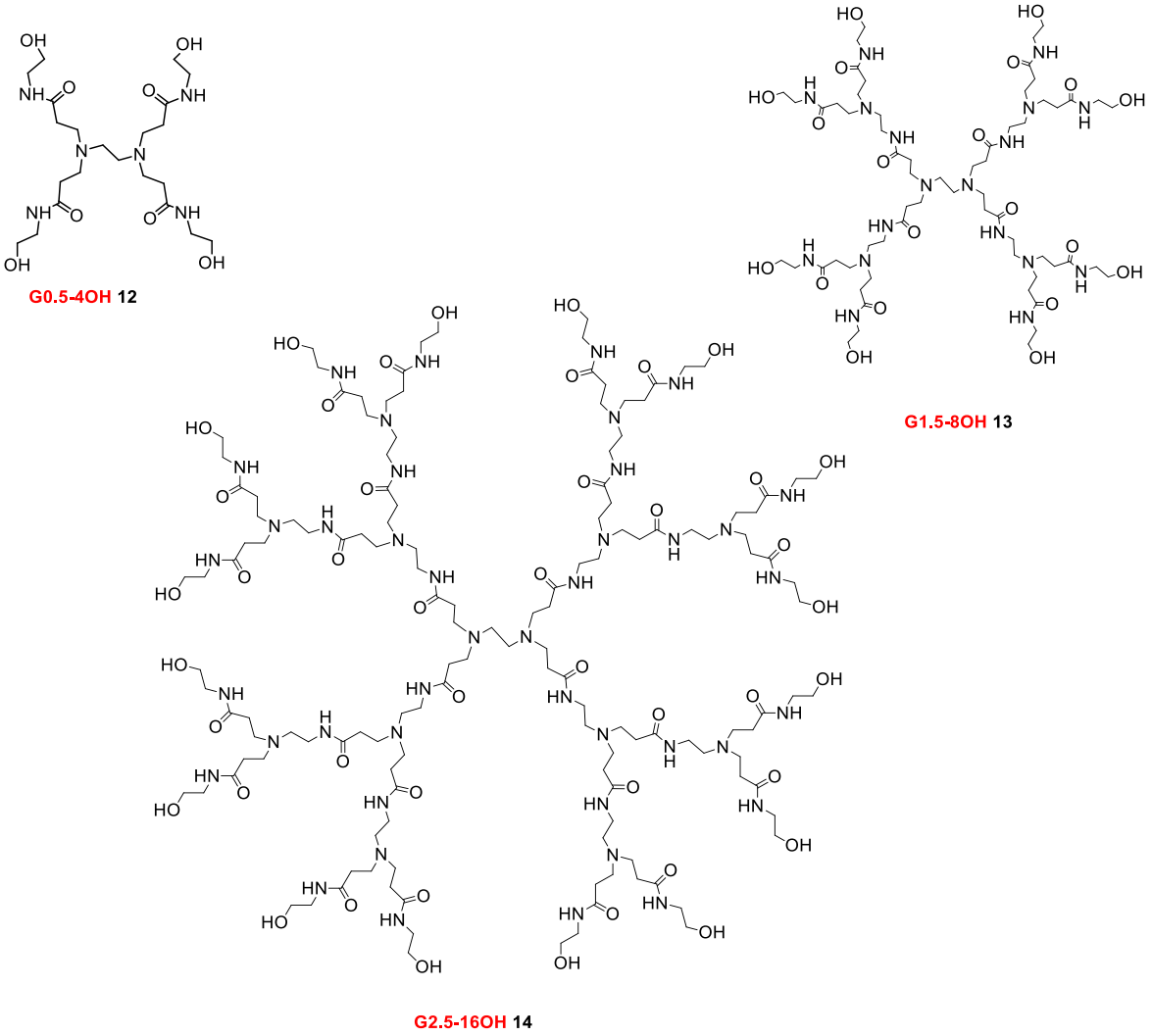


Figure 3.6: Neutral terminated PAMAM-OHs (**12-14**) as prepared

## 3.5 Effect of pH

Enzymes are proteins produced by living organisms to act as catalysts for specific biochemical reactions. Enzymes are thus denatured at extremes of temperature, in organic solvents, and at extreme pH levels, which interfere with the intramolecular forces holding the protein's tertiary structure together and change the enzyme's shape to the point where it is rendered less or even ineffective. Synthetic mimics of enzymes could thus play an important role in catalysis under such conditions, as they are not as sensitive to the reaction conditions described above. To monitor the activity and optimum pH of a copper-dendrimer, catalysis reactions were thus carried out at various pH levels using the methods previously described for non-functionalised dendrimers.

The optimum pH was hypothesised to be between pH 7.0 and 8.5. In an acidic medium, the by-product of hydrolysis is p-nitrophenolate, which is colourless, which prevents the monitoring of any hydrolysis reaction in acidic conditions. However, under basic hydrolysis conditions, the phenolate (PNP **15**) is produced and the rate of reaction can thus be determined by monitoring the formation and intensity of the resulting yellow colour over time.

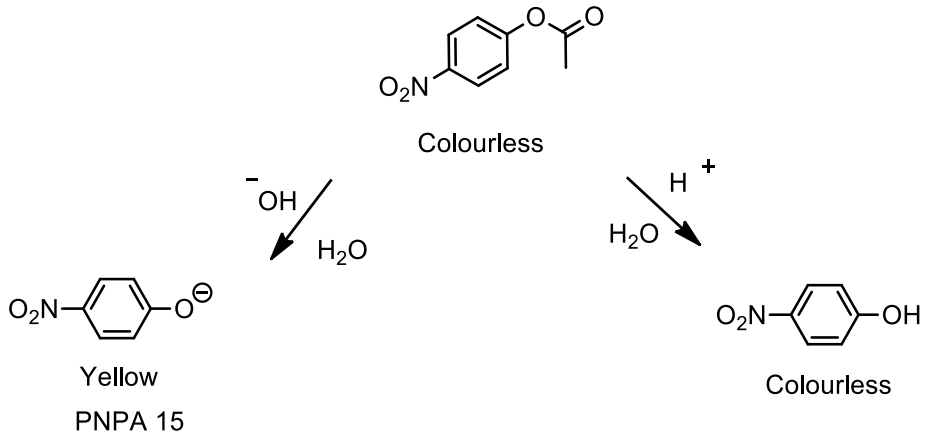


Scheme 3.6**:** Hydrolysis of p-nitrophenol acetate under basic and acid conditions.

## 3.6 Dendrimer catalysis of ester cleavage

The initial experiment was intended to study the effect of the environment in the dendrimer on the rates of ester cleavage reactions at different pH levels. The efficacy of dendrimer catalysis can be improved by the introduction of functional molecules to the inside of the dendrimer, including metals and charged groups.[35-40] As noted earlier, in order to study the PAMAM dendrimer, synthetic enzymes were used to stabilise the intermediary of the reaction.

The first experiment involved the control reaction using PNPA **15** as the ester substrate. PNPA **15** produces an aromatic species of p-nitrophenolate that is characterised by a yellow hue, which can thus be employed to identify the progress of hydrolysis with respect to time. It is thus possible to determine the initial rates using the linear region of the plots of concentration against time for the p-nitrophenolate.

An initial experiment was performed to determine the appropriate concentration of p-nitrophenyl acetate (PNPA **15**) required to obtain good measurable data. This permitted assessment of whether or not the neutral dendrimer could hydrolyse the substrate to a measurable degree.

For the initial experiment, a solution of TRIS buffer (0.1 M) was prepared, and further buffer was used as a diluent to reach pH 7.0. For the control reaction. 1.2 mL of PNPA **15** at a concentration of $3.13 \times 10^{-6}$ M was put into a cuvette and the absorbance measured. In every experiment, the hydrolysis product's concentration was plotted versus time, as shown in **Figure3.7**. GraphPad was then used to identify the initial rate, and the data fitted to a linear regression. The data was further confirmed by calculations within Excel based

on the graph obtained. The results showed that, as expected, hydrolysis was extremely slow. The next step was then to repeat the reaction using the dendrimers and to determine if significant hydrolysis could be detected at a neutral pH.

As in the study of control reactions, PAMAM dendrimers (G0.5-OH **12**, G1.5-OH **13** and G2.5-OH **14** ) were used in the experiments. A total of 1.5 mL of (1 x $10^{-6}$ M) of each dendrimer in TRIS buffer (0.1 M) was put into the relevant cuvette and 100 µL of PNPA **15** (7.5 × $10^{-6}$ M) was added for each dendrimer; the procedure used in TRIS buffer control reaction was then applied.

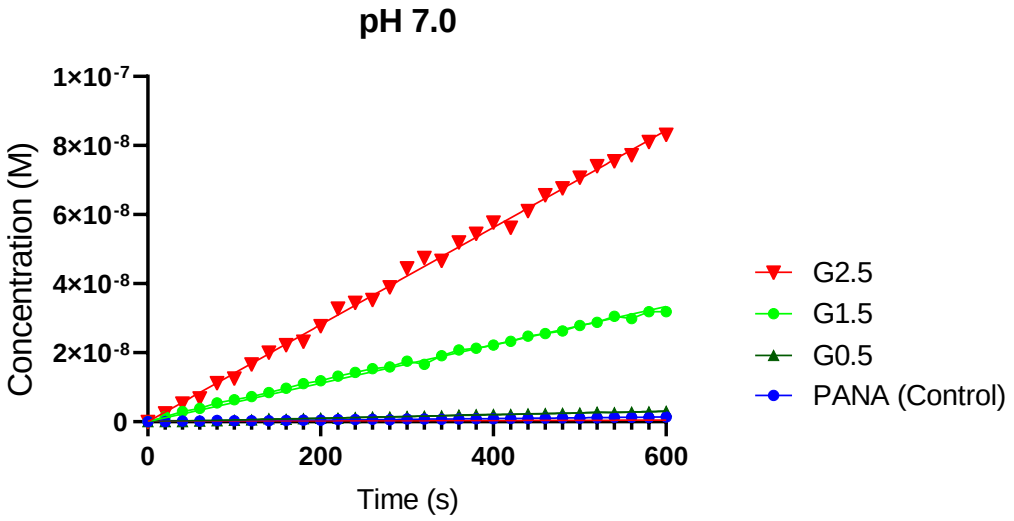


**Figure 3.7:** Rate plots employed to identify initial rates and to show the effect of the neutral dendrimer (G 0.5, G 1.5, and G2.5) in the hydrolysis of PNP at pH 7.0.

From the graphs, it can be seen that the dendrimers had an effect on the rates at pH 7.0, with these rates being higher for the larger dendrimers. The initial rates calculated for all dendrimers at pH 7.00 are shown in Table 3.4.

| pH / Initial Rate ($nMs^{-1}$) | PANA (Control) | G0.5 | G1.5 | G2.5 |
|---|---|---|---|---|
| 7.00 | 0.002 (± 0.0004) | 0.005 (± 0.0001) | 0.056 (± 0.003) | 0.141 (± 0.0002) |

**Table 2.4**: Initial rates identified with different generations of dendrimers, based on data from Figure 1.1

When compared to the G2.5 OH **14,** the initial rates were lower for the G0.5-OH **12** and G1.5-OH **13**, as expected (0.005 and 0.056 $nMs^{-1}$ respectively), due to the non-globular structure of the smaller, lower generation dendrimers and their reduced generation effects. This dendrimer was considered to have a relatively ordered structure that can bind and hold the PNPA substrate **15** in such a way that the dendrimer functionality is close enough to increase the rate of reaction through the terminal or internal functionality (and lowering TS energies).

These results are particularly interesting, as the rate for ester hydrolysis is usually very low at neutral pH, as demonstrated by the control reaction. As previously discussed, ester hydrolysis is very slow due to the poor nucleophilicity of water {or alcohols} and the poor electrophilicity of the ester carbonyl( due to the electron donation from the neighbouring oxygen). The poor reactivity is overcome by increasing the reactivity of the nucleophile or electrophile using base or acid (modifying the pH). The significant increase in rate (at pH7.0) is therefore due to the dendrimers ability to stabilise the TS.

To examine the effect of base concentration on these reactions, the experiments for both the dendrimers and control were repeated at pH 7.5, 8.0, and 8.5. The graph for these reactions at pH 8.0 is represented in Figure 8. As previously, all the findings at different pH levels indicated

that, when the pH increases, the rate of reaction increases both for the control and for all dendrimers studied. In addition, these rates were higher for higher generation dendrimers.

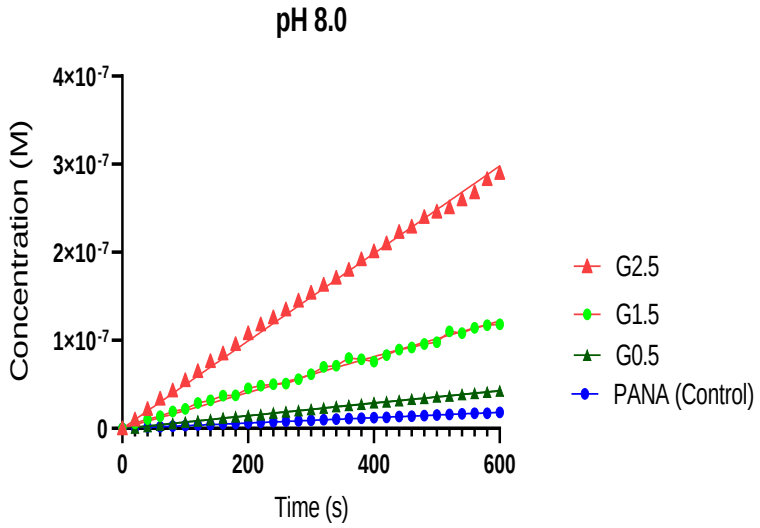


**Figure 8:** Rate plots employed to identify initial rates to show the effect of neutral dendrimers (G 0.5, G 1.5 and G2.5) on the hydrolysis of PNP at pH 8.0

The data was then converted to relative rates {setting lowest rate for each control/ dendrimer at each pH to 1} and plotted graphically, Figure3.9. here we cab clearly seen the significant reduction in the contribution by pH/base. This confirmed that most of the reactions involve the terminal OH group. The hydrolysis reaction still occurs, but is less dominant as the size of the dendrimer increases.

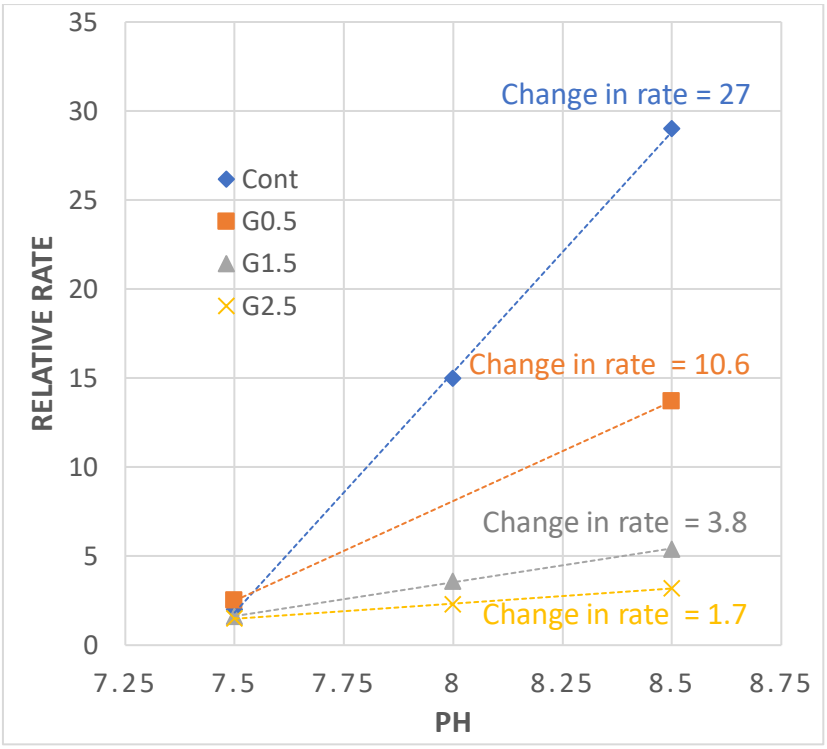


Figure 3.9: Relative rate with pH for different generation of dendrimers

These changes with respect to pH all occurred despite the fact that the dendrimers sped up the reactions (compared to the control reaction). The dendrimer reactions must thus be assumed to be less sensitive to pH than the control reaction (base catalysed hydrolysis), which suggests that the dendrimer reactions cleave the ester in a different way and/or stabilise any intermediaries to a greater extent than the base catalysis process. Thus, dendrimer reactions are not dominated by the simple hydrolysis mechanism, but instead may involve reactions with part of the dendrimer. The obvious candidates for this are the terminal OH groups reacting with the ester substrates in an alcoholysis reaction, via a mechanism as shown in Figure that includes a possible transition state where the intermediate product is stabilised by an internal amide. This is also seen in amine terminated dendrimers. [34]

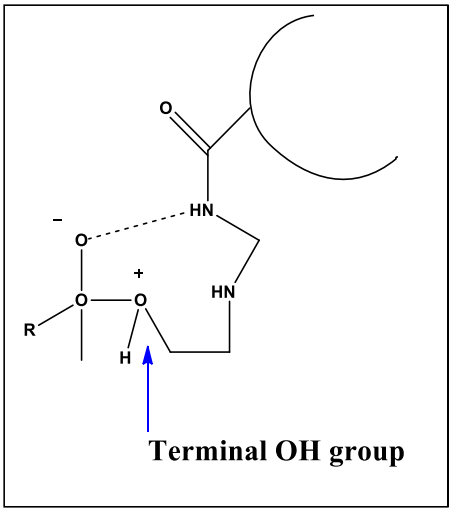


Figure 3.10: proposed reaction of substrate with the terminal OH group and stabilisation of the Td intermediate by the internal amides

### 3.7 Catalysis Reaction of G2.5-OH as Monitored by GC

As previously stated, in order to achieve the study goals, the interior of the dendrimer was changed to include groups that interact more favourably with the tetrahedral intermediate/transition state formed during the hydrolysis reaction. However, if the terminal OH groups are also involved, or are reacting exclusively with the substrate, then an alternative product could form, this is shown in Scheme .

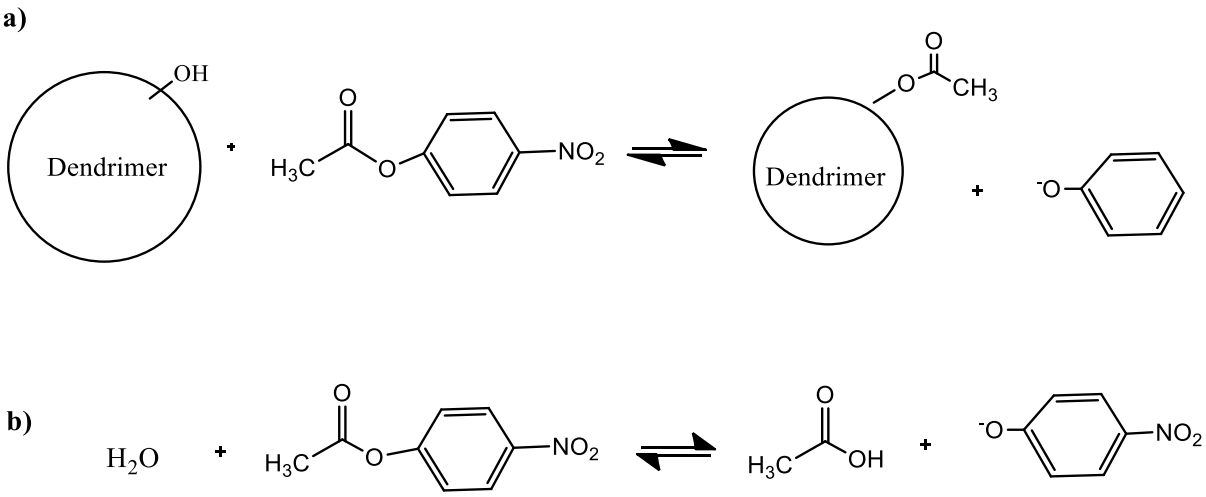


Scheme 3.7: Two possible reaction pathways. (a) Substrate reaction with the terminal groups on the dendrimer, to give a functionalised dendrimer. (b) Simple hydrolysis to give acetic acid as the product.

Therefore we needed to establish which reaction, (a) and (b) from Scheme  was taking place The first step was to obtain GC chromatograms of the various components as reference samples. Figure11 shows the traces for these reference sample using  dendrimer and acetic acid. Catalysis reaction using the same dendrimer and PNPA concentrations was then carried out as previously described. The reaction mixture was stirred consistently at room temperature and samples were taken regularly for analysis using GC. If water catalysed this reaction, then acetic acid would be generated as the by product: however, analysing the traces from the reaction only showed peaks for dendrimer. As such, we can conclude that the catalytic reaction takes place between the terminal dendrimer OH groups and the PNPA.

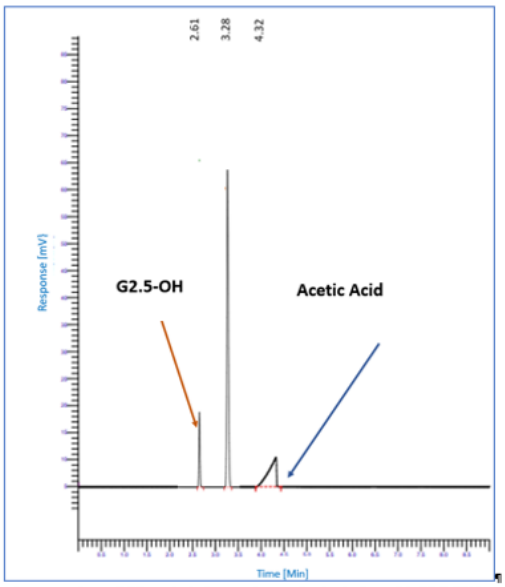


Figure 3.11: Comparison of GC analysis for acetic standard solution with G2.5-OH and acetic solution

Overall, the data suggests that the dendrimer is less pH dependent in terms of reduction, which means that the hydroxyl of the dendrimer is more effective than the OH of any alkaline solution. It also indicates that reactions take place with the OH dendrimer rather than the OH solution,

suggesting that the dendrimer reaction is not dominated by hydrolysis, and the terminal OH group can react with the substrate.

# CHAPTER 4
# Metalation of the dendrimer interior as an enzyme catalyst

## 4.0 Introduction and Aims

The development of metal nanoparticle manufacturing through nanotechnology has opened up new possibilities for a potential revolution in the catalysis industry. Dendrimers are particularly appealing hosts for catalytically active metal nanoparticles, and there are two ways to create nanoparticles using a dendrimer template: encasing the particles inside the dendrimer's internal cavity or creating particles encircled by dendrimer branches. The stronger basic nature is pKa = 9.23 of the surface primary amine as compared to pKa = 6.30 of the interior tertiary amine 13, which may cause the establishment of nanoparticles enveloped by a formation of complexes of metal ions with dendrimeric surface amine groups in the case of amine terminated poly(amidoamine) (PAMAM). [36]

Dendrimers with non-complexing functional groups, such as hydroxyl groups[37] and quaternised amine groups[38] or those created by changing the pH of the solution to specifically protonate the peripheral amine[39] are commonly preferred for creating dendrimer encapsulated nanoparticles (DENs). The method of producing DENs using dendrimer templates offers at least five key benefits: (1) Dendrimer templates produce well-defined nanoparticle copies and have a reasonably homogeneous composition and structure;[39] (2) nanoparticles are stabilised by encapsulation within dendrimers so that they do not aggregate during catalytic reactions; (3) a significant portion of the surface is left unpassivated and thus accessible to participation in catalytic reactions; (4) the branches of dendrimers can be utilised as specific pathways to regulate the access of molecules (substrates) to the encapsulated (catalytic) nanoparticles; and, finally, (5) the dendrimer perimeter can be modified to control the hybrid nanocomposite's solubility and thus employed as a handle to make connecting to surfaces and other polymers easier.[40]

It has been proposed that combining two different metals, such as Au and Pd, in a single nanoparticle could result in the creation of a catalyst, utilising poly(N-vinyl-2-pyrrolidone), or PVP. This idea was demonstrated by stabilising 1-3 nm bimetallic Pd-Au nanoparticles, which demonstrated improved catalytic activity when utilised for the selective partial hydrogenation of 1,3-cyclooctadiene as compared to monometallic mixes of Pd and Au.[41-45] The Pd atoms were found predominantly on the surface of the particles according to an extended X-ray absorption fine structure (EXAFS) spectroscopic examination.[46-49] However, attempts to create core and shell structures by reducing Au and Pd salts successively resulted in dispersions that mixed monometallic Au and Pd nanoparticles,[50] though several metal nanoparticles were successfully synthesised in response to the possibility of dendrimers serving as templates for the production of inorganic nanoparticles to produce catalysts with increased catalytic activity and to develop new catalyst types beyond those available to monometallic catalysts.

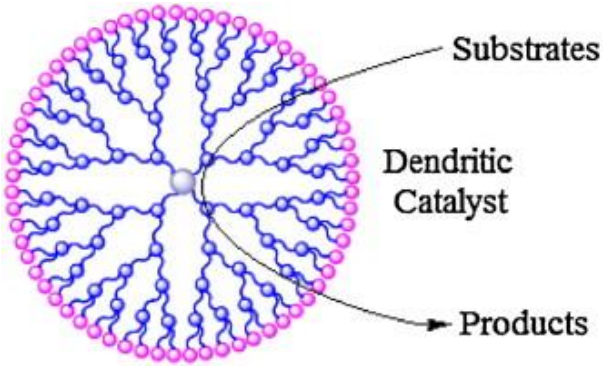


Figure 4.1: Monometallic catalysts

## 4.1 Initial assessment of copper binding to PAMAM dendrimers

The same PAMAM dendrimers were used for this study as in the previous experiment, as they contain multi-functional groups that can bind metals within their inner and outer layers. As previously mentioned, the optimum G2.5 generation of PAMAMs can host various molecules and ions, but for this study, $Cu^{2+}$ ions were investigated because their PAMAM complexes

have well defined topographies and properties that allow for easy binding and analysis via UV-VIS. [21]

The first experiment of this type was designed to establish that $Cu^{+}$ could be inserted and bound, a process achieved by mixing solutions of copper sulphate and dendrimer. This was carried out to achieve a final concentration of 9.8 x $10^{-4}$ M $CuSO_4$ and 1.96 x $10^{-4}$ M solutions of the different generations of PAMAM (from G0.5-OH **12** to G2.5-OH **14**). The solutions were made up in 0.1 M TRIS buffer at pH 7.5. UV/Vis spectroscopy was then used to confirm the coupling of the dendrimers with copper and the spectra obtained were compared to that derived from just copper sulphate and to one from just the dendrimer in buffer.

The $Cu^{2+}$ solution formed in buffer without dendrimer, giving the complex $[Cu\ (H_2O)_6]^{2+}$. Figure 1.26 shows the UV spectra for different concentrations of $CuSO_4$, highlighting that this complex produces a broad absorption band centred around 695 nm, attributable to the d-d transition of $Cu^{2+}$ in the ligand field. Figure 4.29 depicts the absorption spectrum of G1.5-OH **13**, $CuSO_4$, and the mixture of both at a ratio of 1:1. The spectrum of the pure G1.5-OH indicates no absorption response.

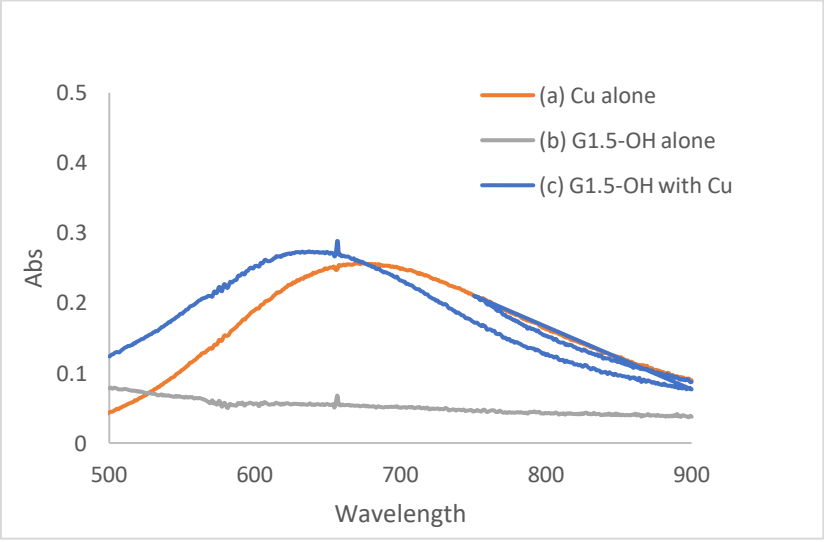


Figure 4.29: Absorption Spectra of (a) $CuSO_4$ (b) G1.5-OH and (c) Mixture of $CuSO_4$G1.5-OH and in the ratio 1:1. All spectra recorded in a 0.1 M TRIS buffer at pH 7.5.

When copper ions were added to G1.5-OH **13**, the $\lambda_{max}$ for the copper shifted to a position around 640 nm, as compared to the $\lambda_{max}$ of 695 for the copper ions alone. This significant change was due to coordination binding between the $Cu^{2+}$ ions and G1.5-OH complexation.

Although this confirmed that the copper formed a complex with the dendrimer, it remained unclear as to whether the complex was formed between the tertiary amines (internal) or the external hydroxyl groups. To investigate this, two further simple experiments were carried out. Initially, a solution of $CuSO_4$ ($9.8 \times 10^{-4}$ M), was mixed with a solution containing nitrogen (EDA -$1.96 \times 10^{-4}$ M) at pH 7.5, and a UV spectrum for this was recorded. The experiment was then repeated using methanol instead of EDA. The spectra for both are shown in Figure4.3**.**

The spectrum displayed a broad absorption band centered at 580 nm for the EDA and $Cu^{2+}$ complex, similar to the one observed for the Cu and dendrimer complex. When, the experiment was repeated using methanol, no significant difference was observed from that recorded for the Cu solution (no dendrimer or ligand). Overall, these simple experiments thus confirmed that the complex was formed between the copper and internal tertiary nitrogens. A representative structure is shown in Figure4.4. Crooks et al.[20] previously demonstrated that the complexation occurring between the nitrogens in the dendrimer and the copper ions was significantly strong because of the d-d transition band, while the ligand-to-metal charge-transfer (LMCT) transition does not decrease remarkably, even during dissolution with water.

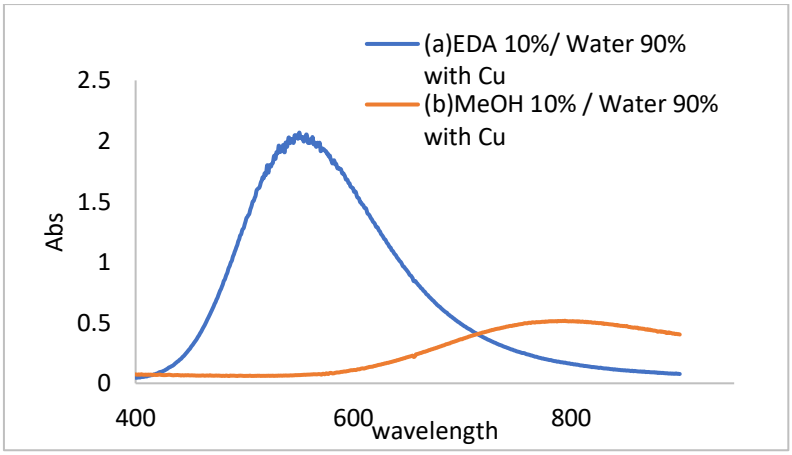


Figure 4.3: Absorbance Spectrum of (a) [10% EDA and 90% Water] with $CuSO_4$ and (b) [10% MeOH and 90% Water] with $CuSO_4$; in a 0.1 M TRIS buffer at pH 7.5

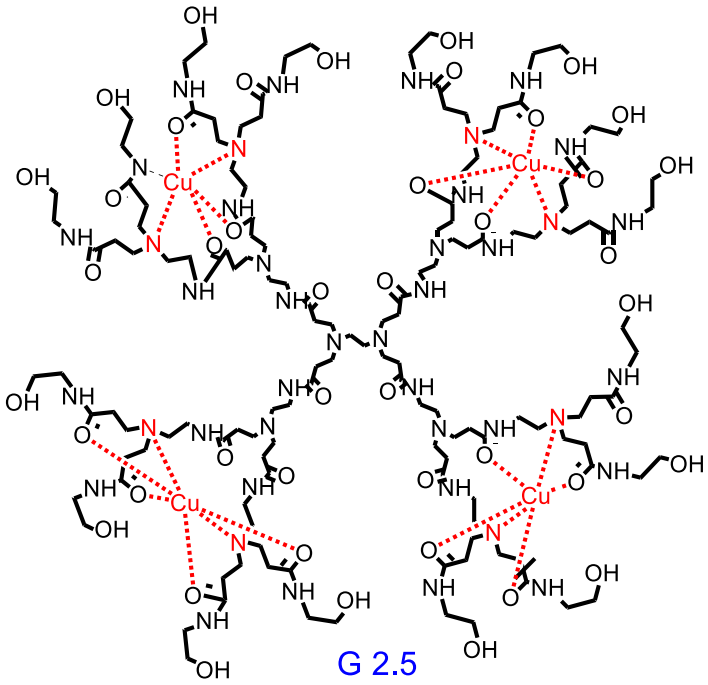


Figure 4.4: Proposed bonding between copper and PAMAM dendrimer

## 4.2 Quantification of copper stoichiometry within PAMAM dendrimers

Although it had been previously demonstrated that it was possible to bind Cu to the interior amines of the dendrimer, a further initial experiment was carried out to determine how the behaviour and coordination of the dendrimer changed with copper concentration in such cases. This was assessed at pH 7.0 using UV-VIS spectrophotometry. A pH 7.0 solution of TRIS

buffer (0.01 M) was prepared and used as a diluent, and this solution was then used to prepare 0.01 M solutions of dendrimer (G0.5-OH **12**, G1.5-OH **13,** and G2.5-OH **14**). The buffer was also used to make a 0.044 M solution of $CuSO_4$. Initial assessment was carried out by adding 1.5 mL of dendrimer solution to a cuvette and measuring its absorbance. As expected, there was no absorbance response across any generation. The $CuSO_4$ solution was then added in 10μL portions, with the absorption spectrum being acquired between each addition. For all samples, an increase in absorbance was observed at low concentrations of $CuSO_4$. However, the absorbance intensity reduced at higher concentrations of $CuSO_4$, which occurred when all binding sites became saturated so that any further addition of $CuSO_4$ resulted in dilution. Although these initial plots were not highly informative, they did help identify the concertation ranges in which Cu-dendrimer binding occurred.

The next experiment thus aimed to determine the precise stoichiometry of Cu ions in each dendrimer, a process achieved using a job plot analysis, with the UV-VIS spectra of various solutions containing different mole fractions of Cu and dendrimer used to determine the stoichiometry. A 0.05 M stock solution of each dendrimer (G0.5-OH **12**, G1.5-OH **13,** and G2.5-OH **14**) and a 0.05 M stock solution of $Cu^{2+}$ ions were prepared in a 0.1 M Tris buffer solution. A job plot analysis requires that the total number of moles (in this case, for $CuSO_4$ and dendrimer) be maintained, while the percentage, or mole fraction of each is varied. Using the two stock solutions, various Cu-dendrimer solutions were prepared with the percentages or mole ratios of dendrimers and $CuSO_4$ ranging from 0 up to 100%, as indicated in Table 4.1**.**

| No | G1.5-OH Conc. / mole | $CuSO_4$ Conc. / mole | G1.5-OH / mole % | Absorbance |
|---|---|---|---|---|
| 1 | 0.05 | 0 | 100 | 0 |
| 2 | 0.045 | 0.005 | 90 | 0.197 |
| 3 | 0.04 | 0.01 | 80 | 0.275 |
| 4 | 0.035 | 0.015 | 70 | 0.400 |
| 5 | 0.03 | 0.02 | 60 | 0.612 |
| 6 | 0.025 | 0.025 | 50 | 0.670 |
| 7 | 0.02 | 0.03 | 40 | 0.772 |
| 8 | 0.015 | 0.035 | 30 | 0.847 |
| 9 | 0.01 | 0.04 | 20 | 0.826 |
| 10 | 0.005 | 0.045 | 10 | 0.680 |
| 11 | 0 | 0.05 | 0 | 0.256 |

Table 4.1: Concentrations of G1.5-OH and $CuSO_4$ in mole percentage and absorbance.

The stoichiometry was then determined by plotting the absorbance against the mole percentage for each dendrimer. This generated the job plots shown in Figure 4.6. Analysis of these plots offers information about the relative amount, or stoichiometry of the copper ions relative to the dendrimer.

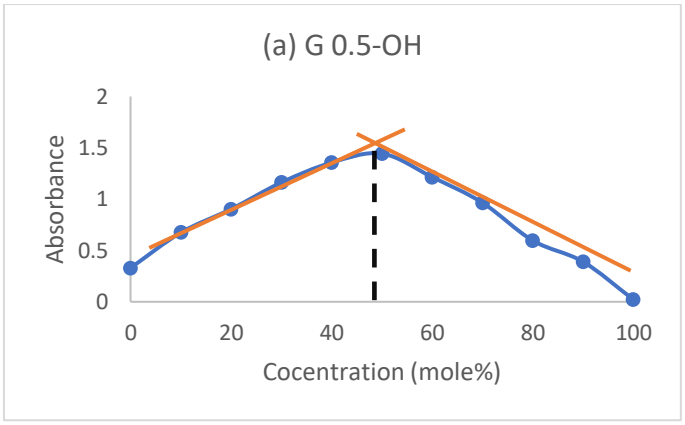


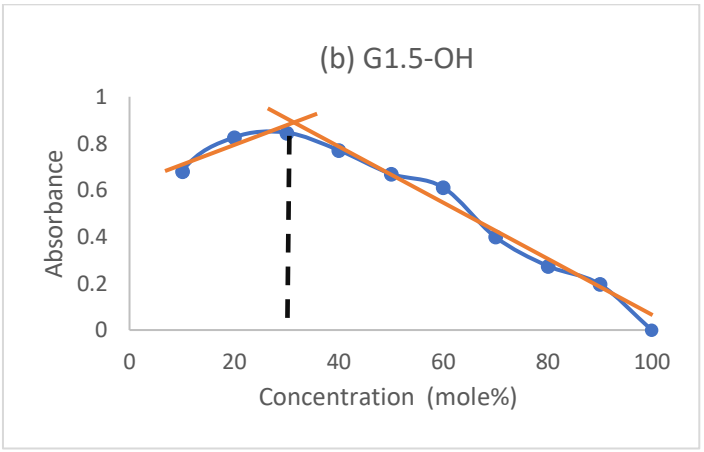


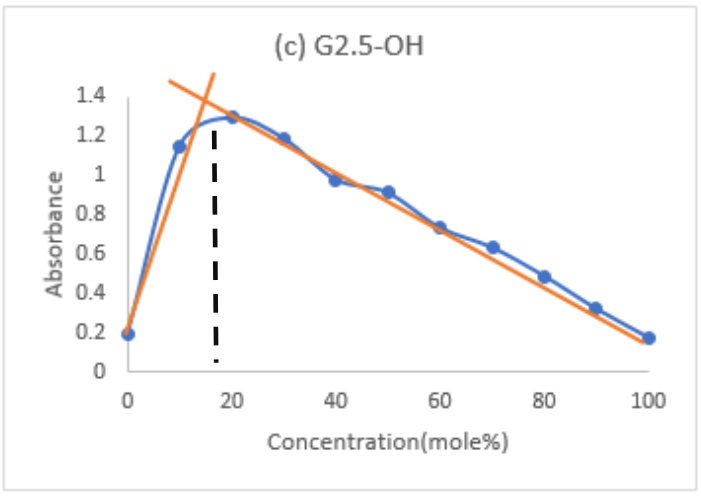


Figure 4.5: Overall data of absorption response vs mole% of a) G0.5-OH, b) G1.5-OH and c) G2.5-OH with Cu ratios at 680 nm ($\lambda_{max}$).

The stoichiometric ratio can be determined from the linear lines connecting each portion of the job plot (the "up" and "down" lines). The point at which these two lines intersect indicates the mole fraction that yields the maximum absorbance ($\lambda_{max}$). As such, the intersection reflects the

number of $Cu^{2+}$ ions that can be inserted into each dendrimer (G0.5-OH **12**, G1.5-OH **13,** and G2.5-OH **14**) at pH 7.0. The data indicates appropriate ratios of 1:1, 1:2, and 1:4 for G0.5-OH **12**, G1.5-OH **13,** and G2.5-OH **14,** respectively, suggesting that only one $Cu^{2+}$ ion is bound within the G0.5-OH **12**: as there are only two tertiary amines, this could have been predicted. For the larger dendrimers, only two and four $Cu^{2+}$ ions are bound to the G1.5-OH **13**, and G2.5-OH **14** respectively, however, despite them having "extra" nitrogens available. The reason for this is steric, as copper will initially bind to the most available nitrogens due to easier access, which are on the outermost layers of the dendrimers. The inner layers are more compact and dense, making it harder to bind any additional copper.

$Cu^{2+}$ binding occurred with the external tertiary amines within each dendrimer. The bound metal can also bind the carbonyl oxygen of an ester substrate and polarise the bond, however, potentially increasing the positive character of the carbon and increasing its reactivity towards nucleophiles.

### 4.3 Assessment of modified dendrimers as catalysts

In an effort to explore the possibility of stabilising the intermediate products and enabling the reaction to proceed faster at a neutral pH, an additional aim was explored, to include copper within the dendrimer. The copper should be able to help speed up the reaction via coordination with the oxygen **(a**cting as a Lewis acid). The copper ions should interact with the oxygen of the carbonyl group (C=O) of the substrate and subsequently make the complex more electrophilic, allowing the second step to form more rapidly and the electrophile carbon to be more easily attacked by good nucleophiles, leading to the stabilisation of the Td intermediate product through a lowering of the activation energy. In this respect, the Cu-dendrimer mimics the structure and active site of many metal containing enzymes.[24]

Copper should thus help speed up the reaction via coordination with oxygen as shown in Scheme  (acting as a Lewis acid). The copper ions will interact with the oxygen of the carbonyl group (C=O) of the substrate, subsequently making the complex more electrophilic so that the second step will be formed more rapidly, and the electrophile compound can be consequently attacked by good nucleophiles, such as the OH group, supporting the stabilisation of the Td. The copper can also coordinate with the charged oxygen in the Td intermediate, stabilising it and lowering the activation energy so that the cu-dendrimer mimics the structure and active site of many metal containing enzymes.[24]

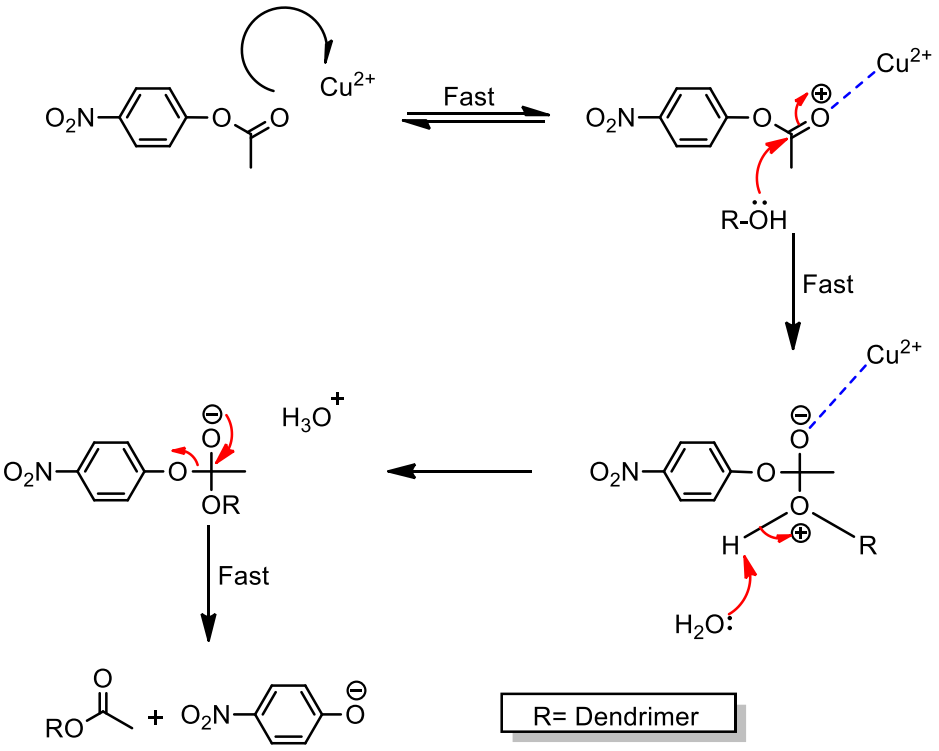


Scheme 4.1: Alcoholysis of PNPA **15** using copper as a catalyst

## 4.4 Assay of dendrimers bound with copper (metalated dendrimers)

Following the discovery of copper stabilisation by dendrimers, the seminal works by Crooks et al. [18-19] and their expansion by several others[20-27] disclosed the catalytic properties of PAMAM dendrimer-encapsulated metals and their functions as substrate nano filters.[18-24] However, this study focuses on metal catalysed cleavage of the esterification process and how encapsulation within the dendrimers affects dependence on pH levels.

It thus examines whether a dendrimer in the presence of copper is able to react with the ester more efficiently and rapidly than non-metalated dendrimers. The experiment used to show this utilised the same method used for the PAMAM dendrimers (see 4.4). The first set was a control using only the substrate PNP **15** and copper in a buffer (pH 7.4) to provide the initial rate for the formation of the by-product PNPA **16**.

The aim of this section was to use PAMAM dendrimers and functionalised PAMAM dendrimers as enzyme mimics to react with substrates at, or close to, neutral pH levels to ensure that some of the product is deprotonated and coloured. In addition, the level of tertiary amine protonation in the dendrimers was expected to be reduced, which is a necessary step, as protonated tertiary amines cannot coordinate with copper. The initial aim was thus to study alcoholysis at pH levels between 7.0 and 8.5.

The experiment was carried out as follow: a solution of TRIS buffer (0.1 M) was prepared and used as a diluent at pH 7.0. This involved 1.2 ml of PNPA **15** at a concentration of $3.13 \times 10^{-6}$ M being added to the cuvette, with the absorbance at 680 nM measured over time. The data retrieved was similar to the profile observed for the PNPA system (Figure 4.5). The analysis confirmed an initial rate of $2.0 \times 10^{-12}$ $Ms^{-1}$, and this low rate confirmed that copper by itself at

pH 7.0 was unable to hydrolyse PNPA. As a result, a system that can support or encourage this metal to be fully functionalised is required.

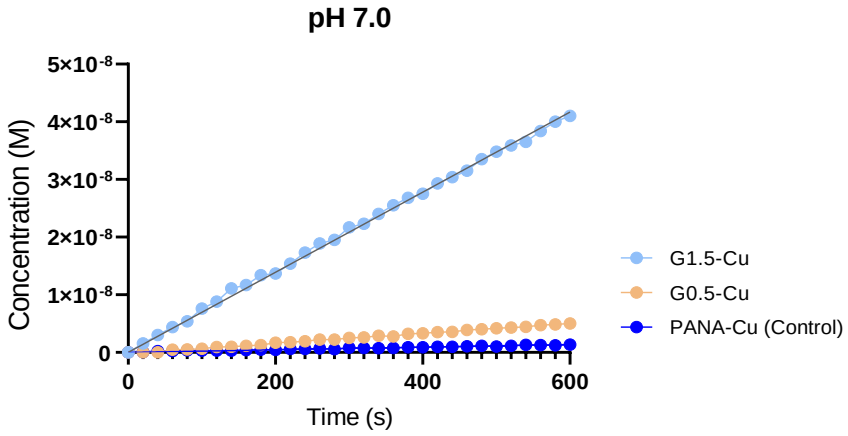


Figure 4.6 : Alcoholysis of PNPA in the presence of copper

The next set of experiments involved metal encapsulated dendrimers. The PAMAM dendrimers (G0.5-OH **12**, G1.5-OH **13,** and G2.5-OH **14**) were dissolved in methanol with excess copper sulphate. Excess copper was then removed by filtration and the methanol evaporated to give Cu-dendrimer coprecipitate. Tris buffer (pH 7.0, 0.1M) was then added to give 1 x $10^{-6}$ M solutions of each dendrimer, and 1.5 mL of each solution was added to a cuvette with 100 µl of PNPA **15** solution (7.5 × $10^{-6}$ M). As before, UV absorption at 680 nm was monitored over time.

The reaction profiles shifted as the copper was added, as seen in Figure 7, which can be seen most clearly in G0.5 and G1.5. This occurred as result of the volume of copper added exceeding these systems dendrimers voids. Table 4.2 shows that as the quantity of copper increased (at ratios of 1:1, 1:2, and 1:4 for the G0.5-OH **12**, G1.5-OH **13,** and G2.5-OH **14** respectively), the rate of reaction also increased. This indicates that copper is stable for use in larger dendrimers to speed up the alcoholysis reactions.

| Cu-PANA (Control) | G0.5-Cu (1:1) | G1.5-Cu (1:2) | G2.5-Cu (1:4) |
|---|---|---|---|
| 0.002 (± 0.0004) | 0.008 (± 0.0003) | 0.069 (± 0.001) | 0.196 (± 0.003) |
| **1.00** | **4.13** | **34.71** | **98.2** |

Table 4.2: Initial rates ($nMs^{-1}$) and relative rates (grey) as identified with metalated dendrimers.

Further research was carried out to learn more about the pH levels of metal catalytic systems. If the pH was altered but the relative pH remained unchanged, that is, if it behaved like a non-metalized dendrimer, the copper would be discounted as a factor in the reaction.

The experiments for the copper dendrimers and controls were thus repeated at pH levels 7.5, 8.0, and 8.5. For each set of pH experiments, the slowest rates were set to 1, and the remaining data presented relative to this to further simplify the study presentation. These rates and the start rates for the systems under study are thus shown in Table. The main finding was that adding more copper allowed the reaction to significantly proceed at neutral pH values, which did not occur for the control reactions. This happens because the copper acts as a catalyst, coordinating the ester and stabilising the Td intermediate produced. The system thus acted as expected in this regard, showing that if dendrimer catalyst is utilised, ester breakage is achievable at pH 7.0.

| Cu-PANA (Control) | G0.5-Cu | G1.5-Cu | G2.5-Cu |
|---|---|---|---|
| 0.002 (± 0.0004) | 0.008 (± 0.0003) | 0.069 (± 0.001) | 0.196 (± 0.003) |
| **1.00** | **4.13** | **34.71** | **98.2** |

| Cu PANA (Control) | G0.5-Cu | G1.5-Cu | G2.5-Cu |
|---|---|---|---|
| 0.014 (± 0.0002) | 0.023 (± 0.0003) | 0.112 (± 0.0016) | 0.230 (± 0.0007) |
| **0.70** | **11.35** | **56.00** | **115.15** |

| Cu-PANA (Control) | G0.5-Cu | G1.5-Cu | G2.5-Cu |
|---|---|---|---|
| 0.1138 (± 0.0002) | 0.1420 (± 0.0001) | 0.295 (± 0.0011) | 0.358 (± 0.0012) |
| **56.9** | **71** | **147.5** | **179** |

| Cu-PANA (Control) | G0.5-Cu | G1.5-Cu | G2.5-Cu |
|---|---|---|---|
| 0.2084 (± 0.0002) | 0.2242 (± 0.012) | 0.3045 (± 0.0005) | 0.537 (± 0.0019) |
| **104.2** | **112** | **152** | **268.5** |

Table 4.3: Relative rates for all dendrimers with copper at varying pH levels ($nMs^{-1}$).

Over the pH range 7.0 to 8.5, the rate for the copper control experiments increased from 0.002 to 0.2084 $nMs^{-1}$, a 100-fold increase in terms of relative rate. This shows that the copper significantly catalyses the basic alcoholysis process.

In pH ranges from 7.0 to 8.5, the G0.5-OH Cu dendrimer's relative rate increased about 30-fold, indicating a definite pH dependence for respective copper oxidation rates. Applying this approach to the larger dendrimers that include more coppers, the effect is noticeably less pronounced, however. The rates increase by only 5 and 4.5 fold, respectively, moving from pH 7.0 to pH 8.5 for the G1.5-OH Cu dendrimer. This indicates that accessible catalytic surfaces are provided by stabilised Cu particles enclosed in dendrimers, which prevent agglomeration or precipitation.

The primary reaction here is alcoholysis, which is sensitive to pH changes. The interiors of the larger dendrimers, along with the regions around their terminal groups and copper can all bind the substrate in metalated dendrimers. The substrate is thus effectively protected from the aqueous environment, including from hydroxide ions, as a result of the higher effective molarity experienced by the substrate in comparison to that seen in reactive groups.

## 4.5 Comparison of metalated and non-metalated dendrimers

. The next study sought to compare the metalated (copper) and non-metalated (without copper) data. The reaction profile shifted as copper was added to the dendrimers, as seen in Figure 4.7. As anticipated, the initial rates were lower in G0.5-OH **12** and G1.5-OH-Cu complex (0.005 and 0.008 $nMs^{-1}$ respectively), due to the relatively open structures of these smaller dendrimers, which result in poor hydrophobic cavities being formed. It is also possible that the rates were lower due to the fact that fewer functional groups were available to interact with and stabilise the substrate and intermediate. The results further showed that, as expected, the rate of reaction was extremely slow for the smallest dendrimer, as this is not capable of holding sufficient copper ions to stabilise the intermediate.

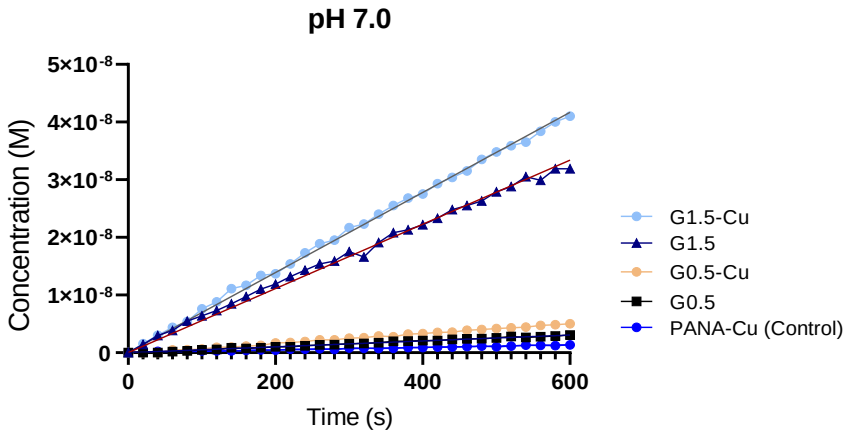


Figure 4.7: Comparison of neutral dendrimer hydrolysed PNPA in the presence of copper

The next step was to study the reaction using the larger generation dendrimers to determine if any significant increase in the rate of reaction could be detected. The plots obtained for the larger dendrimers showed that the initial rate was dramatically raised in the G1.5 OH-Cu (0.069 $nMs^{-1}$) and G2.5 OH-Cu (0.196 $nMs^{-1}$) complexes as compared to that seen in the smaller dendrimer, copper alone, or the non-functionalised neutral dendrimer. This indicated that the copper coordinated G2.5-OH dendrimer can demonstrate an increased rate of 39 % higher than that in the simple non-functionalised dendrimer. This was assumed to be due to the copper and its location within the interior of the dendrimer: specifically, the copper is bound within the hydrophobic region of the dendrimer to the nitrogen closest to the surface, allowing the substrate to bind and react with the external alcohol groups.

In all cases, the copper dendrimers showed higher relative rates of change as compared to the non-metalated dendrimers. One significant observation was that the two larger dendrimers could catalyse the reaction significantly at neutral pH levels, which was not possible for the control reactions, due to the catalytic influence of the copper, which presumably coordinates

with the ester or stabilises the Td intermediate thus formed. In this respect, the system appears to behave as predicted, with ester cleavage possible at pH 7.0 where a dendrimer catalyst, whether metalated or non-metalated, is used.

| **pH / Initial Rate** | **Cu-PANA (Control** | **G0.5** | **G0.5-Cu** | **G1.5** | **G1.5-Cu** | **G2.5** | **G2.5-Cu** |
|---|---|---|---|---|---|---|---|
| 7.00 /$nMs^{-1}$ | 0.002 (± 0.0004) | 0.005 (± 0.0001) | 0.008 (± 0.0003) | 0.056 (± 0.003) | 0.069 (± 0.001) | 0.141 (± 0.02) | 0.196 (± 0.03) |
| 7.5 /$nMs^{-1}$ | 0.014 (± 0.0002) | 0.022 (± 0.0003) | 0.023 (± 0.002) | 0.065 (± 0.008) | 0.112 (± 0.0016) | 0.182 (± 0.08) | 0.230 (± 0.0007) |
| 8.00 /$nMs^{-1}$ | 0.1138 (± 0.0002) | 0.0715 (± 0.0010) | 0.142 (± 0.0032) | 0.203 (± 0.0011) | 0.295 (± 0.0011) | 0.331 (± 0.0015) | 0.358 (± 0.0012) |
| 8.5 /$nMs^{-1}$ | 0.2084 (± 0.0002) | 0.096 (± 0.07) | 0.2242 (± 0.0215) | 0.300 (± 0.0024) | 0.3045 (± 0.0005 | 0.4500 (± 0.0013) | 0.537 (± 0.0019) |

Table 4.4: Effect of dendrimers at different pH levels ($nMs^{-1}$)

The studies for the copper dendrimers and controls were repeated at pH levels 7.5, 8.0, and 8.5 in order to assess the effect and importance of the base concentration on the reactions. Table4.4 thus shows the graphs and data for the relevant responses, illustrating that as the pH increases, the rate of reaction also increases for both the control reactions and the dendrimer-based reactions, with higher rates for the later generation dendrimers.

As previously observed, the relative increases in rates were significantly smaller for the dendrimer systems than for the controls. As a result, the dendrimer reactions must be assumed to be less sensitive to pH than the simple base catalysis control reaction (base catalysed alcoholysis). This again highlights that the dendrimer reactions react with the esters in different ways, stabilising any intermediates more effectively, than the base catalysis control reactions. Dendrimer catalysis is dominated by the reaction with the dendrimer's terminal alcohol groups,

rather than the simple hydrolysis mechanism whose rates are controlled by the relative concentration of hydroxide.

Having acquired data for the copper dendrimers and the non-copper dendrimers, these data were compared to facilitate a better understanding and quantification of the role of copper in the ester reaction (transesterification). To simplify the analysis, the rates were converted into relative values. Table thus shows the rates and initial rates for the systems studied. For the copper control experiments, the rate increased from 0.002 to 0.2084 $nMs^{-1}$ over the pH range 7.0 to 8.5. In terms of relative rate, this represents a 100 fold increase. Examining equivalent data for the non-metalated control, the relative rate increases from 1.00 to 28 (0.002 to 0.057 $nMs^{-1}$) for pH levels 7.0 and 8.5, respectively.

This comparison indicates that the copper has a significant catalytic effect on the simple alcoholysis reaction (presumably by acting as a simple Lewis acid). The data for dendrimer systems shows similarly that the reactions are much faster when larger dendrimers are used as catalysts, while the substrate reaction (alcoholysis with the dendrimer's terminal OH groups) is much more rapid when the copper dendrimers are used: for example, the rate for the G 0.5-OH Cu dendrimer was 1.6 times faster than that for the non-metalated dendrimer **12**.

| Cu-PANA (Control) | G0.5 | G0.5-Cu | G1.5 | G1.5-Cu | G2.5 | G2.5-Cu |
|---|---|---|---|---|---|---|
| 0.002 (± 0.0004) | 0.005 (± 0.0001) | 0.008 (± 0.0002) | 0.056 (±0.0003) | 0.069 (±0.0002) | 0.141 (±0.0002) | 0.196 (± 0.002) |
| **1.00** | **2.5** | **4.13** | **28** | **34.71** | **70.5** | **98.2** |

| Cu PANA (Control) | G0.5 | G0.5-Cu | G1.5 | G1.5-Cu | G2.5 | G2.5-Cu |
|---|---|---|---|---|---|---|
| 0.014 (± 0.0002) | 0.710 (±0.001) | 0.023 (± 0.0003) | 0.065 (± 0.005) | 0.112 (± 0.0016) | 0.182 (± 0.008) | 0.230 (± 0.0007) |
| **0.70** | **35.5** | **11.35** | **32.50** | **56.00** | **91.00** | **115.15** |

| Cu-PANA (Control) | G0.5 | G0.5-Cu | G1.5 | G1.5-Cu | G2.5 | G2.5-Cu |
|---|---|---|---|---|---|---|
| 0.1138 (± 0.0002) | 0.710 (±0.10) | 0.1420 (± 0.0001) | 0.203 (±0.11) | 0.295 (± 0.0011) | 0.331 (±0.15) | 0.358 (± 0.0012) |
| **56.9** | **35.5** | **71** | **101.5** | **147.5** | **165.5** | **179** |

| Cu-PANA (Control) | G0.5 | G0.5-Cu | G1.5 | G1.5-Cu | G2.5 | G2.5-Cu |
|---|---|---|---|---|---|---|
| 0.2084 (± 0.0002) | 0.096 (± 0.0007) | 0.2242 (± 0.012) | 0.300 (± 0.0024) | 0.3045 (± 0.0005) | 0.450 (±0.0013) | 0.537 (± 0.0019) |
| **104.2** | **48** | **112** | **150** | **152** | **225** | **268.5** |

Table 4.5: Relative rates for all dendrimers with copper at different pH levels ($nMs^{-1}$)

Comparing the ***relative rates*** with respect to pH, a 19-fold increase in the rate for the non-metalated G0.5-OH dendrimer is obvious over the pH range 7.0 to 8.5, which is increased to an almost 30-fold increase for the G0.5-OH Cu dendrimer over the same pH range. This indicates a clear pH dependence across the relative rates of both dendrimers. Extending this analysis to the larger dendrimers, a significantly smaller effect is observed, however. For example, the G1.5-OH and G1.5-OH Cu dendrimers display only 5- and 4.5-fold increases,

respectively, as the pH moves from 7.0 to 8.5. A similar but further reduced trend is observed for the G2.5 dendrimers, where the changes in relative rates over the same pH range were just 3 and 2.75 for the non-metalated and metalated dendrimers, respectively. Overall this data confirms that the control and G0.5 dendrimers react in a different manner to the larger dendrimer systems. This is because the G0.5 dendrimers are open and cannot provide an appropriate environment for substrate binding and reaction (with the dendrimer's terminal OH groups).

The principle reaction here is alcoholysis, which is more susceptible to changes in pH level. The substrate can bind within the interior of the larger dendrimers, in close proximity to the terminal groups and copper (for the metalated dendrimers). As such, the substrate is effectively protected from the aqueous environment and any hydroxide ions, whilst also experiencing a higher effective molarity with respect to the various reactive groups (the substrate, stabilising groups, and terminal OH groups).

Further data was sought to analyse the G2.5-OH-Cu complex at different pH levels. As expected, an increase in the reaction rate with the increase in pH was observed, as shown in Figure4.8. Specifically, elevated values were observed at pH levels 8.0 and 8.5, an increase that may be attributed to the base condition in which the reaction takes place, with the existence of an OH- group offering a good nucleophile. As noted, when the alkaline environment increases, this efficiently allows alcoholysis to occur. The carbonyl group (R-OH) of the dendrimer then also reacts to attack the carbonyl group of the substrate and produce PNPA more effectively.

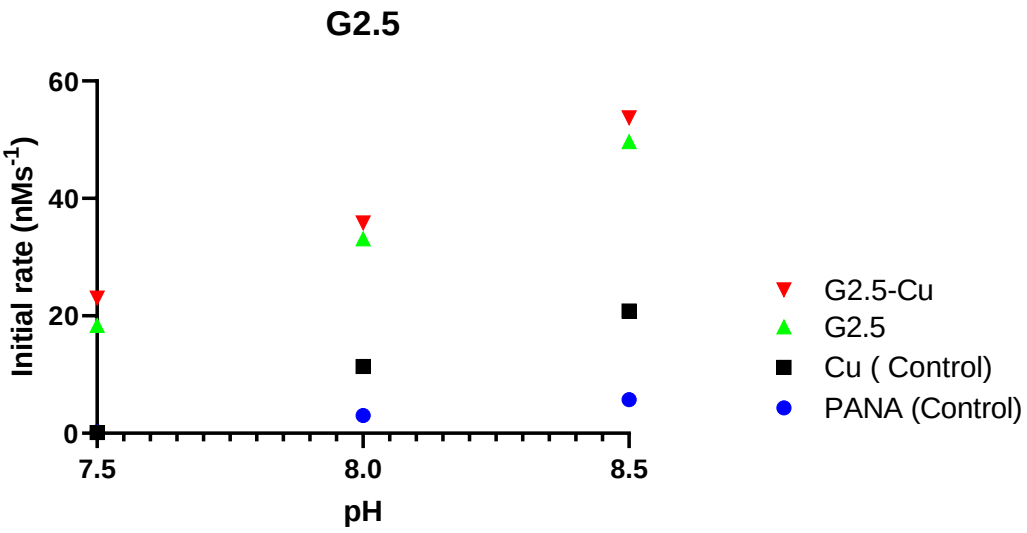


Figure 4.8: Comparison of G2.5-OH hydrolysed PNPA at all pH levels (7.0, 7.5 and 8.0) with and without copper

| Relative Initial Rate | 7.0 | 7.5 | 8.0 | 8.5 |
|---|---|---|---|---|
| Control | 1.0 | 1.0 | 15 | 28.5 |
| G2.5 | 1.0 | 1.3 | 2.3 | 3.2 |
| G2.5-Cu | 1.0 | 1.2 | 1.8 | 2.7 |

Table 4.6: Relative rates for control solution and G2.5-OH at different pH levels

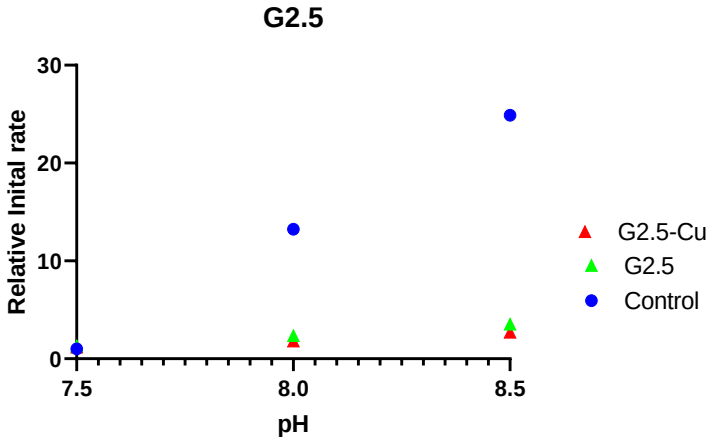


Figure 4.9: Comparison of the relative rates of control and G2.5-OH, with and without copper

As shown in Figure4.9, when the rate of relative growth is compared between the control samples (without dendrimer) at different pH levels, only a small improvement is seen. However, when the rate of relative growth between the control and G2.5-OH **14** is considered, this significantly improves as the pH rises from 7.5 to 8.5. Furthermore, the esterification process enhancement reaches its best value (about 70 fold) at a similar point. Copper is a dynamic component in the dendrimer-Cu system, as it can move to maximise interactions. The enhancement in rate thus results from two factors. The first is that PAMAM dendrimers act as a covalent scaffold and solubilise p-nitrophenol acetate within their external hydrophobic regions, while the second is that the dendrimer's internal amide groups stabilise the transition state.

## 4.6 Conclusions

In order to achieve selectivity or specificity, a water soluble polymeric system with a fixed structure and a controlled microenvironment (interior) is required. In this regard, neutral PAMAM dendrimers can provide the necessary structural, electronic, and solubilising characteristics, while the neutral polar terminal groups of such dendrimers offer water solubility. Additionally, these dendrimers have hydrophobic interior environments that can bind to and dissolve organic molecules, characteristics that can also be used to bind substrates, intermediates, and transition states to then catalyse reactions in a similar manner to enzymes with respect to their structural properties. The main goal of this research was thus to functionalize dendrimers' interiors to explore how this might affect this internal milieu, and to thus decide whether or not dendrimers may be used as efficient enzyme mimics.

Based on their inherent intrinsic functionality, their capacity to catalyse reactions through a .charged intermediate that develops  of during hydrolysis reactions and, as with G2.5-OH,

this intermediate can be stabilised, which leads to a decrease in activation energy and an increase in reaction rate. To track the rate of such reactions, a PNPA substrate was used. Enzymes function at neutral pH levels, but non-catalysed hydrolysis reactions are highly pH dependent; thus, a pH range of 7.0 to 8.5 was chosen, while the ways in which pH affected the speed of dendrimer-catalysed hydrolysis reactions were noted. For the substrate, neutral OH terminated dendrimers (G0.5-OH up to G2.5-OH) were selected, as these were assumed to be less sensitive to protonation and thus to allow a simple hydrolysis reaction to remain the dominant process, allowing exploration of the effect of dendrimer size on catalytic rates.

After examining post-synthetically modified PAMAM dendrimers, simple dendrimers and the capacity of pre-existing functional groups to catalyse hydrolysis reactions were examined. Copper was used to determine any effects of metallic additions on catalytic ability. Groups were also added to the dendrimer interiors that were believed to interact more effectively with the tetrahedral transition state of the hydrolysis reaction, a process completed by post-synthetically metalizing the dendrimer interiors with copper through coordination with the internal amines.

UV-VIS spectrophotometry was then used to analyse and determine the $Cu^{2+}$ incorporation utilised in this investigation, which was conducted at a pH of 7.0. The discovery that only one $Cu^{2+}$ ion had bonded within the G0.5-OH **12** might have been expected, given that there are only two tertiary amines in this complex; however, in the larger dendrimers, only two and four $Cu^{2+}$ ions, respectively, were bound to the G1.5-OH **13** and G2.5-OH **14** despite them theoretically having extra nitrogens available. This is caused by the fact that the dendrimers' outermost layers contain the nitrogens that offer the best access, such that copper will attach to

these first, while the inner layers are denser and more compact, and thus more difficult to bind with for any additional copper.

Furthermore, the ester's carbonyl oxygen is bound by the metal, which then polarises the bond. As a result, the carbon's positive character and nucleophile reactivity are enhanced, including with water. Some metallo-enzymes exhibit this function, which shares similar mechanisms with Lewis acid catalysis. Straightforward quarterisation reactions could also be used to change the interior to contain charged regions so that the charge produced can interact with the negatively charged oxygen that results from the hydrolysis of an ester's carbonyl bond. Binding the tetrahedral intermediate thus causes a faster reaction and lower activation energy, similar to the stabilisation of the amide noted above.

These results show that pH shifts happen even where dendrimers, especially G2.5-OH **14**, speed up reactions as compared to the control reaction. According to the findings, increases in relative rates are caused by increased PAMAM dendrimer generations. Using G1.5-OH **13** as an example, the significance increased from 34.71 to 152 when copper was added where the pH was increased from 7.0 to 8.50. Copper was also shown to enhance the relative initial rate for G2.5-OH **14**, suggesting that dendrimer reactions are less pH-sensitive than the control reaction (base catalysed hydrolysis). The dendrimer reactions stabilise any intermediates to a higher extent than the base catalysis process, as well as cleaving the ester in a different manner. This means that reactions that take only a portion of the dendrimer, rather than the simple hydrolysis process, dominate the dendrimer reactions.

# CHAPTER 5
# Protein Recognition

## 5.0 Introduction

Protein-protein complexes develop from interactions between proteins; these can then be classified as homocomplexes, which normally exhibit both stability and endurance, or heterocomplexes, which exhibit the potential to form or break down more readily due to external influences. Due to these properties, heterocomplexes meet the prerequisites where the involvement of a protein capable of existing on its own is required, and cytoskeletal remodelling, cell control, signal transduction, immunological response, and viral self-assembly are just a few of the biological processes that depend on such protein aggregates.[51] However, if proteins do not interact normally, various disease processes, such as homodimeric complex HIV-1 protease, Alzheimer's, and multiple types of rheumatoid arthritis,[2] may develop. A number of cancer treatment methods can disrupt particular protein-protein interactions: for instance, c-Myc inhibitors are crucial in malignancies linked to extended cMyc activity,[52] and targeting and preventing these interactions may thus prevent the formation of plaque molecules, thereby assisting in the treatment of illness (

Figure 5.110).

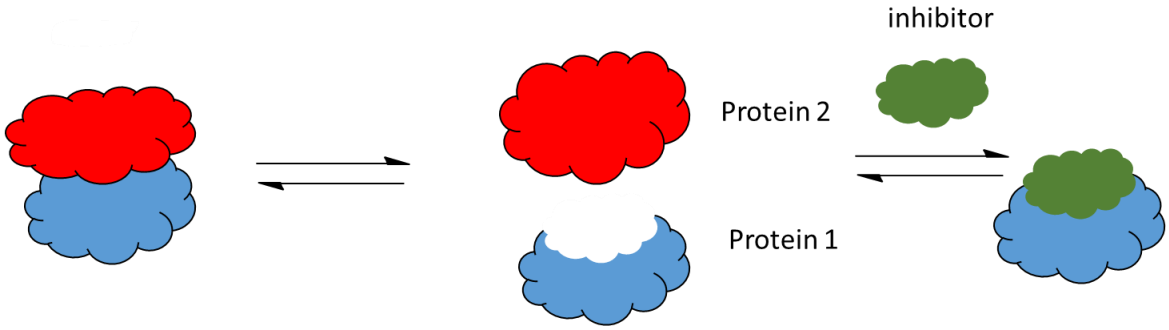


Figure 5.110: Inhibiting protein binding

## 5.1 Understanding protein-protein interactions

The 20 naturally occurring amino acids can be joined in a variety of ways to form primary structures that then fold to form proteins with a range of tertiary and quaternary structures, which may differ significantly. Proteins can perform a multitude of functions due to this diversity,[53] and as shown in Figure5.2, protein-protein complexes can also be created that consist of multiple proteins. The latter are normally created by the non-covalent binding of at least two proteins to create active substances.

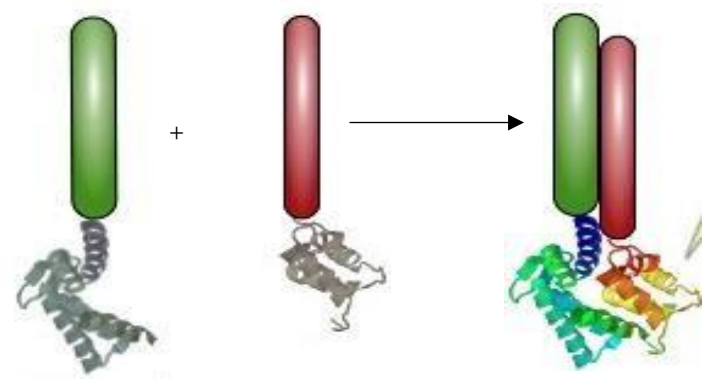


Figure 5.2: A mixed active complex

Cooperative binding confers stability to molecule-molecule interactions, giving such forces a collective strength that they may lack individually.[54] On the basis of this cooperative binding, numerous biochemical and biological processes can take place. Increases in perceived affinity improve the likelihood of a second molecule attaching, as these signal cooperative behaviour. Another explanation for this is where the second binding has relative higher concentration of the necessary ligand.[55]

Figure 5.3 depicts the outcomes of cooperative binding. The first bond between the ligand and the initial binding site is formed at rate $K_1$, and as the relative concentration of the second

ligand is higher than that of other molecules, the creation of the second contact follows the formation of this bond substantially more quickly, and with greater intensity. This effect is non-additive, however, as $K_1$ is significantly smaller than $K_2$: cooperative binding thus has a noticeably larger additive effect.

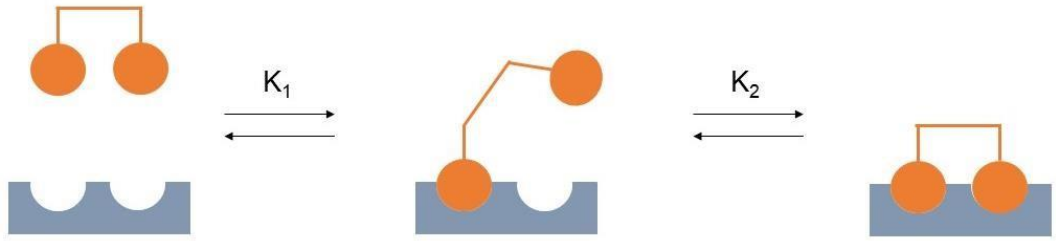


Figure 5.3: Cooperative binding consequences, with $K_1$ being much smaller than $K_2$

Certain amino acids are substantially more concentrated at their binding surfaces than they are elsewhere in the protein molecule. These amino acids show a higher degree of hydrophobicity than the molecule exterior, suggesting that binding interactions between proteins could be improved by utilising hydrophobic interactions. A binding surface is the most likely location for amino acids such as tyrosine to occur in proteins, and this tends to favour aromatic amino acids of larger size.[56]

Table 5.1 lists some potential target proteins that might be used to evaluate a polymers' ability to bind to and to distinguish between protein surfaces across the same enzyme family. The method by which strong associated synthetic subunit complexes of molecules and proteins are formed to prevent protein subunits from interacting with each other thus acts as the basis for the disruption of interactions between proteins with synthetic inhibitors.

| Mechanism | Protein | Amino acid residue | Inhibitor | Cleavage site |
|---|---|---|---|---|
| Serine protease | Elastase | 240 | α-anititrypsin | Ala, Gly |
| | α-chymotrypsin | 241 | Aprotinin | Phe, Tyr, Trp |
| | Trypsin | 233 | p-aminobenzamidine | Arg, Lys |
| | Kallikrein | 619 | Aprotinin | Arg |
| | Thrombin | 308 | Argatroban | Arg |
| Zinc protease | Carboxypeptidase A | 307 | Benzomercapto propanoic acid | Phe, Trp, Leu |
| Aspartate protease | Cathepsin D | 346 | Pepstatin A | Phe-Phe |

Table 5.13: Enzymes for common inhibitor and cleavage locations.[55]

### 5.1.1 Hotspots and the interfacial region

Prior to applying this strategy, it is crucial to gather knowledge about the interfaces seen at protein-protein recognition sites and how these facilitate binding. The size, shape, structure, and characteristics of amino acid residues, the conformational modifications brought on by the formation of complexes, the cooperative relationships between interacting surfaces, and the forces of interaction are all important aspects of protein-protein interfaces that must be taken into consideration in this process.[56] When protein-protein complexes are created, the huge interfacial region on a protein, which generally exhibits hydrophobicity and contains several polar groups, is no longer accessible to solvent.[57] As shown in Figure, most proteins' contact surface areas range from 500 to 5,000 $Å^2$ [58]: for instance, the distance between cytochrome-c and its cytochrome-c peroxidase counterpart is about 1,150 $Å^2$, while the distance between chymotrypsin and its protein analogue is about 2,200 $Å^2$. It was thus initially believed that the connections between proteins were formed by a succession of weak and ad hoc intermolecular interactions throughout the entire interfacial region, and that the hydrophobic binding between interaction amino acid groups was the source of the free energy used in binding.[59]

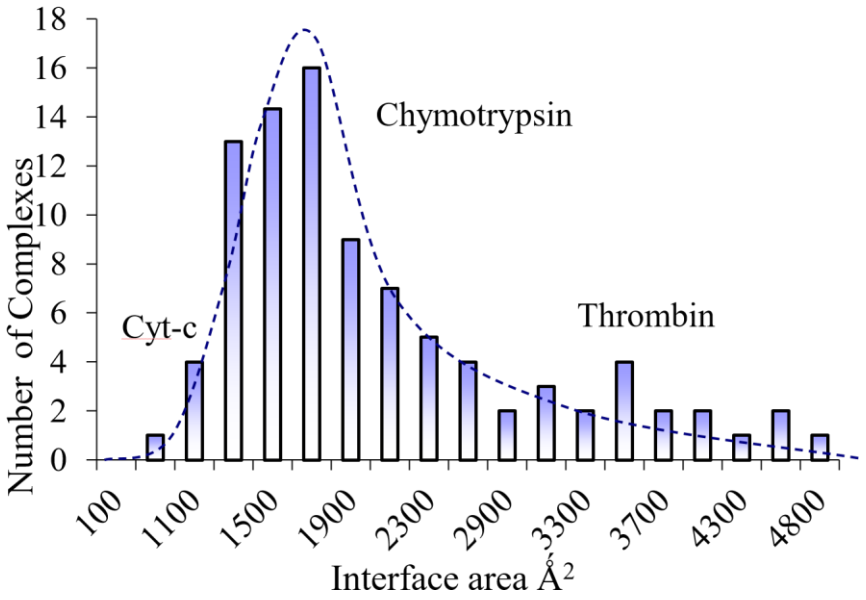


Figure 5.4: Distribution of interfacial regions in common protein-protein complexes

Wells and Clarkson[60] identified the "hot spot" at which binding occurs when contacts with high strength and affinity traverse a surface area with constrained dimensions, however. According to Bogan and Thorn[61], the hot spot is thus a tiny, pre-organised region of the surface of the protein that is supplied with amino acids such as tyrosine, tryptophan, and arginine. Due to the depressions and concavities it exhibits, the fitting of complimentary proteins is frequently conceivable in such an area, and although a protein may have multiple hot spots on its surface, binding through a specific hot spot requires a developing complex to exhibit both stability and low energy in that area.

Furthermore, specific amino acids can be chosen as hot regions do not include random amino acid combinations.[62] The targeting of the protein's internal active site, which is inaccessible to bulk solvent is a distinct mechanism from the targeting of the protein's external surface, which is accessible to bulk solvent; this fact could thus be used to prevent binding between proteins, based on the previously mentioned factors.[63]

### 5.1.2 Small molecule inhibitors

Research into small molecules as potential inhibitors has received a lot of attention in recent years, and generally, the purpose of the development of small compounds is to facilitate contact with the active site or specific location of a given enzyme. The three primary forms of interactions in a protein's active site are hydrogen bonds, electrostatic interactions, and salt bridges. Thus, interactions involving tiny, "drug-like" compounds that exhibit hydrophilicity and hydrogen bond donor groups may be advantageous.[64] However, developing synthetic drugs specifically designed to target protein-protein interactions is not a simple operation, and small molecule inhibitors offer unique challenges due to the relatively wide area (700 to 1,500 $Å^2$ per protein) required for identification[65]. Additionally, selective targeting is difficult because the interacting surfaces appear as shallow depressions devoid of distinguishing features. Replication with simple synthesised peptides is further complicated by these being located in different areas of the binding region of two interacting proteins: proteins can thus present both projections and pockets, rather than only providing and filling pockets, which restricts the creation of inhibitors. As an additional complication, protein-protein interaction surfaces exhibit higher complexity than the interaction surfaces between ligands and enzymes. [66]

### 5.1.3 α-Helix Mimetics

Several peptides exhibiting stability (conformational resilience) and specific secondary structures have been created. More than 15 amino acid residues are needed to obtain a satisfactory conformation stability, however, and recently, interest has focused on the promise of stable 21 hydrogen-bond surrogate-restricted turns, helices, and sheet systems for the treatment of a variety of diseases, notably cancer and HIV.[67]

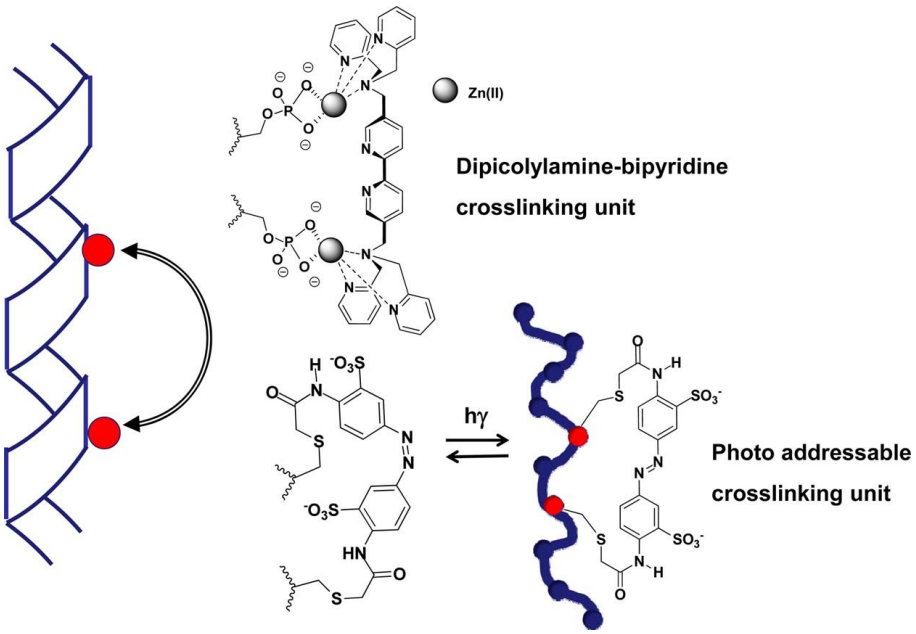


Figure 5.5: Cross-linking units of azobenzene and dipicolylamine-bipyridine

Peptide stabilisation has been explored by the employment of azobenzene photo addressable[68] and dipicolylamine-bipyridine[69] cross-linking units (Figure). Although not all of these peptides have the same three-dimensional orientations, they are equivalent to helices in terms of the side chains they display along a given face. These systems are thus beneficial primarily because they are proteolytically stable and highly conformationally stable as distinct protein secondary structures.

Breslow et al. [70] used a variety of cyclodextrin dimers (-CD) to demonstrate how protein aggregation was specifically disrupted (Figure). Only -CD compounds with depressions facing one another that were sufficiently divided by a linker were able to prevent protein aggregation, however, implying that inhibition is influenced by the linker's characteristics. The scaffold-type helix mimicked terephthalamides, though alkylidene cycloalkanes have also been proposed as potential -helical mimics.[71] Reymond et al.[72] used a -helical conformation to create peptide dendrimers, and the discovery of non-peptidic small molecules that imitate helices as inhibitors of protein-protein interactions received a lot of interest. Meanwhile, Lee et al. [73]

developed a novel pyrrolopyrimadine-based receptor, as depicted in Figure , and the extent to which this scaffold interfered with the interaction between p53 and MDMX was used to gauge its potential as a helical mimic. This required evaluation of the scaffold against a library of 900 different chemicals to facilitate the selection of primary amines with hydrophobic groupings. The side chains of the three amino acids that make up p53 were crucially replicated by these, confirming the scaffold's structural rigidity, high water solubility, and cellular permeability.

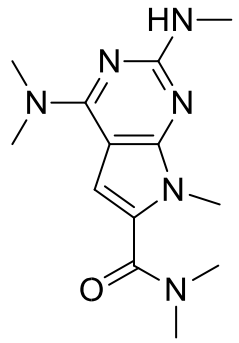


Figure 5.6: Structure of a pyrrolopyramidine-established α-helix mimic

Other strategies for replicating the specific mechanisms of protein interactions have been considered, including the interruption of these interactions through bonding to the protein surface at an area close to, rather than directly on, the active site of the protein. Small molecule inhibitors have proven difficult to develop, however, [74] and thus various other approaches have been considered.

Proteins differ in terms of their peripheral surfaces, which are formed of charged hydrophobic and hydrophilic regions. In addition to electrostatic interactions, the interface between two binding proteins also contains hydrogen bonds and stacking interactions.[75] The majority of compounds under investigation thus work to hinder contact by binding to active depressions on proteins, though little to nothing is known about the mechanism by which synthetic compounds bind to the surface of proteins to disrupt their function. Investigating these

compounds could therefore provide more knowledge about protein periphery and surface recognition, as well as facilitating the discovery of novel potential therapeutic medicines.[76]

### 5.1.4 Supramolecular protein scaffolds

Rotello[77] employed self-assembled systems in order to better recognise surfaces. A-chymotrypsin surface with positive charge was bound with mixed-monolayer protected gold clusters (MMPCs) functionalised with terminal anionic groups as a way to suppress enzymatic activity using a two-step mechanism that involves rapid reversible suppression and a slower irreversible process of gradual enzyme breakdown (Scheme 5.1).

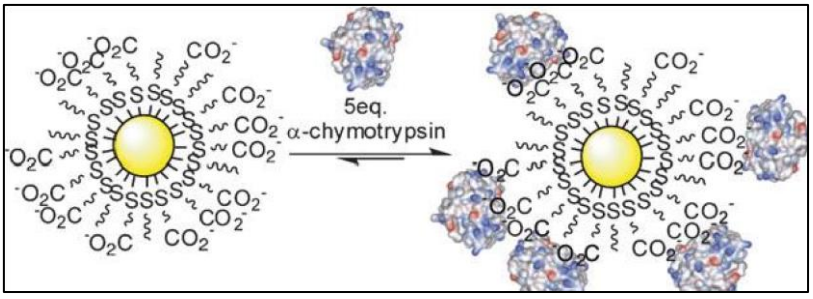


Scheme 5.1: Surface recognition using MMPCs

The procedure demonstrated greater selectivity as compared to elastase, supporting the effectiveness of the created electrostatic contacts. Circular dichroism spectroscopy was used to establish the effectiveness of the association between the gold nanoparticle and -chymotrypsin, which displayed a 10 nM $K_i$(app) and a stoichiometry of five protein molecules per MMPC. Additionally, the inhibitory mechanism demonstrated better selectivity for chymotrypsin as compared to β-galactosidase.

There has also been interest in an inhibitor made from graphene oxide (GO) layers. In terms of dose response (by weight), the surface carboxylate group serves as both a synthetic receptor and an inhibitor of chymotrypsin activity, in such cases, facilitating higher levels of chymotrypsin suppression than the other synthetic inhibitors that have been proposed.[78]

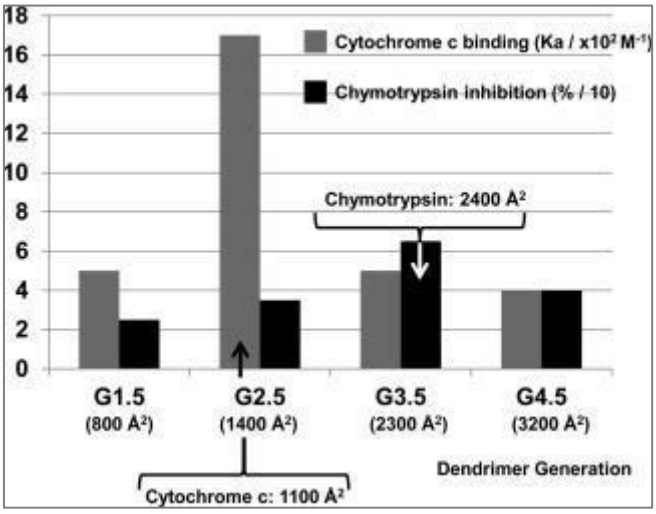


Figure 5.7: PAMAM dendrimers for binding and inhibition

Wang et al.[79] presented proof that GO and iron oxide (IO) may be combined to create a nanocomposite material capable of supporting the creation of brand-new Alzheimer's disease treatment options. Dendrimers, which feature terminal groups that enhance their interactions with hot spot residues, are thus another class of possible protein inhibitors worth mentioning in this context; these are frequently referred to as fake globular proteins because of their resemblance in size and shape to these important proteins.

Fassina[80] proposed two unique dendrimeric peptide mimics, each supported by four copies of the tripeptide Arg-Thr-Tyr (L-amino acids) or a partial-retro-inverso (Arg-Thr-Tyr, D-amino acids), linked to a polysine core with an asymmetric core, though the greatest efficiency was obtained using a natural amino acid sequence. Twyman[81] also provided evidence that dendrimers had the potential to suppress chymotrypsin and cytochrome-c, and as a result, had

the potential to establish a binding mechanism with size selectivity. The PAMAM dendrimers used to achieve this in this work are shown in Figure. That dendrimer that can bind a given protein most effectively is the one whose accessible area is most comparable to the size of the protein's interfacial region, and the interaction between a big ligand and the enzyme active site, essentially blocks the active site, suppressing the enzyme's ability to operate. Based on this, the dendrimers that exhibit the strongest binding are also those with the highest inhibitory potencies.

Using dendrimers as soluble supports was a key component of Ronald's dynamic combinatorial chemistry (DCC) method. High support loadings, homogeneous purification, characterisation, and solution phase chemistry are further crucial DCC characteristics. Effective DCC production of combinatorial libraries is thus possible for the development and study of chemical complexity based on them enhancing molecular network accessibility.[82]

### 5.1.5 Dynamic Combinatorial Libraries

DCLs are collections of molecules that exist in stable, reversible equilibria. These molecules can thus self-assemble into complexes by means of covalent or non-covalent interactions, as well as being thermodynamically regulated. A DCL structure is dictated by exposure to exogenous factors or templates, such as proteins, being further determined by the relative stability of each ingredient (Figure 5.8*11*5.8).[83]

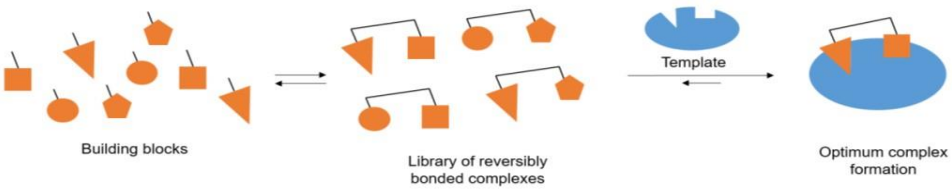


Figure 5.811: Dynamic Combinatorial libraries (DCLs)

A template molecule can be added to the reaction based on the employment of DCLs to drive the end product by demonstrating the strongest affinity for the template in terms of size and noncovalent effects. This has the implication that it may be possible to select the best dendrimer chain complexes by using template molecules, such as proteins, to determine the configuration with the highest binding affinity.

## 5.2 Aims and Objectives

The development of macro-ligands that can interact with vast protein binding surfaces could offer a very effective strategic approach to inhibiting disease-related protein-protein complexes. However, importantly, dendrimers do not natively bind selectively, despite some studies showing them to be effective.

Prior investigations have revealed that carboxylate dendrimers can facilitate binding between proteins and positively charged interfacial sites. The findings of such studies also indicate that selective binding can be accomplished where the size of the dendrimer is effectively matched to the interfacial region of the protein.[15] Binding can also be enhanced by adding different amino acids to the dendrimers: the results of some binding studies show that tyrosine dendrimers bind most effectively with α-chymotrypsin, offering 30% higher affinity than non-functionalised dendrimers of similar size and charge, as seen in Figure.

Previous studies have also shown that mono-functionalised dendrimers offer improved binding. However, this approach is unsuitable for synthesising dendrimers with differing terminal groups, as the three-dimensional position of each group relative to other groups cannot be regulated. Thus, the application of dendrimers and functionalised dendrimers as protein-binding ligands became the focus of the current study.

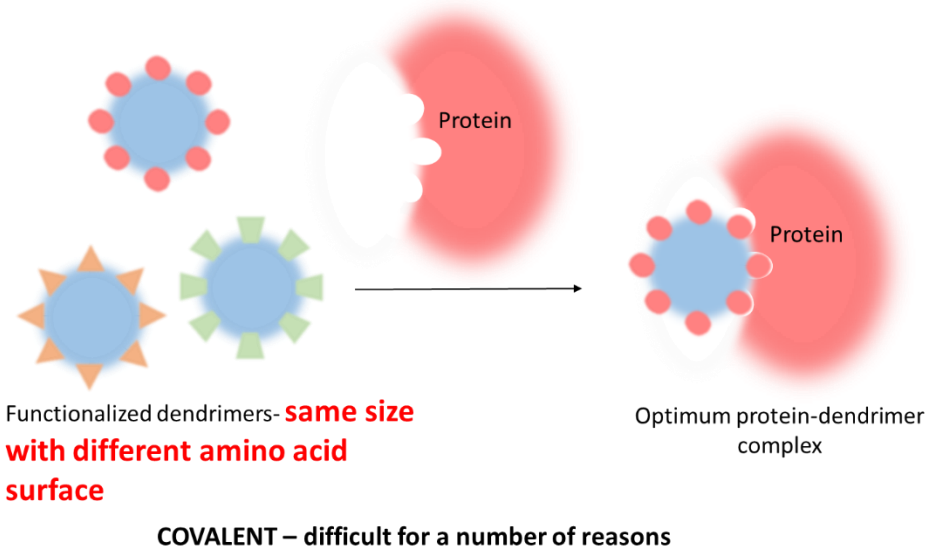


Figure 5.9: Covalently functionalised dendrimers.

Overall, the experimental results supported the assumption that the functionality and size of dendrimers are crucial in producing macromolecular ligands that can be used for selective protein binding. However, despite the findings supporting this as an unambiguous proof of concept, covalent chemistry is extremely time-consuming, as both core functionality and specific terminal groups must be incorporated. Moreover, it is often difficult to rectify design or synthesis errors, and the dendrimer ligand must be resynthesized in most cases where errors arise. Additionally, despite the relative simplicity of incorporating a single specific functional group onto the dendrimer surface (i.e. polyvalency), positioning such moieties with geometric accuracy in a relative manner is extremely complex, while the process of incorporating different numbers of functional groups to establish control multivalency in terms of their relative positions is even more complex. Nevertheless, design accuracy is critical in the covalent synthesis of any therapeutically-feasible dendrimers.

The key purpose of this research was to develop a proof-of-concept mechanism to be used to identify macromolecular ligands for specific proteins. It was thus necessary to develop a system that enabled proteins to “select” the best ligand from a large pool of functionalised macromolecular ligands. This study thus created a non-covalent approach to building target groups in and around a dendrimer framework, with a target protein required to control the relative positions of target groups, ultimately guiding the development of an effective macromolecular protein-ligand.

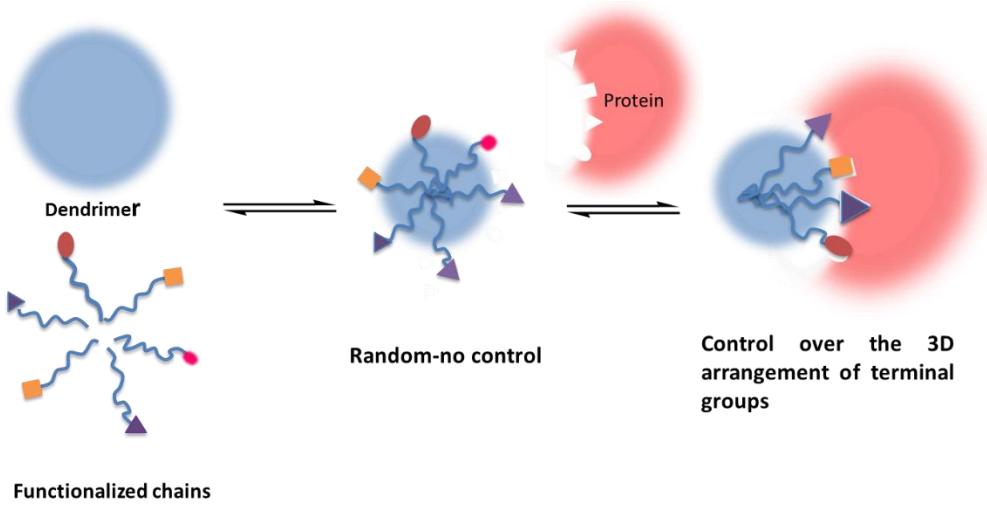


Figure 5.1012: Dynamic multivalent non-covalent method.

As shown in Figure 5.1012, this work developed a new, to improve non-covalent technique. The first objective of this work was to examine the parameters required to maximise the linear chain's encapsulation, including the required hydrophobicity, taking into account the impacts of any extra binding such as hydrogen bonds.

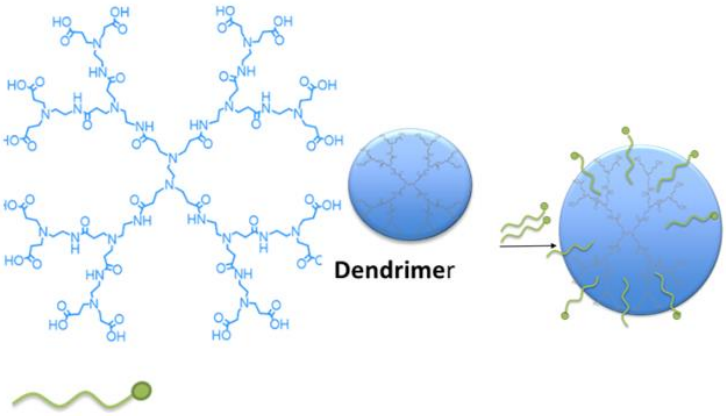


Figure 5.11: Linear chains needed to optimise encapsulation within the dendrimer.

The assessment of binding will take place when functionalized chains are added, despite the fact that binding could not be detected with merely the neutral dendrimer. This will imply that the protein template of α-chymotrypsin (Chy) is under control of the three-dimensional arrangement of terminal groups. Therefore, the functionalized dendrimer's protein binding was assessed using an enzyme inhibition experiment.

The study's second goal is to ascertain the significance and potency of the polyvalent interactions that occur when amino acids bind to proteins. The dendrimers functionalized with amino acids that are implicated in protein-protein binding, if this method is effective, should bind strongly to the surface of -chymotrypsin and suppress its activity Figure(1). Despite the fact that binding could not be identified by utilising only the neutral dendrimer, the assessment of Figure(2), on the other hand, because valine is unrelated to protein binding, a dendrimer functionalized with it would offer less affinity and less inhibition. In the earlier work that Bogan and Twyman discussed, a similar theory was advanced.[12] If polyvalent interactions are absent or the chains' orientation is incompatible with binding, there won't be any change in binding when it will happen when will be place.

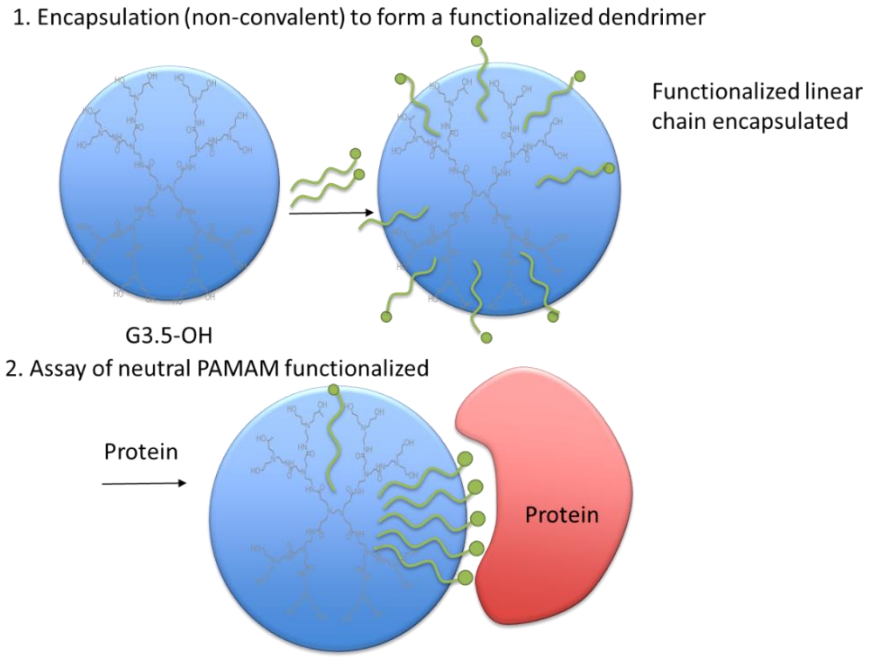


**Figure 5.12**: cooperative contacts between the amino acid and the surface of the α-chymotrypsin.

## 5.3 Synthesis of linear chains

The non-covalent integration of the targeted groups was a crucial component of this process. The end of a hydrophobic linear chain specifically contains the required amino acids to attach to the inside of the dendrimer through the relevant hydrogen and hydrophobic bonding interactions. A functionalised system may therefore be created by synthesising multiple functionalised linear chains and combining them with a dendrimer (Figure 5.1).

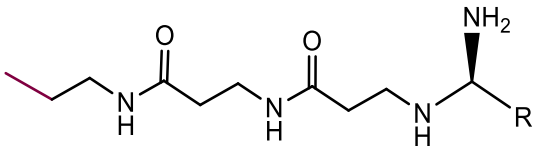


**Scheme 5.2**: Proposed linear chain with hydrophobic site

Previous studies have attempted to employ hydrophobic linear chains; however, the degree of encapsulation within the dendrimer in such cases is very poor.[54] The first step in this work was thus to determine the most straightforward way to create functionalised and hydrophobic linear chains where each has three hydrogen bonding sites, in order to research which method then enclosed the PAMAM dendrimer most effectively.

### 5.3.1 The three amide H-bonding linear chains

The creation of a linear chain that could support three hydrogen bond interactions within the dendrimer was the next step. A smaller alkyl amine was used to create the chain. In a way analogous to that of the other linear chains, it was enlarged by reiterative addition of -alanine **17**.To add the extra amide while keeping the chain length the same, the synthesis began with a shorter alkyl chain. The -alanine **17** was protected with Boc as before, and amide **18** was generated by using the same technique. By using $^{1}$H NMR, the structure of the Boc protection was characterised, and the wide singlets at 2.23 ppm and 3.50 ppm were obtained.

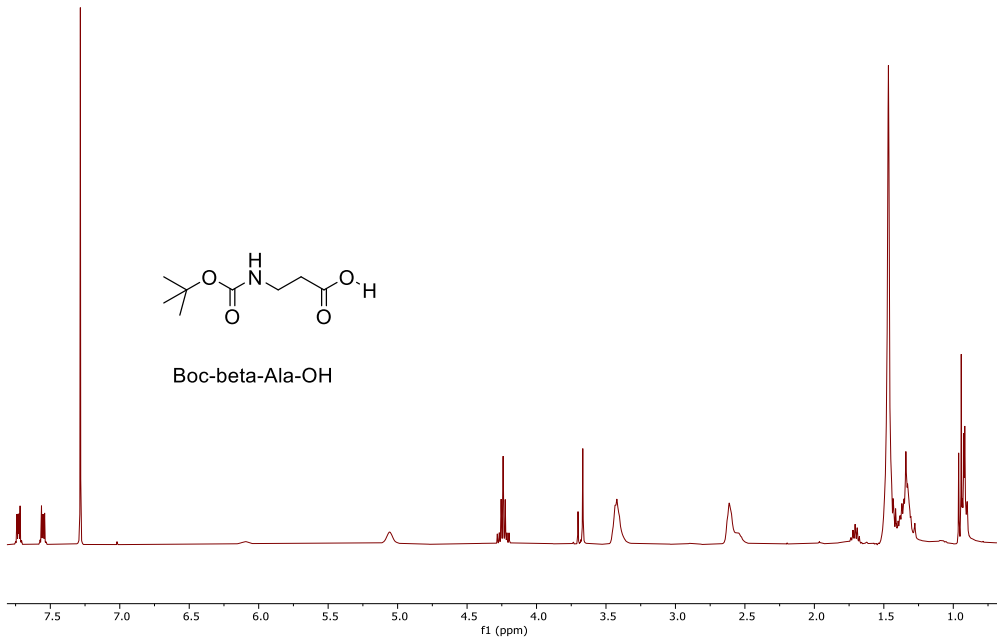


Figure 5.13: $^{1}$H NMR spectrum of chain **18** showing impurities

The production of Boc amide **18** was demonstrated by mass spectrometry, which produced a peak at 212 ($MNa^+$) and at 188 ($MH^+$).

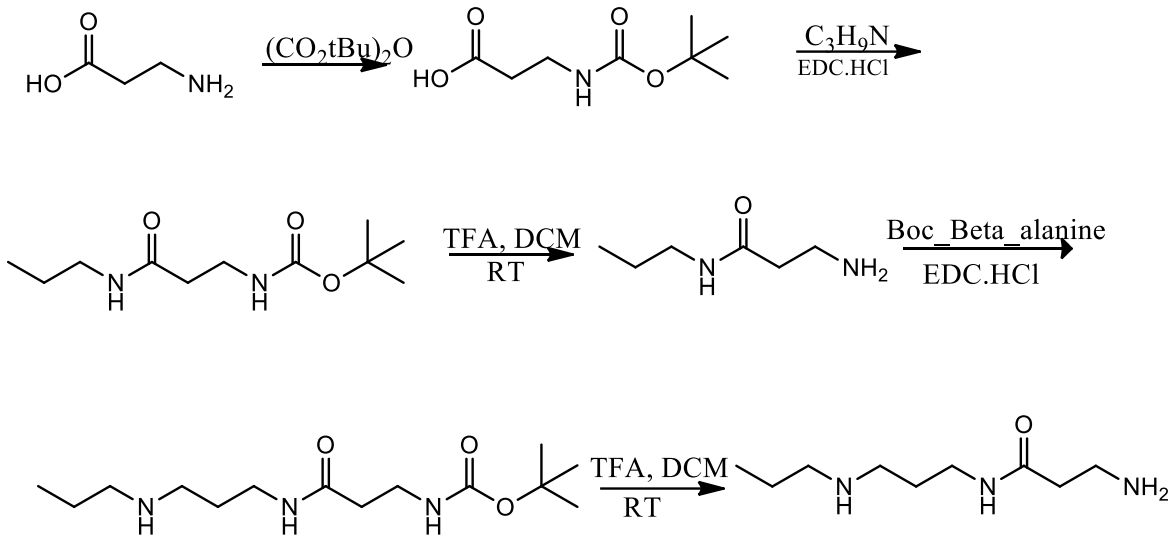


Scheme 5.3: Synthetic of linear chains

Propylamine and chain **18** were joined in the subsequent process in order to produce diamide **19**, as depicted in Scheme 8. At 1.46 ppm, the Boc group's signal was detected; it integrated as 9H. The presence of a molecular ion at 231 for the $MH^+$ ion in the ES-MS spectrum provided a further indication that pure protected chain **19** had been synthesised. It was necessary to extract the Boc group once the protected chain **19** had been successfully synthesised. TFA was removed as previously mentioned, and the chain was deprotected. TFA elimination was ensured by monitoring the pH of the solution. Boc elimination was evident from the absence of the peak at 1.45 ppm (Boc signal) in the $^1H$ NMR study. A mass spectrum ion at 131 also supported deprotection achieved.

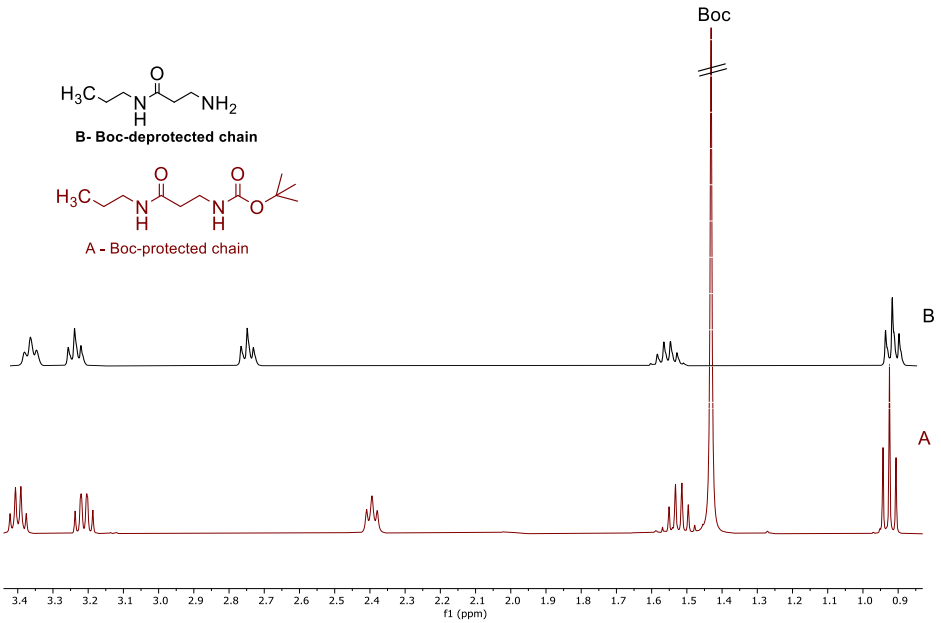


Figure 5.14: $^{1}$H NMR of **19** and **20**

The coupling of a second Boc-alanine group to the chain was accomplished by repeating the EDC coupling. The deprotected molecule was more polar in this instance. Amide **20** was insoluble; DCM was therefore ineffective as a solvent and so tetrahydrofuran (THF) wamids used in its place. Prominent singlet and triplet peaks for the Boc group and the terminal methyl moiety were visible in the 1H NMR spectra at 1.42 ppm and 0.93 ppm, respectively, and were consistent with the product. Mass spectrometry confirmed that the Amide **20** was present.

Once the linear chain was completed, the tyrosine and valine terminal groups had to be added. Figure 1.37 depicts the coupling/deprotection procedures that were used to synthesise the tyrosine and valine chains. The protected 3 HB-Boc-tyrosine chain Amide **20** was successfully synthesised. Mass spectrometry, which revealed at 487.5 ($MNa^{+}$), supported this.

By employing $^{1}$H NMR and mass spectrometry, Boc deprotection with TFA was accomplished. The NMR spectra no longer contained the singlet from the Boc group at 1.4 ppm. The mass spectrum showed a peak at 323 ($MNa^{+}$) and a peak at 299 that corresponded to the molecular ion ($MH^{+}$). This demonstrated that 3HB-LC-Tyr Amide **22** had been prepared with impurities.

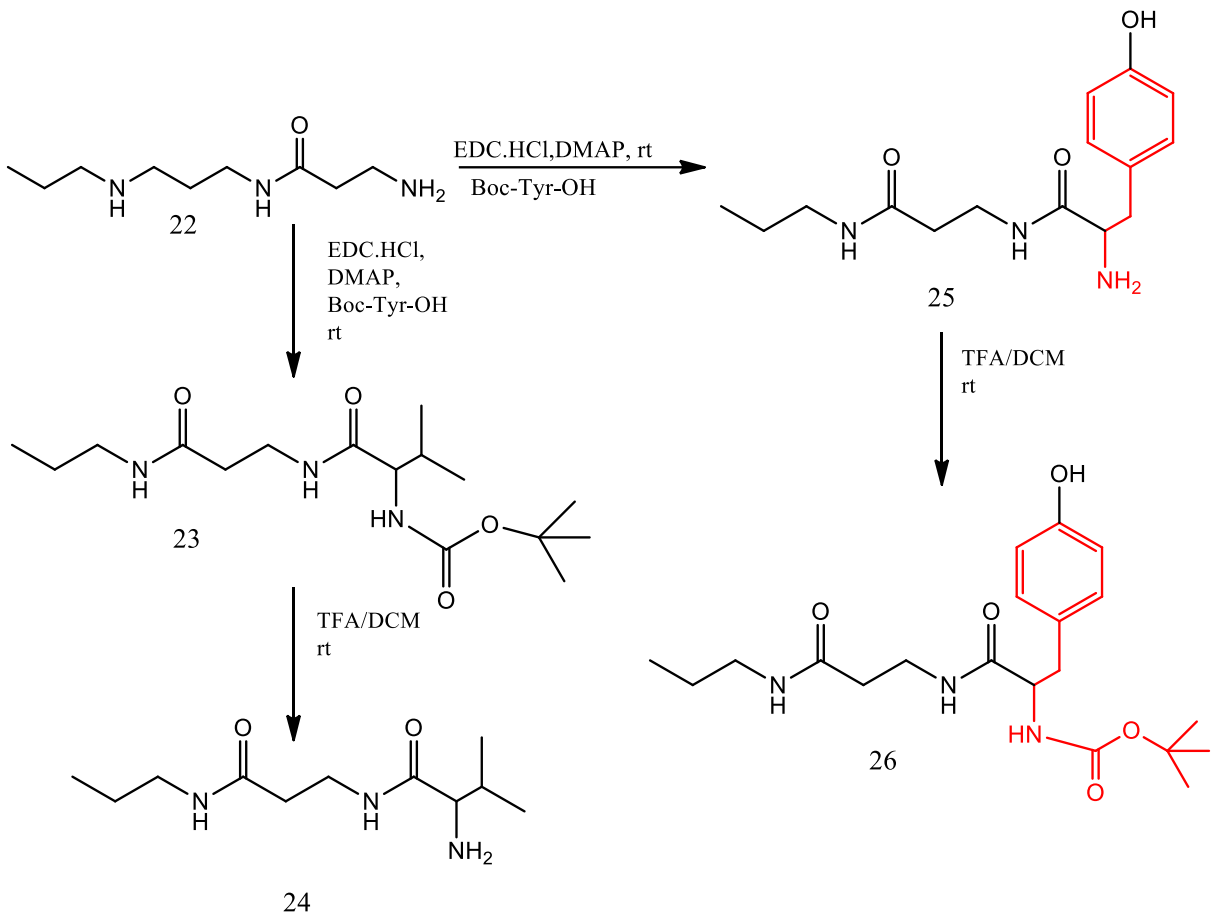


Figure 5.15: shows the process for making the three amides using valine and tyrosine.

In conclusion, the linear chain with a three hydrogen bonding system was difficult to synthesise. However, it had the potential for greater dendrimer encapsulation and, consequently, improved protein binding. Thus, the chain with impurities was still used for the

next study. The created linear chains were subsequently tested so as to establish how well they could fit within a dendrimer in the following stage.

### 5.3.2 Functionalised linear chain encapsulation

As previously indicated, a technique for improving the solubility of pharmaceuticals was identified for this work based on the encapsulation of hydrophobic compounds. The chosen dendrimer for such processes must be water-soluble in order to be organised and **shaped as a** scaffold for the functionalised linear chain, a process that guarantees that the ligand formed is in the same aqueous phase as the protein. The terminal groups of the dendrimer must also be inactive and neutral, so that without any encapsulated functionality, the dendrimer cannot react, bind, or interact with the protein's binding surface.

The inclusion of the binding must not be hindered or constrained by a dense shell or a densely packed structure, and the dendrimer must be sufficiently large to represent the whole size of the target protein's interfacial area.[84, 85] Thus, the scaffold unit was chosen to be the neutral PAMAM **10**, which has 32 end OH groups and a maximum addressable area of 1,200 $A^{o}_{2}$.[86]

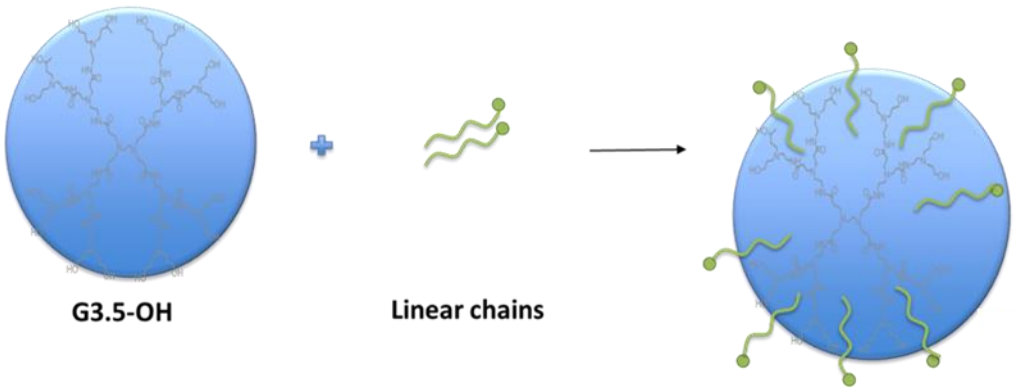


Figure 5.16: The creation of a functionalised dendrimer by encasing a linear chain in G 3.5-OH.

The next step entailed encasing or incorporating the targeting or binding components within the dendrimer's interior. H-bonding interactions π-interactions, electrostatic, and hydrophobic,

were preferred, as the driving forces for encapsulation, which was accomplished by choosing a number of hydrophobic oligomeric amide chains that terminated with amino acids, creating binding functionality. A tyrosine-terminated chain Amide **26** was chosen as the binding/recognition motif for this proof-of-concept experiment, while a valine-terminated chain Amide **39** was chosen as the control, as these amino acids are known to considerably improve or significantly degrade protein-protein interactions, respectively.[87]

An approach comparable to that utilised to solubilise and encapsulate hydrophobic pharmaceuticals within water-soluble PAMAM dendrimers was used to encapsulate the linear chains within the G 3.5-OH dendrimer 10.[88] This step had to be followed using the impure linear chains due to time constraints on this research, however. With respect to the linear chains, methanolic solutions of dendrimer 10 were supplemented with 10 equivalents of each linear chain.

A known volume of buffer (0.01M PBS, pH 7.4) was supplied after the methanol was removed, resulting in a final dendrimer concentration of $1x\ 10^{-6}$ M. As stated in Table 4, the dendrimer's percentage of encapsulated chains was then determined, and each absorbance was divided by the linear chains' extinction coefficient (ε). The dendrimer's concentration was also divided by the functionalised chain's concentration to determine the loading encapsulation.

Meijer[25] employed a similar technique to create dendrimer complexes that can aggregate upon dilution. The experiment was thus carried out again for 3HB-LC-Tyr **26** and 3HB-LC-Val **24**, with encapsulation within the dendrimer confirmed when the bathochromic reading shifted from 270 nm to 275 nm. Six of the chains were found to be enclosed within the dendrimer through supramolecular/non-covalent interactions, and the neutral dendrimer's capability to serve as a scaffold for the linear chain was also confirmed. The next phase thus entailed a series of binding studies to determine whether or not the self-assembled complex could bind to

proteins and, moreover, be detected having done so. This was completed after the encapsulation of the individual components was established and quantified.

### 5.3.3 Conclusions

All dendrimers were fully synthesised, yet the linear chains were not fully achieved due to the impurities that arose. The results of the tests confirmed the importance of size and functionality in the development of macromolecular ligands for specific protein binding.

This research focused on the synthesis of neutral dendrimers with OH ends from ester-terminated dendrimers, which were then given terminal OH groups by adding ethanolamine. With a constant dendrimer concentration of 1.0 $x10^{-5}$ M, a 10 fold excess of linear chains was employed to determine the dendrimer's maximal loading capacity. UV spectroscopy was then used to determine the degree of encapsulation, with results that revealed that more three H-bonding chains could be encapsulated than any other chains; in particular, using the 3 H-bonding system, all 10 linear chains could be enclosed. Meijer[25] utilised a similar technique to create dendrimer complexes that could aggregate upon dilution, yet future research should focus on the purification of 3 H-bonding systems and the development of new methods to achieve this in order to determine which will bind the target protein most effectively. In general, the current work was interested in which complex would best balance protein binding with ease of synthesis, however. The next step was thus to evaluate these complexes' ability to inhibit bonding.

## 5.4 Results and Discussion

### 5.4.1 Design and synthesis of materials.

This novel method builds an idealised macromolecular ligand around a protein template using non-covalent chemistry. Figure depicts the design and process schematically. Water is used to

assemble the dendrimer, its binding components, and a sensing element into random complex **1**. The randomly positioned binding units are unrestricted within the dendrimer and can roam around freely to optimise any cooperative protein-binding interactions when the protein is added. By altering the photophysical characteristics of an enclosed sensing group, the binding can then be identified and quantified.

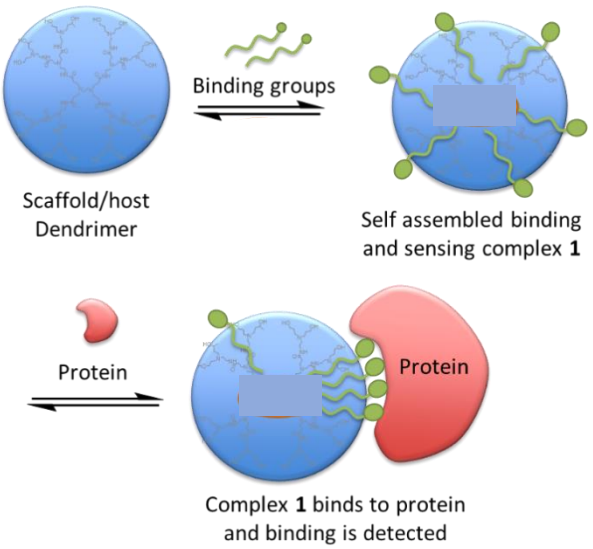


.

Figure 5.17: Self-assembled protein binding complex 1 and its binding to a target protein

The binding and sensing units are supported and enclosed by a neutral/non-binding dendrimer, which serves as a scaffold. When a target protein is present, the utilisation of non-covalent chemistry enables the targeting groups to move and increase the strength of their binding.

This design concept requires three distinct components. To maintain the protein and the formed ligand in the same aqueous phase, the dendrimer must be water-soluble. The terminal groups of the dendrimer must also be inactive and neutral as, in the presence of any encapsulated functionality, the dendrimer must not react, bind, or interact in any manner with the protein's binding surface.

The dendrimer also needs to be big enough to cover the entire binding/interfacial area of the target protein while ensuring that the inclusion of the binding/sensing units is not hindered or constrained by a dense shell or densely packed structure.[19, 20]

An approach similar to that utilised to solubilise and encapsulate hydrophobic pharmaceuticals within water soluble PAMAM dendrimers was used to encapsulate the linear chains and the sensing unit within the G 3.5-OH dendrimer 10. For the linear chains, methanolic solutions of dendrimer 10 were mixed with 10 equivalents of linear chain. A known volume of buffer (0.01M PBS, pH 7.4) was then supplied after the methanol was removed, resulting in a final dendrimer concentration of $1.0 \times 10^{-6}$ M. After that, the solution was filtered to remove any remaining solids. All 10 linear chains were encapsulated, according to Beer Lambert analysis, which resulted in a final concentration of $.1.0 \times 10^{-5}$ M for the 3HBLC-Tyr and 3HBLC-Val molecules.

This is higher than each linear chain's solubility in water ($0.58 \times 10^{-5}$ M for LC-Val and $0.51 \times 10^{-5}$ M for 3HBLC-Tyr **11**). Additionally, when either LC-Tyr or LC-Val were encased within the dendrimer, as illustrated in Figure 13 and Figure, respectively, a 5 nanometre bathochromic shift was seen in the max.

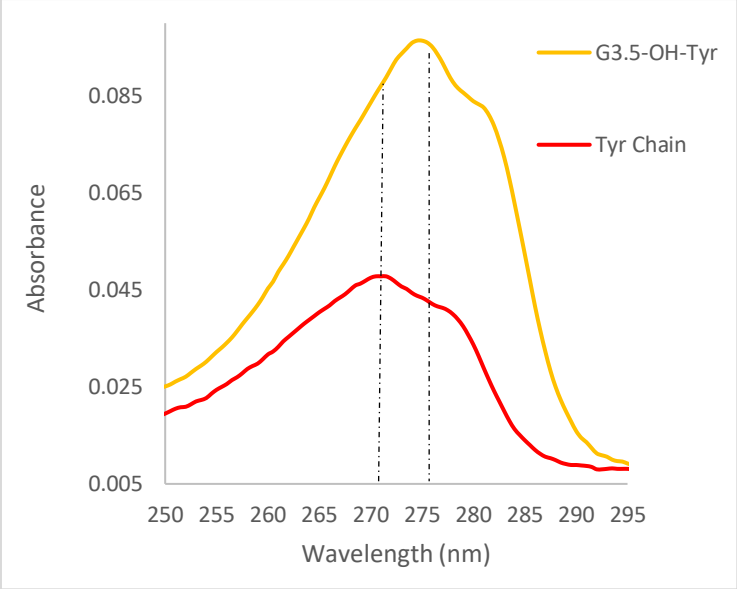


Figure 13: UV spectra of the free of tyrosine and encapsulated 3HBLC-Tyr n at buffer pH 7.4.

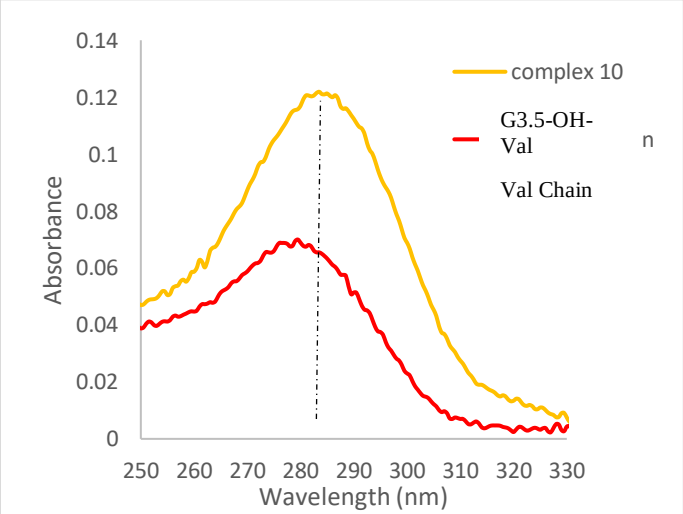


Figure 5.19: UV spectra of the free and encapsulated 3HBLC-Val chains at buffer pH 7.4.

The internal groups of the dendrimer replace of the water solvating the linear chains in this shift, which is compatible with a difference in the environment. The solubility and spectroscopic results for the 3-H bound systems showed that all 10 linear chains were contained within the dendrimer. Shifts in the max once more served as evidence and confirmation of

encapsulation. Hydrophobic and H-bonding interactions are thought to have worked in concert to drive this complexation, as seen in Figure 14.

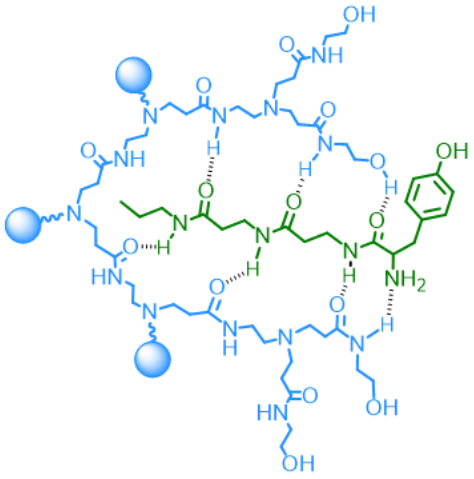

Figure 14: A section of the G3.5-OH dendrimer depicted with the linear chain (3HBLC-Tyr).

### 5.4.2 Inhibition using 3 hydrogen bonding chain

The inhibition and binding investigations were carried out with a groupmate using the identical procedures as for the hydrogen bonding system (Dr Ibrahim Althobaiti). Author contributions made up 60 % of the works. Utilizing simply BTNA and Chy in buffer, the first experiment served as a control to determine the maximum enzyme velocity (pH 7.46). This gave the uninhibited reaction's starting rate (nitroaniline production). Then, in order to establish the kinetic data, we performed binding and inhibition tests employing the three linear H-bonding chains. Tables 8 and 9 include the information that is seen in Figure.19.

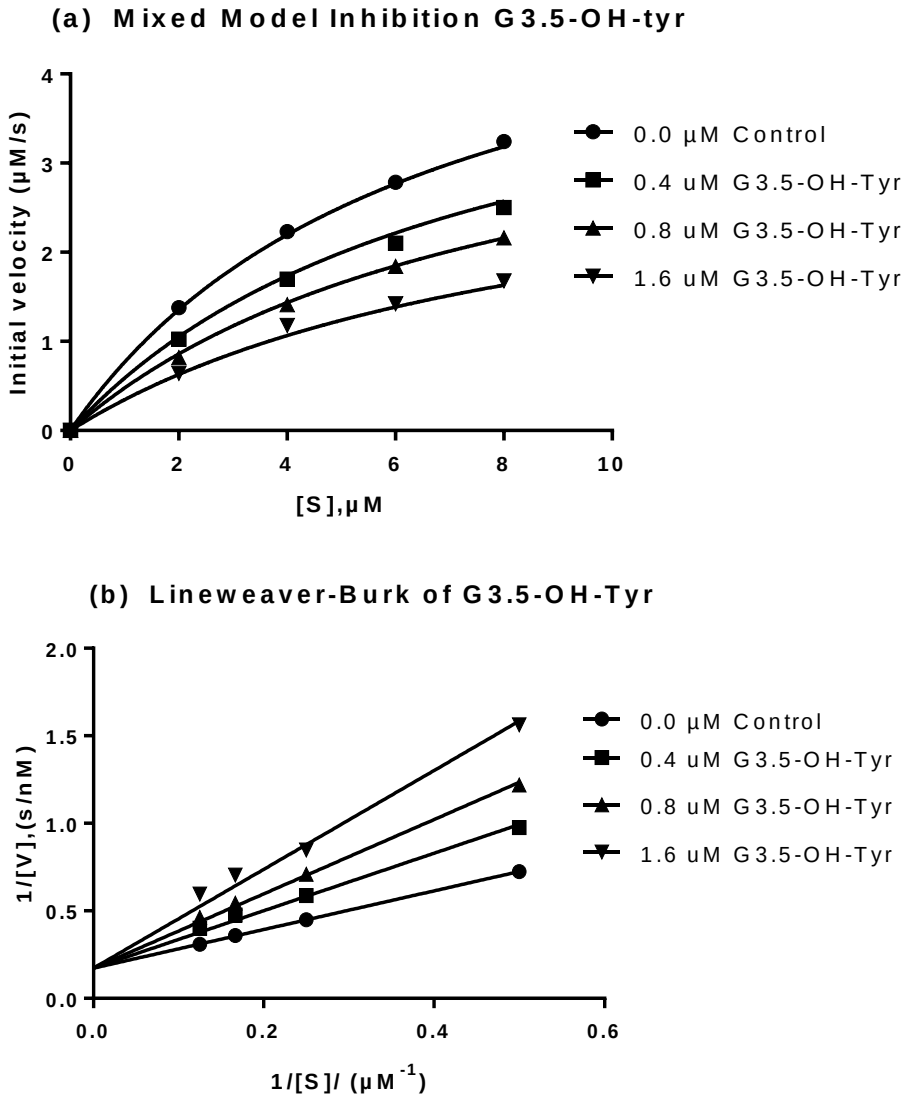


**Figure 15**: For 3HB-LC-Tyr-Tyr at 0.4 M of Chy, (a) mixed mode inhibition and (b) Lineweaver-Burk plots are shown.

Overall, the data supported our hypotheses about the populations at interfacial/binding sites and the availability of amino acids. The binding affinity of functionalized dendrimers further demonstrated that the 3HB-LC-Tyr bound chymotrypsin significantly more strongly than the 3HB-LC-Val functionalized dendrimers, which displayed very little inhibition and subsequently the weakest binding. The beginning rates at the greatest substrate concentrations are shown in Table 5.2. These

concentrations inhibited the tyrosine systems by 48 %. The valine system did, however, bind very weakly, blocking only 8 % (5%).

| Kinetic inhibition data | Control /non-functionalized G3.5-OH | 3HB-LC-Val | 3HB-LC-Tyr |
|---|---|---|---|
| Initial velocity (V), nMs-1 | 3.240 (±0.217) | 2.995 (±0.321) | 1.680 (±0.771 |
| Percentage Inhibition (%) | 0 | 8 | 48 |

**Table5.2:** Initial Velocity converted to percentage of inhibition

| Inhibitor | $K_m$, µM | $K_i$, µM | α |
|---|---|---|---|
| 3HB-LC-Val | 5.50 | 24.60 | 0.85 |
| 3HB-LC -Tyr | 6.56 | 1.23 | 1.23 |

**Table 5.3**: Kinetic parameters of 3HB

Table 5.3 summarises the kinetic and inhibition results. The Lineweaver-Burk plots and values further demonstrated the competitive inhibitory nature of the 3 H-bonding systems, with the 3HB-LC-Tyr having a value of 1.23. Dendrimers that had been given a valine chain functionalization had very poor binding and non-competitive inhibition (= 0.85).

This was once again anticipated. Valine only has limited hydrophobic binding ability, which resulted in a high $K_i$ value of 24.60 M, since it lacks the necessary functionality to engage, whether electrostatically or by H-bonding, aromatic, or - π–π interaction. Tyr, on the other hand, has a $K_i$ value of 1.93 M. An additional piece of evidence supporting the uncompetitive binding mechanism came from a Lineweaver-Burk plot that did not exhibit a common y-intercept. Tyrosine binding was nevertheless more effective than valine, which is explained by the contacts and hydrogen bonding interactions made possible by the tyrosine activity. A further

hydrogen bond on the linear chain maximises its interaction with the dendrimer. Overall, the findings support how crucial hydrogen bonding and the functioning of amino acids.

## 5.5 Conclusions

This work has demonstrated a macro supramolecular technique that has the potential to create novel ligands that can bind specifically or selectively to sizable interfacial binding regions as seen on the surface of target proteins. Although covalently functionalised macromolecules demonstrate promise in this regard, it has previously been challenging to functionalise their surfaces and impossible to manage their relative position with respect to any 3-dimensional geometric constraints within functional groups.

For the creation of macromolecular protein ligands to bind and detect proteins, a supramolecular technique was adopted. The technique made use of a dendrimer scaffold that could accommodate both a targeting/binding group and a sensing group via encapsulation. Hydrophobic, electrostatic, and hydrogen forces were thus combined to create encapsulation. In particular, linear amide chains ending in tyrosine and valine, amino acids known to either significantly or poorly contribute to protein-protein binding affinities, were created. The impure linear chains and dendrimers were combined at a 10:1 ratio to create self-assembling complexes. The linear chain's water solubility was increased by encapsulation, and complexation was verified by UV, which showed a 5 nm bathochromic shift in the linear chain's maximum.

In protein binding assays, it was also noted how crucial it was to maximise the hydrogen bonding contacts between the linear chain and the dendrimer (enzyme inhibition). The dendrimer-encapsulated 3HB-LC-Tyr system was the best overall, with a Ki value of 1.23 M, 25 % higher than 3HB-LC-Val. The outcomes also confirmed the importance of tyrosine as a

protein targeting group. It was crucial to confirm that none of the components individually inhibited the enzyme. This was accomplished by control studies that demonstrated the necessity of both the dendrimer and the linear chain for binding. If either were utilised independently, no binding would be shown.

Future research should be undertaken to find a new method for the synthesis of linear chains, as the chains used in this case featured impurities. This would require combining a range of targeting groups and examining a variety of additional proteins, in addition to creating strategies to fix or trap the linear chains within the dendrimers.

# CHAPTER 6
# Experimental

## 6.0 Experimental details

**Materials**. All chemicals and solvents used were bought commercially (mainly from Sigma-Aldrich) and utilised directly. Dry solvents were obtained through the Grubbs solvent dispensing equipment at the University of Sheffield's Chemistry Department. Before use, all glassware was washed and dried in a 100 °C oven overnight.

**UV spectrum analysis**. WinASPECT was used to evaluate the absorbance data collected using an Analytic Jena AG Specord s600 UV/vis spectrometer. Spectroscopy was performed in the infrared using a **Perkin-Elmer UATR Infrared spectrometer**. Wave numbers were used to indicate the positions of peaks in the spectra, which were then examined using Spectrum100 software ($cm^{-1}$). Spectroscopy of fluorescence at 25 °C was performed, with emissions measured using a **Perkin Elmer Fluoromax-4 Spectrofluorometer,** and FluorEssence V3 software used to analyse the resulting spectra. **Spectroscopy with an NMR system Sigma Aldrich provided deuterated solvents**, and these were used to produce all NMR samples. Spectra were captured using a Brucker AV1400 MHz device for 1H NMR and 13C NMR. Chemical shifts were expressed in ppm, while coupling constants were expressed in Hertz with respect to the signals from the remaining solvents. Topspin 3.0 NMR software was used to analyse the NMR spectra. Spectrometry using a Bruker reflex III MALDI-ToF mass spectrometer was also used to analyse the dendrimers, while e**lectrospray ionisation (ES)** and a Waters LCT Premier XE spectrometer were employed for all other samples. Agilent 6530 Accurate-Mass Q-TQF LC/MS with High Resolution was employed, while

## 6.1 PAMAM dendrimers synthesis

### PAMAM dendrimer G0.5

Instead of using the full generation dendrimer, the conventional procedure for the production of the half-generation dendrimer was used to stir a combination of ethylenediamine (EDA; 10

mL, 0.15 mol), methyl acrylate (57 mL, 0.63 mol), and methanol (50 mL) for 24 hours (G0.5 PAMAM). The combination was then rinsed as previously mentioned to produce the desired result, which was a yellow oil (64.0 g, 106 percent residual solvent). The following description of the product was given:

FTIR ($v_{max}/cm^{-1}$) measurements include 2963, 2900, 1755, and 1183; $^{1}H$ NMR (,400 MHz, MeOD) measurements include 2.50 (8H, t, J 7.0), 2.66 (4H, s), 2.88 (8H, t, J 7.0), and 3.76 (12H, s); $^{13}C$ NMR (,400 MHz, MeOD) measurements include 35.0, 51.5, 52.3, 51.5, and 175.5; MS (ES) $C_{18}$ $H_{32}$ $N_2$ $O_8$ = 405 ($MH^+$)

**Dendrimer G1.0 PAMAM**

The normal procedure for the synthesis of the complete generation dendrimer was followed, and a mixture of the G0.5 PAMAM dendrimer (53.0 g, 0.13 mol), EDA (175 mL, 2.6 mol), and methanol (230 mL) was agitated for 4 days. The combination was then cleaned as previously mentioned to get the desired result, which was a viscous, sticky, dark amber oil (70.9 g, 106 percent residual solvent). The following description of the product was given:

FTIR ($v_{max}/cm^{-1}$) measurements include 3315, 2980, 2833, 1640, 1555, and 1045 $cm^{-1}$; $^{1}H$ NMR (400 MHz, MeOD) measurements include 2.44 (8H, t, J 7.0), 2.63 (4H, s), 2.88 (8H, t, J 6.0), 2.63 (8H, t, J 7.0), 3.35 (8H, t, J 6.0), and 3.51 (4H, s); $^{13}C$ NMR: 31.5, 42.3, 50.3, and 52.5 MS (ES)$C_{22}$ $H_{48}$ $N_{10}$ $O_4$ 516 ($MH^+$)

**Dendrimer G1.5 PAMAM**

Following the conventional procedure for the production of the half-generation dendrimer, a mixture of the G1.0 PAMAM dendrimer (38.5 g, 0.07 mol), methyl acrylate (107 mL, 1.18 mol), and methanol (350 mL) was agitated for 48 hours. The combination was then rinsed as

previously mentioned to produce the intended end product, which was a brown oil (74.4 g, 88 percent ). The following description of the product was given:

FTIR ($\nu_{max}$/ $cm^{-1}$): 3504, 2866, 2968, 1745, 1631, 1533, and 1100; $^{1}H$ NMR (400 MHz, MeOD): 2.55 (8H, t, J 7.0), 2.51 (16H, t, J 7.0), 2.65 (8H, t, J 6.5), 2.77 (4H, s), 2.92 (24H, m), 3.34 (8H, t, J 6.5), 3.44 (4H, s) 3.75 (24H, s); $^{13}C$ NMR (400 MHz, MeOD): 51.5, 52.3, 51.4, 48.7, 39.0, 35.5, and 175.5; MS (ES) $C_{54}H_{96}N_{10}O_{20}$ = 1205 ($MH^{+}$),

**Dendrimer G2.0 PAMAM**

The normal procedure for the synthesis of the full-generation dendrimer was followed, and a mixture of the G1.5 PAMAM dendrimer (63.6 g, 0.053 mol), EDA (282 mL, 4.22 mol), and methanol (250 mL) was agitated for 7 days. After washing the combination, the desired product—a viscous, sticky, dark amber oil—was obtained (86.7 g, 114 percent residual solvent). The following description of the product was given:

: FTIR ($\nu_{max/}$ $cm^{-1}$): 2888, 2900 ,1645 , 1545 , 1100 $cm^{-1}$; $^{1}H$ NMR (400 MHz, MeOD): 2.44 (24H, t, J 6.5), 2.56 (12H, m), 2.67 (16H, t, J 6.5), 2.79 (24H, tr, J 7.0), 3.13 (24H, t, J 6.5), 3.44 (12H, s); $^{13}C$ NMR ( 400 MHz, MeOD): 55.6, 50.3, 42.5, 42.0, 38.7, 34.5, 32.5 ,174.5 ,176.7 ; MS (ES) $C_{62}$ $H_{128}$ $N_{26}$ $O_{12}$ = 1429 ($MH^{+}$)

**Dendrimer G2.5 PAMAM**

According to the conventional procedure for the manufacture of the half-generation dendrimer, a mixture of the G2.0 PAMAM dendrimer ( 51.0g, 0.035 mol), methyl acrylate (, 105 mL, 1.15 mol), and methanol (, 350 mL) was agitated for 72 h. After washing the mixture, the desired product—a thick, brown oil was obtained (87.3 g, 86 %). The following description of the product was given:

FTIR ($\nu_{max/}$ $cm^{-1}$): 3333, 2798 , 1755, 1638 , 1555 $cm^{-1}$; $^{1}H$ NMR ( 400 MHz, MeOD): 2.55 (24H, J 7.0), 2.53 (32H, t, J 7.0), 2.73 (28H, m), 2.96 (56H, m), 3.14 (24H, t, J 6.5), 3.55 (12H, s) ,3.88 (48H, s ); $^{13}C$ NMR (400 MHz ,MeOD): 51.0 , 53.4, 53.1, 50.0, 49.8, 36.5, 34.5, 33.6, 32.0, 31.5 ,176.7; $C_{126}$ $H_{224}$ $N_{26}$ $O_{44}$ 2807 ($MH^{+}$)

**G3.0 PAMAM dendrimer**

The normal procedure for the synthesis of the full-generation dendrimer was followed, and a mixture of the G2.5 PAMAM dendrimer (44.2 g, 0.0158 mol), EDA (2.50 mol, 167 mL), and methanol (200 mL) was agitated for 6 days. After washing the combination, the desired product—a viscous, sticky, dark amber oil was obtained (51.3 g, 100 %). The product's attributes were as follows:: FTIR ($\nu_{max/}$ $cm^{-1}$): 3300, 3216 ,3000, 2760, 1800,1645 ,1100; $^{1}H$ NMR (400 MHz, MeOD): 2.44 (56H, t, J 6.5), 2.56 (28H, m), 2.67 (24H, t, J 6.5), 2.79 (56H, t, J 6.5), 3.30 (56H, t, J 6.5) , 3.44 (28H, s); $^{13}C$ NMR (400 MHz, MeOD): 55.5, 48.7, 43.4, 41.5, 38.9, 37.6 ,176.7, 178.9 ; $C_{142}$ $H_{288}$ $N_{58}$ $O_{28}$ 3256 ($MH^{+}$)

## 6.2 Functionalized PAMAM PAMAM

**G3.5-OH dendrimer synthesis**

In 7 mL of anhydrous DMSO with potassium carbonate, a PAMAM G3.5 dendrimer (11.07g, 1.83 mmol) with 32 terminal methyl ester groups was mixed (9.1 g, 66 mmol). The mixture was heated at 50 $^{o}C$ for 72 hours while being agitated and ethanolamine (4.42 g, 72 mmol) was added. The solid residues in the crude product were filtered out under reduced pressure, and the solution was then placed to a large conical flask. The crude product produced a thick oil or paste at the bottom of the flask after acetone (600 mL) was added. Carefully decanting the acetone off, enough distilled water was added to dissolve the substance (5 mL). With the least amount of acetone possible, the product was precipitated, then let to settle. The initial solid

result turned out to be hydroscopic and, when left, quickly turned into a paste. After decanting the acetone, the precipitation process was carried out once more. The result was dissolved in methanol and placed to a flask with a round bottom, where the solvents were extracted under vacuum to provide the final PAMAM-G3.5 OH dendrimer, which was a 90 percent pale yellow/cream paste. synthesis of a linear chain with two hydrogen bonds.

FTIR ($\nu_{max}/cm^{-1}$), 3500, 3623, 2987, 2900, 1633, 1553; $^{1}H$ NMR (400 MHz, $D_2O$), 3.76 (62H, *t*, J 7.0), 3.55 (120H, *m*), 2.80 (120H, *m*), 2.63 (60H, *t*, J 7.0), 2.44 (120H, m); $^{13}C$ NMR (100 MHz, $D_2O$), 176.7, 174.2, 63.4, 56.7, 53.0 , 50.0, 45.3, 43.3 , 38.9 , 34.0; MS (ES), $C_{302}H_{576}N_{90}O_{92}$ [MH+]: 6940

## 6.3 Synthesis of three hydrogen bond

### Boc-protected amide chain

DCM was used to dissolve n-propylamine 15 (1.1 g, 0.017 mol), boc-alanine 16 (3.40 g, 0.017 mol), and DMAP (4.39 g, 0.035 mol) (100 mL). Triethylamine (5.16 g, 0.0506 mol), EDC.HCl (3.44 g, 0.017 mol), and other ingredients were added, and the mixture was agitated under nitrogen for 24 hours. The mixture was moved to a separating funnel, where the crude product was washed with brine solution (3100 mL), and the aqueous layers were extracted using DCM. $Mg_2SO_4$ was used to collect and dry the organic layers. The Boc protected chain 17 (3.96 g, 96 percent) was obtained as a white powder after the solvent was condensed at decreased pressure and dried under a high vacuum.

FTIR ($\nu_{max}/cm^{-1}$) , 3544, 3001, 1632, 1588, 1544; $^{1}H$ NMR (400 MHz; $CDCl_3$) 5.60 (1H, *s*), 5.55 (1H, *s*), 3.51 (2H, *q*, J 7.0), 3.33 (2H, *q*, J 7.0), 2.35 (2H, *t*, J 7.0), 1.66 (2H, *m*), 1.55 (9H, *s*), 0.98 (3H, *t*, J 7.0); $^{13}C$ NMR (100 MHz; $CDCl_3$); 173.4, 156.5, 81.2, 44.3, 38.3, 37.0, 29.3, 24.5; MS (ES), $C_{11}H_{22}N_2O_3$ [MH+]: 230.

**Deprotected amide chain**

DCM (25 mL) was used to dissolve Boc protected chain 17 (3.0 g, 0.013 mol), then TFA (25 mL) was added. For 24 hours, the solution was agitated under nitrogen before being poured into a separate funnel and given a wash with water (50 mL). A rotary evaporator was used to collect, dry ($MgSO_4$), and then remove the organic layer. A high vacuum was employed to dry the end product, which produced amide chain 18 (1.4 g, 82 %) in the form of a yellow oil that was immediately applied in the following phase.

FTIR ($\nu_{max}/cm^{-1}$), 2888, 1653, 1558; $^1$H NMR (400 MHz; $D_2O$) 3.33 (2H, *t*, J 7.0), 2.87 (2H, *t*, J 7.0), 2.66 (2H, *t*, J 7.0), 1.44 (2H, *m*), 0.86 (3H, *t*, J 7.0); $^{13}$C NMR (100 MHz; $D_2O$) 173.4, 44.4, 43.6, 37.6, 33.8, 27.8; MS (ES), $C_6H_{14}N_2O$ [M+]:131.

**Boc-protected di-amide chain**

The following ingredients were used to create the title compound: EDC.HCl (3.82 g, 0.020 mol), Boc—alanine 16( 3.8 g, 0.019 mol), deprotected amide chain (18, 2.63 g, 0.019 mol), DMAP (4.88 g, 0.04 mol), and triethylamine (6.1 g, 0.06 mol). The Boc-protected diammide chain 19 was produced as a white solid following work up and purification (4.7 g, 78 %)

FTIR ($\nu_{max}/cm^{-1}$), 3400, 2988, 2956, 2900, 1678, 1600, 1544; $^1$H NMR (400 MHz; $CDCl_3$) 6.99 (1H, *s*), 6.67 (1H, *s*), 5.44 (1H, *s*, NH), 5.25 (1H, *s*, NH), 3.62 (2H, *q*, J 7.0), 3.44 (4H, *m*), 3.23 (2H, *q*, J 7.0), 2.88 (2H, *m*), 2.54 (4H, *m*), 1.48 (2H, *m*), 1.38 (9H, *s*), 0.90 (3H, *t*); $^{13}$C NMR (100 MHz; $CDCl_3$) 176.7,155.4, 80.6,36.7, 35.6,32.6, 35.8, 30.2, 25.6, 29.8, 13.5; MS (ES), $C_{14}H_{27}N_3O_4$ [MH+]: 302.5.

**Deprotected di-amide chain**

Di-amide chain 19 that has been boco-protected (4.5 g, 0.016 mol) was dissolved in 25 mL of DCM, 25 mL of TFA was added, and the mixture was then allowed to react for 24 hours under nitrogen. The crude product was produced as a thick brown oil after the DCM was removed using a rotary evaporator. 100 mL of water was added, and it was then decanted out. The product was then dried under a strong suction after repeating this washing process twice more. The crude product was dissolved in 100 mL of DCM, twice washed with 2 mL of 2M HCl diluted in 100 mL of water, and then dried. $Mg_2SO_4$ was used to dry the organic layer, and a rotary evaporator was used to evaporate the solvent. After that, the product was placed in a high vacuum to dry. With a 93 % yield, the crude product was produced as dark oil and used immediately in the following process.

FTIR ($\nu_{max}/cm^{-1}$), 3001, 1800, 1623, 1200 and 1199; $^1$H NMR (400 MHz; $CDCl_3$), 7.77 (2H, *t*, J 7.0), 7.63 (2H, *s*), 3.44 (2H, *dd*, J 13.0, 7.0), 3.22 (4H, *s*), 3.01 (6H, *m*), 2.65 (2H, *t*, J 7.0), 2.53 (4H, *m*), 1.44 (2H, *m*), 0.97 (3H, *t*, J 7.0); $^{13}$C NMR (100 MHz; $CDCl_3$) 177.8, 172.0, 171.5, 44.5, 38.9, 37.6, 36.9, 34.5, 33.3, 27.6, 13.5; HRMS (ES), $C_9H_{19}N_3O_2$ [MH+]: 202.1

**Boc-protected tyrosine chain**

Deprotected di-amide chain 20 (1.0 g, 4.98 mmol), Boc-Tyrosine-OH (1.4 g, 4.98 mmol), DMAP (1.21 g, 9.96 mmol), triethylamine (1.52 g, 0.015 mol), and EDC.HCl were used to create the title chemical using the procedure described above for the Boc-protected amide chain 25. (0.78 g, 4.0 mmol). A pale yellow material known as the crude product was obtained, and it was refined using silica chromatography with DCM (MeOH 1 percent) as the eluent. A white powder known as Boc product chain 25 was acquired.

(1.5 g, 71%): UV (MeOH) $\lambda_{max}$ (nm) 273, 225. FTIR ($\nu_{max}/cm^{-1}$) , 3400, 3000, 2888, 2750, 1690, 1588, 1557, 1233; $^1$H NMR (400 MHz; MeOD) 7.33 (2H, *d*, J 8.5, *m*), 6.88 (2H, *d*, J

8.5), 4.32 (1H, *t*, J 7.0), 3.88 (4H, *m*), 3.22 (2H, *t*, J 7.0), 2.86 (1H, *dd*, J 14.0, 7.0), 2.74 (1H, *dd*, J 14.0, 7.0), 2.44 (2H, *t*, J 7.0), 2.24 (2H, *q*, J 7.0), 1.38 (2H, *m*), 1.23 (9H, *s*), 0.98 (3H, *t*, J 7.0); $^{13}$C NMR (100 MHz; MeOD) 177.8, 177.1, 144, 135.5, 124.5, 55.7, 48.9, 40.0, 38.9, 24..5, 22.2; MS (ES) $C_{23}H_{36}N_4O_6$ [M+]: 465

**Tyrosine linear chain - 3HB-LC-Tyr**

Using the procedure outlined above for the deprotected amide chain 26, the title compound was created using the following: Boc-protected tyrosine chain 25 (1.0 g, 2.15 mmol), DCM (20 mL), and TFA (10 mL). A white powder known as 3HB LC-Tyr 26 was acquired (510 mg, 65 %)

. UV (MeOH) $\lambda_{max}$ (nm) 287, 256. FTIR ($\nu_{max}$/cm$^{-1}$) 3678, 3334, 3000, 1634, 1601, 1456, 1200, 1120; $^{1}$H NMR (400 MHz; MeOD) 7.12 (2H, *d*, J 8.5), 7.00 (2H, *d*, J 8.5), 4.01 (1H, *t*, J 7.0), 3.55(4H, *m*), 3.23 (2H, t, J 7.0), 2.98 (1H, *dd*, J 14.0, 7.0), 2.77 (1H, *dd*, J 14.0, 7.0), 2.56 (2H, *t*, J 7.0), 2.44 (2H, *q*, J 7.0), 1.33 (2H, *m*), 0.94 (3H, *t*, J 7.0); $^{13}$C NMR (100 MHz; MeOD) 176.6, 175.0, 173.0 , 140.0, 135.5, 116.8, 65.5, 44.4, 39.6, 35.6, 33.2, 31.0, 28.7, 27.6, 15.0, HRMS (ES), $C_9H_{19}N_3O_2$ [MH+]: 425.9 ( with impurities)

**Boc-protected valine chain**

Deprotected diamide chain 20 (1.0 g, 4.98 mmol), Boc-Valine-OH (1.1 g, 4.98 mmol), DMAP (1.21 g, 9.96 mmol), triethylamine (1.52 g, 0.015 mol), and EDC.HCl were used in the synthesis and purification of the title chemical (0.78 g, 4.0 mmol).

UV (MeOH) $\lambda_{max}$ (nm) 287, 240; FTIR ($\nu_{max}$/cm$^{-1}$) , 3150 , 1700 , 1560, 1400, 1200 and 1199 ; $^{1}$H NMR (400 MHz; MeOD), 5.03 (1H, *d*, J 5.5), 3.66 (4H, *m*), 3.25 (2H, *t*, J 7.0), 2.77 (1H, *sept*), 2.55 (2H, *t*, J 7.0), 2.42 (2H, *q* J 7.0), 1.58 (2H, *m*), 1.54 (9H, *s*), 0.98- 0.95 (6H, *d*), 0.92 (3H, *t*, J 7.5); $^{13}$C NMR (100 MHz; MeOD) 175.6, 173.5, 163.6, 86.5, 70.0, 46.8, 40.0, 38.9,

33.5 , 30.0 , 20.0,18.0; 72 % yield ; MS (ES), Calculated for $C_{19}H_{36}N_4O_5$ [M+]: 400, found 401.

**Valine linear chain – 3HB-LC-Val**

The Boc-protected valine chain 27 (1.0 g, 2.50 mmol), DCM (20 mL), and TFA were used in the process described above for the deprotected amide chain 28 to create the title compound (10 mL). A white powder known as 3HBLC-Val 28 was produced (435 mg, 58 %).

UV (MeOH) $\lambda_{max}$ (nm) 322, 280; FTIR ($\nu_{max}$/$cm^{-1}$) , 3100, 1650, 1400, 1333, 1280; $^1$H NMR (400 MHz; MeOD), 5.55 (1H, *s*), 3.88 (1H, *d*, J 5.5), 3.58 (4H, *m*), 3.24 (2H, *t*, J 7.0), 2.68 (2H, *t*, J 7.0), 2.43 (2H, *q* J 7.0), 2.33(1H, *sept*), 1.66 (2H, *m*), 0.98-0.95 (6H, *d*), 0.88 (3H, *t*, J 7.5); $^{13}$C NMR (100 MHz; MeOD) 175.6, 174.3, 44.5, 37.6, 36.8, 33.6, 28.9, 20.0,18.0; 55 % yield;MS (ES), Calculated for $C_{14}H_{28}N_4O_3$ [MH+]: 301.2, found 345 ( with impurities).

# CHAPTER 7
# REFERENCES

## REFERENCES


1. G. Odian, Principles of polymerization, John Wiley and Sons, Fourth Edi., 2004.
2. M. Irfan and M. Seiler, *Ind. Eng. Chem. Res*., 2010, 49, 1169–1196.
3. W. Jiang, Y. Zhou and D. Yan, *Chem. Soc. Rev*., 2015, 44, 3874–3889.
4. U. Boas, J. B. Christensen, and P. M. H. Heegaard, *J. Mater. Chem*., 2006, 16, 3785–3798.
5. C. Gao and D. Yan, *Prog. Polym. Sci*., 2004, 29, 183–275.
6. D. A. Tomalia and J. M. J. Fréchet, *J. Polym. Sci. Part A Polym. Chem*., 2002, 40, 2719–2728.
7. Y. H. Kim, *J. Polym. Sci. Part A Polym. Chem.*, 1998, 36, 1685–1698.
8. B. Voit, *J. Polym. Sci. Part A Polym. Chem.*, 2000, 38, 2505–2525.
9. M. Jikei and M. Kakimoto, *Prog. Polym. Sci.*, 2001, 26, 1233–1285.
10. A. Sunder, J. Heinemann and H. Frey, *Chem. Eur. J*., 2000, 6, 2499–2506.
11. B. Klajnert and M. Bryszewska, Acta Biochim. Pol., 2001, 48, 199–208.
12. A. Carlmark, C. Hawker, A. Hult and M. Malkoch, *Chem. Soc. Rev*., 2009, 38, 352–362.
13. S. M. Grayson and J. M. J. Fréchet, *Chem. Rev.*, 2001, 101, 3819–3867.
14. E. Buhleier, W. Wehner and F. Vögtle, *Synthesis (Stuttg*)., 1978, 2, 155–158.
15. D. A. Tomalia, H. Baker, M. Hall, G. Kallos, S. Martin, J. Roeck, J. Ryder, and P. Smith, *Polym. J*., 1985, 17, 117–132.
16. G. R. Newkome, Z. Yao, G. R. Baker and M. J. Saunders, *J. Am. Chem. Soc*, 1986, 18, 849–850.
17. C. J. Hawker, R. Lee, and J. M. J. Frécnet, *J. Am. Chem. Soc.*, 1991, 113, 4583–4588.
18. D. Hölter, A. Burgath and H. Frey, *Acta Polym*, 1997, 48, 30–35.
19. C. J. Hawker, P. J. Farrington, M. E. Mackay, K. L. Wooley, and J. M. J. Fréchet, *J. Am. Chem. Soc*., 1995, 117, 4409–4410.
20. S. R. Turner, F. Walter, B. I. Voit and T. H. Mourey, *Macromolecules*, 1994, 27, 1611–1616.
21. K. L. Wooley, J. M. J. Fréchet and C. J. Hawker, *Polymer (Guildf)*, 1994, 35, 4489–4495.
22. C. J. Hawker, E. E. Malmström, C. W. Frank, and J. P. Kampf. *J. Am. Chem. Soc.* 1997, 119, 41, 9903–9904
23. P.G. De Gennes and H. Hervet, *J. Phys. Lett. Paris*, 1983, 44, 351.

24. S. Rosenfeldt, N. Dingenouts, D. Pötschke, M. Ballauff, A. J. Berresheim and K. Müllen, *Angew. Chemie* - Int. Ed., 2004, 43, 109–112.
25. J. F. Jansen, E. M. M. de Brabander-Van den Berg and E. W. Meijer, *Science* (80)., 1994, 266, 1226–1229.
26. R. L. Lescanec and M. Muthukumar, *Macromolecules*, 1990, 23, 2280–2288.
27. U. Boas, J. B. Christensen, and P. M. H. Heegaard, *J. Mater. Chem*., 2006, 3785–3798.
28. D. A. Tomalia, H. Baker, J. Dewald, M. Hall, G. Kallos, S. Martin, J. Roeck, J. Ryder, and P. Smith, *Polym. J*., 1985, 17, 117–132.
29. C. J. Hawker and J. M. J. Fréchet, *J. Am. Chem. Soc*., 1990, 112, 7638–7647.
30. L. J. Twyman, A. S. H. King and I. K. Martin, *Chem. Soc. Rev*., 2002, 31, 69–82.
31. P. J. Flory, *J. Am. Chem. Soc.*, 1952, 74, 2718–2723.
32. Y. H. Kim and O. W. Webster, *Am. Chem. Soc. Polym. Prepr. Div. Polym. Chem*., 1988, 29, 310–311.
33. B. I. Voit, *Comptes Rendus Chim*., 2003, 6, 821–832.
34. C. Schlenk, A. W. Kleij, H. Frey and G. Van Koten, *Organometallics*, 2000, 3773, 3445–3447.
35. C. J. Hawker, R. Lee, and J. M. J. Frechet, *J. Am. Chem. Soc*., 1991, 113, 4583–4588.
36. K. E. Uhrich, C. J. Hawker, J. M. J. Fréchet and S. R. Turner, *Macromolecules*, 1992, 25, 4583–4587.
37. C. J. Hawker and F. Chu, *Macromolecules*, 1996, 29, 4370–4380.
38. J. F. Miravet and J. M. J. Frechet, *Macromolecules*, 1998, 31, 3461–3468.
39. C. R. Yates and W. Hayes, *Eur. Polym. J.*, 2004, 40, 1257–1281.
40. M. Jikei, S. H. Chon, M. A. Kakimoto, S. Kawauchi, T. Imase and J. Watanebe, *Macromolecules*, 1999, 32, 2061–2064.
41. J. M. J. Fréchet, M. Henmi, I. Gitsov, S. Aoshima, M. Leduc and R. B. Grubbs, *Sci*, 1995, 269, 1080–1083.
42. K. Matyjaszewski, S. G. Gaynor, A. Kulfan and M. Podwika, *Macromolecules*, 1997, 30, 5192–5194.
43. M. Suzuki, A. Ii, and T. Saegusai, *Macromolecules*, 1992, 25, 7071–7072.
44. A. Sunder, R. Hanselmann, H. Frey and R. Mülhaupt, *Macromolecules*, 1999, 32, 4240–4246.
45. M. Liu, N. Vladimirov, and J. M. J. Fréchet, *Macromolecules*, 1999, 32, 6881–6884.
46. K. Inoue, *Prog. Polym. Sci*., 2000, 25, 453–571.

47. F. Vögtle, S. Gestermann, R. Hesse, H. Schwierz and B. Windisch, *Prog. Polym. Sci*., 2000, 25, 987–1041.
48. H. N. Patel and P. M. Patel, *Int. J. Pharma Bio Sci*., 2013, 4, 454–463.
49. R. Dong, Y. Zhou, and X. Zhu, *Acc. Chem. Res*., 2014, 47, 2006–2016.
50. W. Wu, R. Tang, Q. Li and Z. Li, *Chem. Soc. Rev*., 2015, 44, 3997–4022.
51. A. M. Caminade, D. Yan and D. K. Smith, *Chem. Soc. Rev*., 2015, 44, 3870–3873.
52. C. Chothia, and J. Janin, *Nature*, 1975, 256, 705–708.
53. M. Hashimoto, E. Rockenstein, L. Crews and E. Masliah, *Med*, 2003 4, 21–35
54. S. C. Tao, Y. Li, J. Zhou, J. Qian, R.L Schnaar, Y. Zhang, I. J. Goldstein, H. Zhu and J.P. Schneck, *Glycobiology*, 2008, 18, 761–769 .
55. D. Whitford, Proteins: Structure and Function. (John Wiley and Sons Ltd, 2005).
56. S. Jones, and J. M. Thornton, Principles of protein-protein interactions. Proc. *Natl. Acad, Sci* 93, 13–20 (1996).
57. M. I. Stefan and N. L. Nove, Cooperative Binding. PLOS *Comput. Biol*., 2013, 9, 2–7.
58. W. Stites, *Chem. Rev*, 1997, 97, 1233–1250.
59. L. Conte, L. C. Chothia, and E. Janin, *J. Mol. Biol*, 1999, 285, 2177–2198.
60. D. Reichmann, O. Rahat, M. Cohen, H. Neuvirth and G. Schreiber, *Curr. Opin. Struct. Biol*, 2007, 17, 67–76 .
61. P. Argos, *Protein Eng. Des. Sel*,1998, 2, 101–113
62. C. J. Tsai, S.L. Lin, H. J. Wolfson and R. Nussinov, *Protein Sci*,1997, 6, 53–6
63. A. Bogan and K. S. Thorn, *J. Mol. Biol*.1998, 280, 1–9.
64. T. Clarkson and J. Wells, J. *Science*. 1995, 267, 383–386.
65. R. K. Jain and A. D. Hamilton. *Org. Lett*, 2002, 2, 1721–1723
66. H. Yin and A. D. Hamilton, *Angew. Chemie* - Int. Ed., 2005, 44, 4130–4163.
67. D. C. Fry, *Drug Discovery*, 2006, 84, 535–552.
68. D. Kuritzkes, S. K. and P. K. Nat. Rev. Drug Discov.,2008, 7, 15–16 .
69. M. R. Arkin, Y. Tang, and J. A. Wells, *Chem. Biol*, 2014 21, 1102–1114.
70. W. K. Alderton, C. E. Cooper, and R. G. Knowles, *Biochem*, 2001, J 615, 593–615.
71. B. Carrington, W. K. Myers, P. Horanyi, M. Calmiano and A. D. G. Lawson, *Natural. Biophys.* J, 2017, 113, 371–380.
72. S. E. Miller, P. F. Thomson and P. S. Arora, *Chem. Biol*, 2014, 6, 101–116
73. D. Wang, M. Lu, and P. S. Arora, *Angew. Chemie* - Int. Ed, 2008, 47, 1879–1882.
74. C. Renner, U. Kusebauch, M. Löweneck, A. G. Milbradt and L. Moroder, *Chem. Biol. Drug Des.*, 2005, 65, 4–14.

75. A. Ojida, I. Masa-aki, M. Yasuko and H. Itaru. *J. Am. Chem. Soc*. 2003, 125, 10184–5.
76. D. K. Leung, Z. Yang and R. Breslow, *Proc. Natl. Acad, Sci*, 2000, 97, 5050–5053.
77. D. A. Tomalia and J. M. J. Frechet, *J Polym Sci A Polym Chem*;2002, 9,2719–2728.
78. S. D. Emerson, R. Palermo R and C. M. Liu, *Protein Sci*.;2003, 12(4):811–822.
79. J. H. Lee, Q. Zhang, S. Jo, S. C. Chai, M. Oh, W. Im, H. Lu and L. Hyun-Suk. *J. Am. Chem. Soc*, 2010, 133, 676–679.
80. W. Guo, J. A. Wisniewski and H. Ji, *Bioorg. Med. Chem. Lett*, 2014, 24, 2546–2554.
81. S. Srivastava, A.Verma, B. L. Frankamp and V. M. Rotello, *Adv. Mater,* 2005, 17, 617–621.
82. M. De, S. S. Chou and V. P. Dravid, *J. Am. Chem. Soc*, 2011, 133, 17524–17527
83. I. Ahmada, A. Mozhia, L. Yanga, Q. Hana, X. Lianga, C. Lia, R. Yanga and B. Chen Wang. *Biointerfaces,* 2017,159, 540–545.
84. S. Svenson, and D. A. Tomalia, *Drug Deliv. Rev,* 2005, 57, 2106–2129 (2005).
85. D. Moiani, M. Salvalaglio, C. Cavallotti, A. Bujacz, I. Redzynia, G. Bujacz, F. Dinon, P. Pengo and G. Fassina, *J. Phys. Chem*, 2009,113, 16268–16275.
86. F. Chiba and T. C. Hu, *Chem Commun*, 2008, 4351–4353. doi:10.1039/b806517a
87. R. M. Kim, M. Manna, S. M. Hutchins, P. R. Griffin, N. A. Yates, A. M. Bernick and K. T. Chapman, *Sci. U. S. A*, 1996, 93, 10012–10017.
88. J. Li, P. Nowak and S. Otto, *J. Am. Chem. Soc*, 2013, 135, 9222–9239.
89. R. Huang and I. K. H. Leung, *Discovery Molecules*, 2016, 27, 910.
90. R. Liu, X. Li, and K. S. Lam, *Curr. Opin. Chem. Biol*, 2017, 38, 117–126.
91. S. Fletcher and A. D. Hamilton, *J. R. Soc. Interface*, 2006, 3, 215–233.
92. P. L. Toogood, *J. Med. Chem*, 2002, 45, 1543–1558.
93. R. E. Babine and S. L. Bender. *Chem. Rev*, 1997, 97, 1359–1472.
94. S. Shaunak, S. Thomas, E. Gianasi, A. Godwin, E. Jones, I. Teo, K. Mireskandari, P. Luthert et al. *Nat. Biotechnol*. 22, 977–984 (2004).
95. V. P. Torchilin, *Eur. J. Pharm. Sci*. 2000, 11, S81–S91.
96. E. Abbasi, S. Aval, A. Akbarzadeh, M. Milani, H. Nasrabadi, S. Joo, Y. Hanifehpour, K. Nejati-Koshki and R. Pashaei-Asl, *Nanoscale Res. Lett.,* 2014, 9, 247 .
97. L. K. Tsou, R. K. Jain and A. D. Hamilton, *J. Porphyr. Phthalocyanines,* 2004, 08, 141–147.
98. A. A. G., You, C., De, M., Han, G. and Rotello, V. M., Tunable, *Gold Nano*-.2005, 23 12873–12881 .